SAND REPORT
SAND2003-1869
Unlimited Release
Printed June 2003

Geologic Investigation: An Update of Subsurface Geology on Kirtland Air Force Base, New Mexico

Dirk Van Hart

Prepared by
Sandia National Laboratories
Albuquerque, New Mexico 87185 and Livermore, California 94550

Sandia is a multiprogram laboratory operated by Sandia Corporation, a Lockheed Martin Company, for the U.S. Department of Energy under Contract DE-AC04-94AL85000.

Sandia National Laboratories

SAND2003-1869
Unlimited Release
Printed June 2003

Geological Investigation: An Update of Subsurface Geology on Kirtland Air Force Base, New Mexico

Dirk Van Hart
GRAM, Inc.
8500 Menaul Blvd., Suite B-370
Albuquerque, New Mexico 87114

Abstract

The objective of this investigation was to generate a revised geologic model of Kirtland Air Force Base (KAFB) incorporating the geological and geophysical data produced since the Site-Wide Hydrogeologic Characterization Project (SWHC) of 1994 and 1995. Although this report has certain stand-alone characteristics, it is intended to complement the previous work and to serve as a status report as of late 2002.

In the eastern portion of KAFB (Lurance Canyon and the Hubbell bench), of primary interest is the elevation to which bedrock is buried under a thin cap of alluvium. Elevation maps of the bedrock top reveal the paleodrainage that allows for the interpretation of the area's erosional history.

The western portion of KAFB consists of the eastern part of the Albuquerque basin where bedrock is deeply buried under Santa Fe Group alluvium. In this area, the configuration of the down-to-the-west, basin-bounding Sandia and West Sandia faults is of primary interest. New geological and geophysical data and the reinterpretation of old data help to redefine the location and magnitude of these elements. Additional interests in this area are the internal stratigraphy and structure of the Santa Fe Group. Recent data collected from new monitoring wells in the area have led to a geologic characterization of the perched Tijeras Arroyo Groundwater system and have refined the known limits of the Ancestral Rio Grande fluvial sediments within the Santa Fe Group.

Both the reinterpretation of the existing data and a review of the regional geology have shown that a segment of the boundary between the eastern and western portions of KAFB is a complicated early Tertiary (Laramide) wrench-fault system, the Tijeras/Explosive Ordnance Disposal Area/Hubbell Spring system. A portion of this fault zone is occupied by a coeval "pull-apart" basin filled with early Tertiary conglomerates, whose exposures form the "Travertine Hills."

This page left intentionally blank.

Acknowledgements

Susan Morrison (GRAM, Inc.) of the Environmental Restoration Geographic Information System worked hand in glove with me to construct the four plates. Geologists John Copland (Weston Solutions, Inc.) and Joe Pavletich (GRAM, Inc.) each gave the report an in-house peer review. Geophysicist Dave Hyndman (Sunbelt Geophysics) provided a reality check on some of the geophysical interpretations. Geophysicist Chuck Reynolds (Geological Associates) read over the entire report and made numerous suggestions. Finally, W.K. (Kelly) Summers, retired and well-known New Mexico hydrologist, conducted an intense review. All of this greatly appreciated input has been incorporated into this report.

This page left intentionally blank.

Contents

Figures

Tables

This page left intentionally blank.

Appendices

Appendix A—Catalog of Subsurface Bedrock Control Points, Lurance Canyon and Hubbell Bench Area (Exclusive of Inhalation Toxicology Research Institute) (Plates II & III)

Appendix B—Catalog of Subsurface Bedrock Control Points, Hubbell Bench—Inhalation Toxicology Research Institute Area (Plate III)

Appendix C—Catalog of Important Subsurface Bedrock Control Points, Manzano Base West Area (Plate IV)

This page left intentionally blank.

Plates

I	Lurance Canyon, Hubbell Bench, and Manzano Base West Areas with Bedrock Elevations, SNL/KAFB (scale 1:36,000)
II	Lurance Canyon with Bedrock Elevations (scale 1:12,000)
III	Hubbell Bench and Lower Lurance Canyon with Bedrock Elevations, SNL/KAFB (scale 1:18,000)
IV	Manzano Base West Area with Bedrock Elevations (scale 1:18,000)

This page left intentionally blank.

Acronyms and Abbreviations

ARG	Ancestral Rio Grande
bgs	(Depth) below ground surface
CSAMT	Controlled-Source Audio-Frequency Magnetotelluric
CTA	Central Training Academy
°C	degrees Celsius
°	degrees
E	East
EM	electromagnetic
EOD	Explosive Ordnance Disposal Area
EGIS	Environmental (Restoration) Geographic Information System
ER	Environmental Restoration
FGU	Fine-grained alluvial-fan unit of upper Santa Fe Group
ft	feet
ITRI	Inhalation Toxicology Research Institute
Ka	Thousand years ago
KAFB	Kirtland Air Force Base
K_{sat}	Saturated hydraulic conductivity
m	meter(s)
Ma	Million years ago
mag	magnetometer
M-M'	Fault located in EOD Hills
N	North
NMBG&MR	New Mexico Bureau of Geology and Mineral Resources
S	South
sec	second(s)
SNL/NM	Sandia National Laboratories/New Mexico (located on KAFB)
SP	Seismic shot point
SWHC	Site-Wide Hydrogeologic Characterization Project
TAG	Tijeras Arroyo Groundwater area
TA	Technical Area
USGS	U.S. Geological Survey
W	West

This page left intentionally blank.

1. Introduction

This report presents the results of the geological investigation of Kirtland Air Force Base (KAFB) and includes 55 figures produced in Adobe Illustrator 9.0 and four plates. Plate I is a composite top-of-bedrock map of the entire area at a scale of 1:36,000. Plates II and III are more detailed plates covering Lurance Canyon and the Hubbell bench at scales 1:12,000 and 1:18,000, respectively. Plate IV covers the eastern flank of the Albuquerque basin at a scale of 1:18,000 and, because bedrock data of this area are sparse, serves mainly as an index map.

1.1 Project Scope

This project was conducted for Sandia National Laboratories/New Mexico (SNL/NM) Environmental Restoration (ER) Project, Department 6133. The investigation was planned by Sue Collins (SNL/NM ER, Dept. 6133), Bill Schneider (Weston Solutions, Inc.), Amy Bruckner (Weston Solutions, Inc.), and Dirk Van Hart (GRAM, Inc.) at a meeting held on August 22, 2001. As originally conceived, the result was to be a set of elevation maps of the top-of-bedrock surface spanning three contiguous areas in the eastern portion of KAFB including: 1) Lurance Canyon, 2) the Hubbell bench, and, where possible, 3) the eastern flank of the Albuquerque basin west of Manzano Base (referred to as "Manzano Base West"). This investigation was intended to supplement the geologic mapping done during the Site-Wide Hydrogeologic Characterization Project (SWHC) in 1994 and 1995 (SNL/NM 1996). The map data were entered into the Environmental Restoration Geographic System (EGIS), and personnel from Weston Solutions, Inc. used the data to generate a three-dimensional model with earthVision®, which will support public education about SNL/NM ER.

Although the investigation began with mapping the elevation of the top-of-bedrock surface, it progressed to an analysis of recently-acquired geophysical data, revisitation of 1984 reflection-seismic data, correlation of new wells, and reconsideration of KAFB geology in its regional context. It led to the rethinking of various structural, stratigraphic, paleodrainage, and hydrogeologic issues. Some elements of the interpretation, e.g., deep structure, are, and will remain, speculative. The interpretations presented in this report should therefore be considered a status report as of late 2002 and a reasoned attempt to correlate all the available data.

1.2 Procedure

In 1994 and 1995, the SWHC geologists mapped the bedrock on the Hubbell bench and in the lower Lurance Canyon. Their work involved two components: 1) construction of a geologic map that integrated the surface and the subsurface bedrock geology (SNL/NM 1996, Plates XII, XIII, and XIV), and 2) construction of a top-of-bedrock elevation (i.e., paleotopographic) map (SNL/NM 1996, Plates XV and XVI). The present investigation of those areas deals with only the top-of-bedrock elevation. The procedure was to tie the surface bedrock elevations from the topographic maps to all the existing subsurface and geophysical control. This project was intended to build upon and update the SWHC work.

The Domino Theory rules geologic investigations, i.e., the modification of one element of an interpretation forces the revision of other related parts. A reconsideration of pre-alluvial paleodrainage and bedrock structure became necessary. The problematic Travertine structural block, renamed the Travertine basin (see Section 3.1), and a unique fault exposed on the east side of the Explosive Ordnance Disposal Area (EOD) Hills had to be reevaluated in the context of early Tertiary, Laramide wrench-faulting. The study of new geophysical data acquired in 2001 and 2002 and a revisitation of a 1984 reflection seismic line required reinterpretation of the fault pattern in the Manzano Base West area, including the location of the elusive West Sandia fault. This led to a revision of structural and stratigraphic elements at the eastern part of KAFB east of the Tijeras Arroyo Groundwater (TAG) and Technical Area (TA)-V areas.

1.3 Geologic Setting

KAFB spans a segment of the eastern flank of the Albuquerque basin and the uplifted basin margins. The basin, in turn, is a segment of the Rio Grande rift, a linear extensional feature extending from southern Colorado to Mexico and West Texas (Figure 1-1). The southern and southwestern part of the rift merges with the broad extensional province of the Basin and Range Province. The rift was formed under a regional extensional regime active during the last 30 million years and affecting most of western North America. Rift structures were superimposed on both the pre-existing northeast grain of the Precambrian basement and structures formed during the Pennsylvanian and the early Tertiary Laramide compressional episodes. On KAFB, the structural scenario is quite complex, but it can be simplified as consisting of four tectonic provinces (Figure 1-2). From west to east these are:

- The eastern part of the Calabacillas subbasin of the Albuquerque basin, where bedrock is deeply buried below late Tertiary, Santa Fe Group alluvium, and has been encountered by only a single deep well on KAFB.

- The uplifted basin margins, where bedrock generally crops out and forms rugged topography. The uplifted terrain is highly segmented and includes the elevated blocks of Manzano Base (i.e., Four Hills) and the Manzanita Mountains.

- The Hubbell bench, which occupies an intermediate structural position between the Albuquerque basin and the uplifts. Bedrock is generally buried by less than 200 ft of alluvium and is frequently encountered during well installation. A few scattered outcrops reveal that the bench has been beveled by erosion to deep stratigraphic levels.

- The Travertine basin, which developed within a zone of early Tertiary, Laramide-age shear on the western rim of the Hubbell bench.

The stratigraphic section preserved on KAFB varies with province and is controlled by the amount of uplift and the attendant depth of erosion (Figure 1-3). The buried bedrock geology can be projected into the subsurface across the Hubbell bench and the Travertine basin using the scattered bedrock outcrops and monitoring wells (Figure 1-4).

1.4 Summary of Relevant Previous Geologic Work on KAFB

Numerous studies have been conducted on the bedrock exposures in the Manzanita and Manzano mountains on KAFB. However, because this project focuses primarily on the surface and subsurface bedrock geology west of the uplifts, most of these studies will not be cited here. The first work relevant to this project was that of Reiche (1949), who mapped the Hubbell bench and was the first to study the unusual conglomerates in the Travertine basin. Myers and McKay (1970) mapped the eastern part of the Hubbell bench, and Myers and McKay (1976) mapped the Manzano Base (Four Hills) area. Riddle and Grant (1981) performed a Controlled-Source Audio-Frequency Magnetotelluric (CSMAT) survey on the west flank of Manzano Base to determine depth to bedrock. Grant (1981 and 1982) described the "travertines" of the Travertine basin. Sigma Geoservices, Inc. (1984) shot a reflection seismic survey on KAFB, and Dobecki (1985) interpreted the results. Krumhansl and McConnell (1994) mapped the EOD Hills and the Travertine basin. The SWHC effort included extensive surface and subsurface geologic mapping during 1994 and 1995 (SNL/NM 1996). The U.S. Geological Survey (USGS) conducted an extensive aeromagnetic survey (USGS 1998) of the area. Fritts and Van Hart (1997) and Van Hart (2001) studied the geology of the TAG area. Van Hart et al. (1999) incorporated the USGS aeromagnetic data into the unfolding geologic picture. Karlstrom et al. (1999a) mapped the bedrock geology of Lurance Canyon and the northern rim of the Hubbell bench. Hyndman and Brandwein (2002) conducted geophysical investigations on the west flank of Manzano Base. Finally, Geological Associates (2002) ran a reflection and refraction seismic line along a portion of the north boundary fence of KAFB.

This page left intentionally blank.

2. Lurance Canyon (Plates I and II)

Lurance Canyon consists of the upper reach of the Arroyo del Coyote that is narrowly confined by outcrops of Precambrian rocks. It begins on the east side of the Burn Site and extends west of Coyote Springs (Figure 1-4, Plates I and II).

The method of investigation in this area was straightforward. I took the top-of-bedrock elevations from the topographic coverage in the areas of bedrock exposure and projected the values into the subsurface using the existing subsurface control where the bedrock is covered by alluvium.

In Lurance Canyon, subsurface data exist at ten monitoring well locations, including one well (CYN-MW5) that was drilled by SNL/NM ER in 2001 (Appendix A). The bedrock elevation was mapped at a contour interval of 40 ft. The map was first constructed on a scale of 1:6,000 to show detail and then reduced to a scale of 1:12,000 for presentation (Plate II).

This page left intentionally blank.

3. Hubbell Bench (Plates I and III)

The SWHC mapped the northern part of the Hubbell bench during 1994 and 1995 at a contour interval of 50 ft (SNL/NM 1996, Plates XV and XVI). For this investigation, I converted the SWHC contour interval to 40 ft to facilitate the linkage of Lurance Canyon (Plate II) with the Hubbell bench (Plate III). The rather abundant well monitoring on the Hubbell bench includes 4 points along the Manzanita Mountain front, 6 along Arroyo del Coyote, 12 in the central part of the bench, and 44 in and around the Inhalation Toxicology Research Institute (ITRI) facility (Appendices A and B). Only five of these monitoring wells were drilled since the SWHC, and only one forced a revision.

3.1 Travertine Basin Complex

The Travertine basin (Plate III and Figure 3-1) is arguably the most interesting and most problematic structural feature on KAFB. This fault-bounded basin has attracted the attention of researchers for years, but no subsurface data existed until the SWHC. The SWHC geologists referred to it as the "Travertine block" and recognized that it was a unique element on KAFB. At the time, the structure was considered to be a transitional stair-step between the Albuquerque basin to the west and the Hubbell bench to the east, and to have been formed during late Tertiary, Rio Grande rifting. This investigation has revised this scenario. Therefore, it is appropriate to review the past work done in this area.

Reiche (1949) surveyed the area around Travertine Hills and observed that:

> ... several low hills and a flat district to the east are formed of ill-sorted sandy coarse Tertiary gravels (fanglomerate). These are essentially impermeable, owing to an interstitial clay fraction which is about half calcite and half kaolinitic clay. Along their western margin the gravels are dragged to easterly dips as high as 48° [degrees], exposing a section 1100 feet thick.

Geothermal investigations on KAFB (Grant 1981 and 1982) took note of the bona fide travertine deposits in the area (north of North Travertine Hill) and coined the term "Travertine Hills" for what was interpreted as a pair of travertine mounds built up by springs. The "hills" are a pair of semicircular features aligned along a north-south (N-S) axis north of Magazine Road (Figure 3-1A), consisting of "North" Travertine Hill, the most prominent of the two with more than 100 ft of relief, and its more subdued southern neighbor lying between North Travertine Hill and Magazine Road with about 70 ft of relief. In this report, I call the second one "Middle Travertine Hill" because of a third feature on the south side of Magazine Road, barely a hill at all with less than 20 ft of relief, which I refer to as "South" Travertine Hill.

The term "travertine" for the rock underlying these hills is a misnomer. Travertine is defined as a dense finely-crystalline or concretionary limestone formed by rapid chemical precipitation of calcium carbonate ($CaCO_3$) from solution in surface-water and groundwater via agitation of stream water or by evaporation around the mouth or in the conduit of a spring, especially a hot spring (AGI 1987). Grant (1982), however, pointed out that all the so-called travertine deposits

are actually conglomeratic, in fact consisting of calcium carbonate ($CaCO_3$)-cemented, bouldery to cobbly conglomerates and some coarse sandstones.

Travertine Hills Arroyo cuts between North and Middle Travertine Hills (Figure 3-1A). The floor of the arroyo contains a number of conglomerate outcrops. In the westernmost outcrop, the conglomerate beds dip 55° to the east. Precambrian quartzite crops out less than 100 ft to the west of this outcrop, but the contact between the quartzite and conglomerate is not exposed. Eastward along the arroyo, the dips in the conglomerates gradually decrease to about 15° to the southeast. The length of traverse combined with the dip data indicates that the thickness of the conglomerate unit could be as great as 1,450 ft. This compares favorably with the 1,100 ft of Reiche (1949). The single monitoring well in the basin, STW-2 (STW-1 was abandoned at 180 ft) was drilled in 1995 about 1,000 ft southeast (SE) of Middle Travertine Hill and penetrated conglomerate to a total depth of 521 ft (Figure 3-1B).

Magazine Road cuts through the southern part of Middle Travertine Hill (Figure 3-1A). Dips in the bouldery conglomerate cannot be measured with accuracy, but the occasional sandy beds reveal dips of about 35° to the east. Most of the large clasts consist of Madera limestone, with many fewer clasts of red mudstone possibly derived from the Abo Formation (Figure 1-3). An exemplar of the coarse nature of this unit occurs near the top of Middle Travertine Hill where a very large boulder of Madera limestone was encountered during the SWHC. Partial excavation and size measurement (4.3 by 3.5 by 1.3+ ft) reveals that it is in fact a boulder weighing more than 1 ½ tons.

Reiche (1949, cross section B-B' in Plate 5) recognized the basic geometry of the conglomerate unit, but supposed that the unit was a coarse-grained variant of the Santa Fe Group. Krumhansl and McConnell (1994), in their excellent and comprehensive investigation of this area, agreed that the conglomerates are of Tertiary age, but speculated that because these sediments were old enough to be tectonically deformed, they must be no younger than lower Santa Fe (late Oligocene or early Miocene). The authors went a step further and boldly stated that these sediments were probably the depositional product of a mountain-building event and were therefore probably of early Tertiary, Laramide age.

It is difficult to draw a satisfying transverse cross section through this basin. Outcrops and subcrops of bedrock surround the feature on three sides. To the east, flat-lying Madera limestone crops about 1,800 ft east of the Solar Tower (Figure 3-1A). About 4,000 ft to the northeast, Permian Abo redbeds exist in the shallow subsurface (Well LMF-1) and dip to the west, opposite the dip of the conglomerates. To the west and northwest of the westernmost outcrop of conglomerate are two exposures of Precambrian quartzite. Finally, about 1,000 ft northwest of the latter quartzite, there is a single small outcrop of Madera limestone, suggesting that the quartzite body between it and the conglomerates is contained in a fault sliver (Figure 3-1B).

I have reinterpreted the area and, in the course of doing so, have gained a profound appreciation of the work and insight of Reiche (1949) and Krumhansl and McConnell (1994). The following elements are germane to this discussion:

- A long history of wrench-faulting along the Tijeras fault
- Similarity of the Tijeras fault to wrench-faults in other basins
- The EOD Hills, the newly-named EOD fault, and an "old" fault between the main body of the EOD Hills and the EOD fault, identified as M-M' by Krumhansl and McConnell (1994)
- The possible connection of the EOD fault and the Hubbell Spring fault
- The grain size, thickness, and pervasive cementation of the Travertine Hills conglomerates
- The occurrence of lower Tertiary sedimentary formations in the subsurface
- A possible Hubbell Spring "pop-up" structure.

3.1.1 Tijeras Fault

The Tijeras fault zone has a long history of strike-slip movement, from the late Precambrian to at least the late Pleistocene (Lisenbee et al. 1979; Abbott and Goodwin 1995; Kelson et al. 1999). The zone is one of a number of NE-striking structural lineaments in northern New Mexico that influence the configuration of the Rio Grande rift and probably represent NE-striking anisotropy inherited from the northwest-directed, late Precambrian assembly of the lithosphere (Figure 1-1). Early Tertiary, Laramide regional compression later exploited this structural grain. In the vicinity of KAFB, the Tijeras fault follows the sheared, weakened base (southeast side) of the 1.4-billion-year-old Sandia granite pluton (Figure 3-2). East-stepping of compressional, thrust faults, from the Montosa fault to the south to the Sangre de Cristo Mountains to the northeast, suggest right-lateral slip along the Tijeras fault during the Laramide (Karlstrom et al. 1999b). During late Tertiary Rio Grande rifting, the Tijeras fault experienced left-lateral strike-slip that was a factor in the regional extension. The Travertine basin should therefore be interpreted in the context of the Tijeras wrench-fault system (Figure 3-3).

3.1.2 Other Wrench-Fault Basins

A characteristic of wrench-fault systems is the development of associated syntectonic basins, commonly referred to as "pull-apart basins." Excellent examples are the late Tertiary Ridge basin of southern California (Wilcox et al. 1973; Figure 3-4A), the modern Sea of Marmara basin along the Anatolian fault in western Turkey (Aksu et al. 2000; Figure 3-4B), and the modern Dead Sea basin along the Dead Sea fault in the Middle East.

The geometry of these basins is as complicated as the variable strength of the bedrock involved and the stresses acting on it (Figure 3-5). The basins are typically bound by split segments of the wrench-fault system that partition the stresses. The result is a complex pattern of branching and cross-linking faults (Dooley and McClay 1997; Figure 3-6). The subsidence and sedimentation history of wrench-fault basins can be highly complicated, and speculations about the subsurface structure within the Travertine basin without supporting data are tenuous at best. The inability to

construct balanced cross sections across such basins is often the result of lateral transport of bedrock slivers into the plane of cross section (Harding 1973; Figure 3-7).

3.1.3 EOD Hills, M-M' and EOD Faults

The broad uplift referred to as the EOD Hills (in contrast to the smaller feature called EOD Hill, on which Monitoring Well EOD was drilled) is anomalous. It is adjacent to the Tijeras fault system, but its deep structure and relationship to the fault are not understood (Figure 3-3).

An area on the east side of the EOD Hills provides an important piece of data (Figure 3-8). Well-defined formlines in the limestones of the Madera Group appear to be truncated to the west. In a small portion of this zone of apparent truncation, a chaotic zone at least 30 ft wide separates ESE-dipping Sandia Formation on the west from ESE-dipping Madera limestone on the east (Figure 3-9). Within the zone is a 2-by-30-ft slab, an exotic block of Madera limestone that has been rotated a high angle relative to the outcrops on either side. Eight ft north of the block is a patch of Madera striking N 5° W (west) and dipping about 30° west, and 12 ft east of that is a patch of Madera with subhorizontal dips. Despite a lack of obvious stratigraphic separation, these highly variable strikes and dips present an argument for disruption along a major fault. The earlier view was that the EOD fault is an up-to-the-west Laramide thrust fault (SNL/NM 1996; Van Hart et al. 1999). I interpret the chaotic zone as a Laramide wrench fault and call it the "EOD fault."

Krumhansl and McConnell (1994) noted a mineralized fault on the eastern part of the EOD Hills that they identified only as M-M' on their geologic map (see inset map in Figure 3-9, and Plate III) and wrote that:

> ...mineralizing fluids percolated along this fault depositing barite ($BaSO_4$) and fluorite (CaF_2), along with traces of galena (PbS) and sphalerite (ZnS). Judging from the gossans (massive iron oxide deposits) found in the same area, iron pyrite (FeS_2) was also abundant at one time, though prolonged exposure to the air has apparently oxidized it completely.

The authors speculated that this mineralogy indicates the presence of a deep circulation system and that the mineralization of the fault may be of early Tertiary (Oligocene) age. Fault M-M' is subparallel to a prominent fault to the south on the east flank of EOD Hill proper and may be an en echelon extension of it (see inset map in Figure 3-9). I interpret these two faults as a composite splay of the EOD fault.

3.1.4 Possible Connection of EOD Fault with Hubbell Spring Fault

During the SWHC, the southern extension of the EOD fault had been left unresolved (SNL/NM 1996, Plates 12 and 13; Van Hart et al. 1999, Plate II). However, if it is a wrench fault, its lateral extent should be significant. The only nearby candidate that is subparallel is the Hubbell Spring fault. However, this fault has down-to-the-west slip related to Rio Grande rifting

(Personius et al. 1999). Could the Hubbell Spring fault be a segment of the Laramide EOD fault that was reactivated during the late Tertiary?

There are precedents for such structural behavior in the Albuquerque basin. Kelley (1977), in his classic memoir on the Albuquerque basin, presented two cross sections in the southern part of the basin (Figures 3-10 and 3-11). Each cross section reveals an early Tertiary, Laramide fault on the east side of the basin, and Kelley's companion map (Kelley 1977) labels it the Montosa thrust fault. In each case, he interprets the thrust faults exposed at the surface in the mountains as connecting at depth to normal, late Tertiary, Rio Grande rift faults. Hayden (1991) determined that the fault is not a simple thrust but rather a right-lateral wrench with a complex geometry and variable directions of dip, and Cather (1992) successfully incorporated the wrench character of the fault into a comprehensive scenario of regional Laramide compression. Structural weaknesses created by Laramide compressive shearing may have provided a ready-made detachment surface for structural foundering during Rio Grande rift extension. Based upon these considerations, I provisionally interpret the Hubbell Spring fault to be a reactivated segment of the longer, Laramide-age Hubbell Spring/EOD wrench fault.

3.1.5 Travertine Hills Conglomerates

The large boulders present within the conglomerate suggest a nearby source with significant relief. However, the grain-size argument is not in itself compelling. During the SWHC, a limestone boulder 6 ft in diameter was observed in the Arroyo del Coyote, about one-half mile west of "G" Spring (Plate III). It had to have been derived from Lurance Canyon, a significant distance to the east. The large volume of bouldery material in the Travertine Hills, however, argues for a nearby source.

The conglomerates are well cemented by $CaCO_3$. The SWHC (SNL/NM 1996) considered the possibility that either groundwater moving up along a complex array of faults or near-surface water moving down the faults during late Tertiary Rio Grande rifting had caused the cementation. However, if the conglomerates are of Laramide age (i.e., Eocene), they have had more than 40 million years of opportunity to become cemented and late Tertiary spring activity need not be invoked.

Finally, the conglomerates have been tectonically deformed, with dips of 55° on the west side of the outcrop. The available evidence therefore suggests that the conglomerates were deposited syntectonically with the uplift of the basin rims as part of the early Tertiary, Laramide compressive and transpressive episode.

3.1.6 Lower Tertiary Strata in Subsurface

Lower Tertiary mudstones have been encountered in the subsurface below two three-well pads located along South Fence Road on the southern edge of KAFB: SFR-3 and SFR-4 (Figure 1-4 and Appendix B). Mudstone samples from SFR-3P were age-dated as lower Tertiary (Paleocene) based on palynology (MICROPALEO, 1993). Two of the wells on the SFR-3 pad (SFR-3P and SFR-3T) penetrated Santa Fe Group alluvium on the hanging-wall block of the Hubbell Spring fault and Lower Tertiary mudstones and possible Triassic strata on the footwall block.

Each of the wells on the SFR-4 pad (SFR-4D, SFR-4P, and SFR-4T) encountered Lower Tertiary rocks under less than 40 ft of alluvium on the footwall block of the Hubbell Spring fault. Wells located about 2,000 ft east of SFR-4 near the ITRI encountered Lower Permian Abo Formation in the shallow subsurface. Accordingly, I interpret a down-to-the-west fault to separate the two areas. Directly south of and on trend with the interpreted fault on Isleta Pueblo land is a series of up-to-the-west reverse faults (Love et al. 1996). The apparent scissor-type movement along this fault trend and the preservation of relatively young bedrock are compatible with the Laramide wrench-fault origin suggested for the Travertine basin and argues for inclusion of this block, east of the Travertine basin, as part of a Travertine pull-apart-basin complex.

3.1.7 Pop-Up Structures

"Pop-up" structures are structural uplifts commonly associated with wrench-fault systems. Two such features are apparently associated with the Tijeras fault system in the vicinity of KAFB. I interpret the EOD Hills, north of the Travertine basin, as being such an uplift. A second, less well-defined one is located to the south of KAFB near Hubbell Spring on the Isleta Pueblo Reservation (Figure 1-4). A sequence of upper Triassic through lower Permian strata crops out east of the spring (Love et al. 1996), and the extent of the exposures permits the interpretation of the suballuvial bedrock geology. South of the spring, the bedrock is downfaulted into the basin along the NW-trending East Hubbell Spring fault. Structural dip in the bedrock outcrop is generally down to the north, but an anticlinal rollover is developed just north of the East Hubbell Spring fault. The Permian Bursum Formation crops out on a portion of the crest of this anticline.

The easternmost outcrops in the Hubbell Spring area occupy a fault slice, part of an up-to-the-west reverse fault zone with possible right-lateral slip (Love et al. 1996; Figure 1-4). Furthermore, according to apatite fission-track data, a group of outcrops on the Hubbell bench (about 15 miles south of the Hubbell Spring area) was uplifted and deeply eroded more than 40 million years ago (Ma), i.e., during Laramide time (May et al. 1994), and subsequently downfaulted to its intermediate structural position. Therefore, the location of the Hubbell Spring structural high within an area affected by Laramide transpression leads to the conclusion that the high may be a pop-up feature similar to the smaller EOD Hills to the north and formed during the same episode (Figure 3-3).

3.2 Geologic History

3.2.1 Laramide Wrench-Faulting

I interpret the Travertine basin on KAFB to be a pull-apart basin associated with right-lateral motion along the Tijeras/EOD/Hubbell Spring wrench-fault system during Laramide, NE-directed regional transpression. The basin formed within an environment of local tension produced along a releasing bend of the Tijeras fault (Figure 3-3). The EOD Hills and the structural high near Hubbell Spring are interpreted to be pop-up structures developed under transpression within the same system (Figures 3-3 and 3-12). As the Travertine basin opened and the flanks were uplifted to significant relief, a synsedimentary sequence of bouldery

conglomerates was deposited in the adjacent topographic low. The active faults were the Tijeras, the EOD/ancestral Hubbell Spring, the M-M' splay, and the Travertine faults.

3.2.2 Rio Grande Rifting

Regional tension affected the area beginning in the early Miocene, resulting in the formation of the Rio Grande rift. Some of the normal faults associated with the rift apparently formed early and became inactive shortly afterwards, such as the Coyote fault, which is beveled flat in outcrop near the Manzanita Mountain front, and the northern part of the Manzano fault (Maldonado et al. 1999). Continued rifting shifted the focus of normal faulting basinward. The later faults were the Hubbell Spring, the Sandia, and the West Sandia faults.

3.2.3 Post-Laramide Erosion and Plio-Pleistocene Incision

A long period of erosion followed the Laramide faulting. Strata as young as Paleocene were once present (SNL/NM 1996; Van Hart et al. 1999), but on most of KAFB the bedrock has been stripped down to the Permian level or deeper. Lurance Canyon and the upper reach of the Ancestral Arroyo del Coyote (more appropriately considered an ancestral Coyote Creek) were probably developed in response to differential erosion of heterogeneous Precambrian rocks after breaching of the protective cap of Paleozoic strata.

The final carving of the bedrock surface occurred during the late Pliocene(?) to Pleistocene. Earlier courses of the Ancestral Arroyo del Coyote had been outlined by the SWHC (SNL/NM 1996). The SWHC shot four refraction seismic lines, "A" through "D" (Hyndman 1995) and drilled five hollow-stem auger holes (95B2, 95B4, 95B5, 95B6, and 95B7) in the present Arroyo del Coyote (Plate III). In 2001, SNL/NM ER drilled a monitoring well (CTF-MW2) into a portion of an Ancestral Arroyo del Coyote (Plate III). These data have been synthesized by a series of cross sections, B-B' through I-I' (Figures 3-13 through 3–17), modified from Hyndman (1995) and summarized by three paleodrainage maps (Figures 3-18 through 3-20) modified from the SWHC (SNL 1996).

Drainage Course #1. The earliest course of the Ancestral Arroyo del Coyote probably veered from the mouth of Lurance Canyon to the southwest (Figure 3-18; SNL/NM 1996). This course was probably controlled by reactivation of the Travertine and Hubbell Spring faults, which resulted in local lowering of base level and accelerated incision of the soft Permian strata exposed at the time on the upthrown block in the ITRI area during Late Pliocene(?) to early Pleistocene(?) time. The bulk of the sediment was transported to the Albuquerque basin west of the Travertine basin. The present subsurface expression of a portion of this early drainage course east of the EOD Hills and south of the present Arroyo del Coyote is very subdued and indistinct (Figure 3-17 and Plate III). Why sediments deposited by this stream do not crop out is not clear; perhaps they have since been eroded away or perhaps the river course never aggraded its valley sufficiently to produce a deposit.

Drainage Course #2. During the middle Pleistocene, the drainage flowed to the west from Lurance Canyon, bypassed the former course of Drainage #1, and veered sharply to the southwest when it encountered the elevated prong of Precambrian rocks on the west side of the Tijeras

fault (Figure 3-19). Evidence of the drainage consists of remnants of high terrace deposits (SNL/NM 1996, Plate I, designated Pt2). A paleochannel had been postulated here earlier (SNL/NM 1996, v. 1, Figure 2.1-14c). I expand on that interpretation in Figure 3-14A.

In 2001, Monitoring Well CTF-MW2 was drilled into a more southerly portion of this paleochannel (Figure 3-13) located about 1,500 ft WNW of the LMF-1 well drilled in 1995. LMF-1 encountered Permian, Abo Formation bedrock at the shallow depth of 18 ft and bottomed at 410 ft in the upper part of the Madera Group. In contrast, CTF-MW2 encountered alluvium to a depth of 110 ft, followed by highly fractured and brecciated granite to total depth of 190 ft. The position of the paleochannel and the nature of the granite bedrock seen in CTF-MW2 suggest that the drainage preferentially followed the trend of easily eroded, crushed granite along the Tijeras fault and the soft Permian mudstones. The stream incised deeply into the mudstones as much as 200 ft but downcut only slightly into the resistive Madera limestones upgradient (Plate III).

Sometime between the time Coyote Creek incised its valley into bedrock during the middle to late Pleistocene and the subsequent aggradation, the drainage was disrupted by faulting. Cross sections E-E', F-F' (Figure 3-15), G-G', and H-H' (Figure 3-16) show profiles of the valley that were verified by combinations of refraction seismic and hollow-stem augering data collected during the SWHC. The deep portions of the valley are filled with a clay-rich unit, suggesting fault-induced ponding. Evidently, the ponds filled with fine-grained sediment until the spill point was reached and the through-drainage was reestablished.

Drainage Course #3. Sometime after cutting its channel into bedrock in Drainage Course #1, the river likely aggraded its bed on the east side of the southern prong of Precambrian rocks. Raising the stream level and lateral cutting together may have allowed the stream to incise a path across the bedrock prong, allowing the drainage to escape to the west into the basin and to incise the water gap near the Arroyo del Coyote bridge (Figure 3-20).

4. Manzano Base West Bedrock Geology (Plates I and IV)

The area termed "Manzano Base West" is the western piedmont of the uplifted Precambrian-rock mass of Manzano Base (Four Hills). A pair of normal, Rio Grande rift faults is buried below its surface (Figure 1-4). The inboard, Sandia fault is closest to the Manzano Base uplift and is the best constrained. The outboard, West Sandia fault has been and remains an obscure feature. Its location is inferred by indirect means.

The data considered for structural analysis of this region include:

- Surface outcrops
- A CSAMT survey done in 1981
- Gravity data
- An extensive aeromagnetic survey flown by the USGS in 1997
- Ground-based magnetometer (mag) data from the SWHC
- Data from new monitoring wells and boreholes
- A series of geophysical surveys run in 2001, including electromagnetic ground conductivity, ground-based magnetometry, and refraction seismic
- An old water-supply well driller's log
- A reflection seismic line shot in 1984
- A seismic survey run in 2002

4.1 Surface Outcrops

The surface geology reveals the surface trace of a number of faults (SNL/NM 1996). These traces are taken as starting points for positioning the main faults in the area (Plate IV).

4.2 CSAMT Survey

A CSAMT survey was conducted in 1981 as part of an effort to identify potential hydrothermal energy sources on KAFB as an alternative to natural gas (Riddle and Grant 1981). The CSAMT technique is an electromagnetic (EM) induction method that uses signals produced by a transmitter operating at selected (controlled source) frequencies. The primary EM field is produced by a long dipole laid out along, in this case, a 2,000-ft line on the surface and grounded

at each end with a transmitter located at the center of the line. The receiver antenna consists of a short dipole in contact with the ground surface at both ends that measures the electric field parallel to the line (E_x), and a wound ferrite coil to measure the magnetic field normal to the transmitting antenna (H_y). In simplified terms, an equation converts the E_x/H_y ratio to apparent resistivity values. The apparent isoresistivity contours are used to estimate the depth of the sediment/granite contact.

The CSAMT survey estimated the top-of-bedrock contact to be at depths between 165 and 230 ft (50 and 70 meters [m]) at the eastern section of its Line 1. However, subsequent surface mapping (SNL/NM 1996) found granite outcrops in this area (Plate IV). For this reason, I did not use the results of the CSAMT survey in this analysis.

4.3 Gravity Data

USGS Bouger gravity data exist for the Albuquerque basin (Heywood 1992) and from several lines on KAFB (IT 1993). Van Hart et al. (1999, Figure 3-4) constructed a horizontal gradient map of the Bouguer gravity that presents a very broad-brush picture of lateral gravity contrasts but provides little insight as to fault locations or trends.

4.4 1998 Aeromagnetic Survey

The USGS flew its Isleta/KAFB Aeromagnetic Survey in 1997 (USGS 1998). The project covered much of KAFB. The USGS data were subject to further editing and reprocessing by Dave Hyndman (Van Hart et al. 1999, Plate I).

The aggregate amount and proximity of the mineral magnetite (Fe_3O_4) to the surveying instrument control the aeromagnetic response. Igneous and some metamorphic rocks commonly contain trace amounts of magnetite. In contrast, metamorphic quartzites and most sedimentary rocks contain little magnetite and are essentially nonmagnetic. The Sandia granite, which makes up most of the core of Manzano Base, typically contains from less than 1 to as much as 4 percent magnetite (Kelley 1975). The recording instrument is therefore sensitive to changes in both bedrock composition and bedrock depth.

The weathering products of the granite, such as much of the alluvium of the Santa Fe Group, contain detrital magnetite that can be locally concentrated by running water. Anyone living in Albuquerque's Northeast Heights has observed the wispy black streaks of magnetite in arroyo bottoms. In many cases at KAFB, the bedrock is at depths beyond the detection range of the instrument. In some cases, faults that cut the bedrock propagate upwards into the alluvium. If the faults are young and the propagations disturb the ground surface, sedimentary processes commonly modify the surface distribution of detrital magnetite in the alluvium and are detectable by the aeromagnetometer.

Sharp linear aeromagnetic trends in shaded-relief maps of the magnetic gradients are indicative of shallow faults. Such trends are pronounced west and south of KAFB (Van Hart et al. 1999, Plate I and Figure 1-3). Either the faults on Manzano Base West do not cut the shallow alluvium or the linear trends are overwhelmed by the huge magnetic response from the granite mass of

Manzano Base. However, the total field map (Figure 4-1) and especially the angular response patterns shown on the horizontal gradient map (Figure 4-2), indicate that bedrock occurs at detectable depths and strongly suggest that displacement along the Sandia fault is partitioned along its northern trace. The strike and apparent segmentation of the aeromagnetic data guide the interpretation of the Sandia fault complex in Plate IV.

4.5 1995 Ground-Based Magnetometry

Prior to 1998, the location of the Sandia fault had been constrained only by poor surface exposures near its southern end and a ground-based mag line run in 1995 during the SWHC. The 1,000-ft Mag Line "E" crossed the interpreted trace of the fault just north of the Arroyo del Coyote bridge near where the fault is exposed (Plates III and IV). The data show a sharp change of the magnetic signature at the interpreted location of the fault (Figure 4-3).

The drop in magnetic values on the upthrown east side of the fault is counterintuitive. The magnetometer reads the sum of 1) the earth's present, ambient magnetic field, 2) the magnetism induced in the rock by the earth's present, ambient field, and 3) the rock's remanent or permanent magnetic field. The remanent field is that given to the rock by the earth's ambient field as the rock is being formed. Lines of force of the ambient field dip downward to the north at an approximate 65° angle. If the rock's remanent field were of similar polarity, the two would complement each other and increase the signal. If, on the other hand, the remanent field were of opposite polarity (the earth's field has reversed many times in the past) the two would partly cancel and the sum would be less than the ambient field. This is probably the case here.

4.6 Recent Well Data

In 1998, KAFB drilled four boreholes at the Manzano Landfill (LF-20) located in the Central Training Academy (CTA), including KAFB-2001, KAFB-2002, KAFB-2003, and KAFB-FT14-BH1 (Figure 4-4). Monitoring wells KAFB-2001, KAFB-2002, and KAFB-2003 were drilled to 270, 274, and 291 ft, respectively, and all bottomed in weathered granite. The nature of the top-of-granite surface at this location has important repercussions for the entire area. Therefore, these well data are discussed in some detail below.

The broad slope on the west flank of Manzano Base is a "pediment" developed on a granite surface. A pediment is defined as a broad, gently-sloping, rock-floored erosion surface developed by subaerial agents in an arid or semiarid region at the base of an abrupt and receding mountain front; the surface may be bare but is more often mantled with a thin discontinuous veneer of alluvium derived from the mountain (AGI 1987).

The suitability of the word "erosion" in the above definition has been strongly disputed (Moss 1977; Cooke et al. 1993). Mounting evidence suggests that many pediments in the arid Southwest are, for the most part, the product of subaerial weathering developed during earlier periods of higher rainfall. Therefore, the bedrock surface is a downward-moving weathering front that has been partly buried during the ensuing drier climate. Granite typically weathers by downward penetration of moisture along joint surfaces followed by lateral movement from those sites. Chemical breakdown of biotite and hydration of the feldspars cause swelling and

disintegration of the granite. The result is development of residual, rounded bodies of fresh granite "corestones" surrounded by *in situ* granular disintegration products, or "grus." The weathered zone can be quite thick. On a pediment in south-central Arizona, a borehole was drilled through a 60-ft-thick canopy of grus before reaching fresh granite (Moss 1977).

When such a weathering front is drilled, the cuttings resemble coarse sand alternating with fresh granite chips. At the KAFB-2001, KAFB-2002, and KAFB-2003 monitoring wells, the deep cuttings were described variously as coarse to fine sand with occasional boulders and cobbles of fresh to weathered granite. Rather than a sharp contact, the weathering front is a transitional boundary that severely attenuates the velocity contrast between overlying grus and underlying fresh granite. The contact therefore may be barely detectable by reflection-seismic imaging techniques.

Two lines of evidence facilitate picking the top of bedrock in these wells. First, the gamma ray curve tends to record higher counts in the granite because of a higher concentration of residual feldspar (Figure 4-5). The gamma ray log records the natural radioactivity of the material opposite the borehole. The potassium feldspar minerals in granite contain the unstable isotope K^{40}, which emits gamma rays. Second, logs for all three wells documented a moderately abrupt, subtle color change, from mainly yellow-brown and brown above, i.e., Munsell 10YR 5/3 and 5/4, to gray and gray-brown below, i.e., Munsell 2.5 YR 6/2, 5/2, and 4/3 (Macbeth 1992). The two criteria do not coincide perfectly and the picks in Figure 4-5 are therefore an educated compromise.

Groundwater in these three wells was encountered at approximately 250 to 260 ft bgs. The fourth borehole, KAFB-FT14-BH1 (Fire Training Area 14), originally intended to be a monitoring well, was drilled about 400 ft west of KAFB-2001 to a depth of 500 ft in dry alluvium. The supporting floor that clearly exists below the water table to the east must lie deeper than 500 ft at KAFB-FT14-BH1 (Figure 4-6). The Sandia fault evidently passes between KAFB-FT14-BH1 and the three shallow wells (Figure 4-7).

In 1949, the KAFB-9 well was drilled to a total depth of 650 ft (Figures 4-4 and 4-7). A document in the well file indicates that an unnamed interpreter suspected the top of granite to be located at about 750 ft, but the evidence to support this is not cited. According to a KAFB cross section (KAFB 1993), the well actually bottomed in granite at the total depth of 650 ft (elevation 4,849 ft), but again no supporting evidence is provided. Lacking sound data, I assume that KAFB-9 bottomed in alluvium. In 1999, KAFB drilled the KAFB-6301 well about 2,800 ft west of KAFB-FT14-BH1 and 1,500 ft west of KAFB-9. The KAFB-6301 well bottomed in alluvium at a depth of 640 ft (elevation 4,814 ft), and supports my interpretation of KAFB-9. Therefore, bedrock west of the Sandia fault here must lie below an elevation of about 4,800 ft. Minimum throw on the fault at this location is about 650 ft (Figures 4-7 and 4-8).

The northern extent of the Sandia fault is unconstrained by wells. The configuration of the fault in Plate IV relies on the 1997 USGS aeromagnetic data mentioned in Section 4.4 and on the three 2001 ground-based mag lines discussed in Section 4-7.

4.7 2001 Geophysical Surveys

In 2001, three geophysical lines were laid out normal to interpreted structural trends and located as the existing KAFB facilities allowed (Figures 4-1 and 4-2). EM ground conductivity, ground-based magnetometry, and limited refraction seismic surveys were run on the lines (Hyndman and Brandwein 2002). The principal purpose of the work was to identify, if possible, the positions of the Sandia and West Sandia faults. The resultant geophysical-data profiles represent the maximum capability of these inexpensive methods to determine fault locations.

4.7.1 EM Ground Conductivity

EM surveys measure the ability of near-surface materials to conduct an induced electrical current (Figure 4-9). The amount of moisture present within the depth range of the instruments controls the ability of the near-surface to conduct electricity. The presence of porosity and the availability of moisture, in turn, mainly control the moisture content. Moist soils, dry soils, and hard bedrock generally demonstrate high, intermediate, and low conductivity, respectively. Ideally, low conductivity values would indicate the top of shallow bedrock, and higher values to the west would suggest bedrock that has been down-faulted to a depth beyond the range of the instruments. However, such factors as a weathered and gradational top of bedrock influence the detectable moisture content, as discussed in Section 4.6. The locations of the West Sandia and Sandia faults shown on the profiles in Figure 4-9 are therefore not compelling from these data alone, but are based upon a compromise with the ground-based magnetometry (see below).

4.7.2 Ground-Based Magnetometry

A ground-based magnetometer line had been run in 1999 (Van Hart et al. 1999) parallel to and about 300 ft from a portion of 2001 Line-2, and the data are similar. Therefore, the discussion of ground-based magnetometry will cover only the three 2001 lines (Hyndman and Brandwein 2002).

As with aeromagnetic surveys (Section 4.4), the aggregate amount, proximity, and magnetic properties of the mineral magnetite (Fe_3O_4) control the ground-based magnetic response. On magnetic-data profiles, changes in line slope, signal magnitude, and, to a lesser degree, overall line character are typically used to identify probable faults (Figure 4-10). However, a level of subjectivity is often involved in the interpretative process and the fault locations picked must take into account other data.

Having said that, the data show two significant features. First, a sharp change in magnitude and slope occurs on the eastern ends of all three lines. This is the position of the Sandia fault. The second feature is a subtle change in character on the western part of Lines 1 and 2, which suggests a deep change in bedrock depth and/or composition. The readings on the western ends of the two lines reach a minimum value of about 51,100 nano-teslas. Line 3 is different. Not only does the character change seen on Lines 1 and 2 appear to be absent, but the lowest values on the west end of the line are significantly greater at about 51,300 nano-teslas. The mapped position of this character change in Lines 1 and 2 indicates a possible fault-cut trending

northeast. If this pick is correct, the fault passes to the west of Line 3 (Plate IV). This interpretation would explain why the data in Line 1 are different.

The current tentative interpretation is that this northeast-trending feature is the buried trace of the down-to-the-west West Sandia fault. Prior interpretations oriented the trace in a north-trending direction (SNL/NM 1996; Van Hart et al. 1999).

4.7.3 Seismic Refraction Survey

Seismic surveys record the surface response to a compressive (sound) wave generated by an energy source and transmitted into the subsurface. A group of receivers (geophones) arrayed along the survey line measure the surface response. In seismic refraction surveys, the pulse travels downward through a low-velocity layer (shallow alluvium) until it encounters a high-velocity layer (usually bedrock). The wave travels (refracts) along the top of the high-velocity layer and transmits compressive waves upward. The geophones record these secondary waves.

Logistical and budgetary restrictions permit only weak, low-energy seismic sources on KAFB. Therefore, the seismic work was limited to the eastern ends of Lines 1 and 3, where the bedrock was interpreted to be shallow. The Line 1 seismic work was located entirely east of the Sandia fault and will not be discussed further. Line 3 revealed a fault with about 110 ft of offset (Hyndman and Brandwein 2002). This lies about 800 ft east of the trend suggested by the well data at the CTA about 3,000 ft to the south. Because the minimum throw on the Sandia fault at the CTA is about 650 ft (Figure 4-8), this fault on Line 3 is considered to be an intermediate in-board splay of the Sandia fault.

4.8 Well KAFB-10

The water-supply well, KAFB-10, located in TA-V (east of the trace of the West Sandia fault noted in Section 4.7.2) was drilled to a depth of 1,042 ft bgs in 1959. The driller's log noted 17 ft of "limestone" from 1,025 ft bgs to total depth. This anomaly was noted during the SWHC investigations (SNL/NM 1996) and during the 1999 aeromagnetic analysis (Van Hart et al. 1999, Plate II). Both times, I considered the pick with skepticism and, accordingly, placed it "on the shelf" for future consideration. If the West Sandia fault indeed passes west of this point, as suggested by the geophysical data (Section 4.7), this speculative top-of-bedrock elevation (+ 4,391 ft) is generally compatible with the minimum values indicated by KAFB-6301 (< 4,814 ft) and KAFB-9 (< 4,849 ft) (Figure 4-8). Furthermore, if the bedrock pick is correct, the western face of the West Sandia footwall block lies below the level of the regional water table (about 500 ft bgs) and may not be an important factor in the TAG area (discussed in Section 5.4).

4.9 1984 Reflection Seismic Data

In 1984, Sigma Geoservices, Inc., of Englewood, Colorado, ran an east-west reflection seismic line across a portion of KAFB for the U.S. Army Corps of Engineers (Sigma Geoservices 1984; Figure 4-11A). The line had been revisited before (Van Hart et al. 1999) and again during this investigation. The relevant parameters of the survey are as follows:

Length of line:	3 miles
Shot point (group) spread:	110 ft
Energy source:	Hydrapulse
Number of pops per shot point:	16
Common depth-point stack:	30-fold
Datum on seismic record section:	5,400-ft elevation

Because 1984 was not that long ago, the field and processing technologies used for this type of a limited two-dimensional survey have not changed drastically since then. The energy source, a Hydrapulse, is essentially a hydraulic ram that pounds the surface at "shot points" spaced 110 ft apart. Sixteen "pops" were done at each shot point along the 3-mile line. The seismic impulses were recorded by geophones placed on the ground 10 ft apart along the line. The term "30-fold common depth-point stack" indicates that the seismic trace plotted below each shot point on the record section consists of the summed ("stacked") simultaneous records from 30 different positions along the line. Stacking is performed to improve the signal-to-noise ratio by canceling out the random noise. The data processing was done to exceed petroleum industry standards. The main limitation was the sandy surface sediment, which provided generally poor energy-to-geophone coupling. In sum, the seismic record section presented on Figure 4-11A is a high-quality product, and the presence or absence of data is likely the result of the geology rather than the technology. However, persistent and severe constraints on the interpretation of this line include the lack of deep well control and reliable velocity control. Because these data may never be available, interpretations will always remain speculative.

Sigma consultant Thomas L. Dobecki (1985) wrote an interpretative report to accompany the contractor's report and included an annotated seismic record section (Figure 4-11A) that shows fair-to-good east seismic dips on the western segment of the line as far east as seismic shot point (SP) 155. The fair-to-good data to the west indicate that the seismic method used was fully capable of imaging the subsurface stratigraphy and that adequate velocity contrasts exist below at least that part of the line.

I have overlain my provisional interpretation on the annotated record section (Figure 4-11B). On the east end of the line, from SP 110 to SP 101, a few poor, west seismic dips are recognizable. In the center of the line between SP 155 to SP 110 a zone of no reflections occurs. The magnetic data mentioned in Section 4.7 suggest that a fault (West Sandia fault) trends northeast and crosses the line somewhere near SP 155. Seismic imaging is always optimized by lines oriented normal to the structural grain. However, at the time the line was laid out, the subsurface structural grain was unknown. This departure from optimum conditions would be enough to scatter the seismic energy into an unusable condition. It also demonstrates the risk of relying on a single line for structural interpretation.

A second possible contributor to the lack of data between SP 155 and SP 110 may be the result of the stratigraphy. Rising fault blocks typically shed coarse-grained material or "clastic wedges" into proximal basins. Such sequences typically lack sharp and continuous velocity contrasts. Transparent seismic zones produced by clastic wedges are known from half-graben rift basins

elsewhere in the world (Figure 4-12). Accordingly, I interpret the blank zone between SP 155 and SP 110 to be due to both the incident 45° angle between the line and the fault, and to a clastic wedge.

The best deep data exist between the west end of the line and SP 155. Between SP 195 and SP 155, reflective stratigraphy abruptly terminates downward at about 1.1 second (sec). I interpret this boundary to be the top of unstratified Precambrian basement (purple in Figure 4-11B). The relatively strong and continuous reflections, about 0.215 sec thick, that overlie that contact probably represent well-stratified, reflective Paleozoic rocks (blue in Figure 4-11B). The reflections above those rocks to about 0.4 sec may represent exclusively Santa Fe Group basin-fill sediments, or Santa Fe Group overlying an unknown thickness of weakly-reflective upper Paleozoic, perhaps Permian Abo Formation. Dobecki (1985) interpreted the top of the Paleozoic (Abo Formation?) to occur at about 0.7 sec on the western part of the seismic line (Figure 4-11A), and this could be correct. More recent seismic evidence suggests that shale or mudstone bedrock (e.g., Abo?) is indeed preserved on some downfaulted blocks (see Section 4.10). However, I have elected to take a conservative view and to interpret a full thickness of Pennsylvanian Madera Group and Sandia Formation on the seismic record section and zero thickness of Permian rocks.

With the minimal Paleozoic seismic thickness of 0.215 sec, Pennsylvanian formation thickness and lithology from Myers and McKay (1976), and revised Pennsylvanian stratigraphy from Kues (2001), I interpret the interval to consist of about 1,400 ft of the Madera Group overlying 200 ft of the Sandia Formation. Above the Madera there may be as much as 3,300 ft of Santa Fe Group based on recently-acquired sonic-velocity data (Table 4-1 and Figure 4-13).

4.10 2002 Seismic Survey

In late September and early October 2002, Geological Associates, an Albuquerque contracting entity headed by geophysicist Charles B. Reynolds, conducted a shallow seismic survey for SNL/NM on a speculative basis to demonstrate the feasibility of a new seismic system. The energy source was an accelerated weight drop, i.e., a "thumper" device, mounted on the back of a pickup, with two strings of self-orienting geophones pulled behind. The line was run along an east-west dirt road at the northern boundary of KAFB, between the KAFB Four Hills water tank battery on the west and Manzano Base to the east, and south of Albuquerque's Four Hills neighborhood (Figure 4-14). The geologic objectives were to identify major faults, to determine bedrock lithology from refraction velocities, and, if possible, to image structure within the bedrock and the Santa Fe Group basin-fill material. The survey produced good-quality shallow reflection and refraction data (Figure 4-15). The final report (Geological Associates 2002) is a separate, stand-alone document. Only a summary of the survey and the results are presented here. The relevant parameters of the survey are as follows:

Length of line:	1,845 m (6,000 ft)
Recording station spacing:	5 m (16.4 ft)
Energy source:	Gisco Electronic Seismic Source accelerated drop system
Geophone spread:	120 m (393.7 ft)
Average number of drops per record:	2
Common depth-point stack:	12-fold

4.10.1 Refraction Data

It is not possible to reliably correlate seismic reflections across discontinuities in the data. Therefore, the refraction data provide the best indicators of faults across which contrasting bedrock lithologies are juxtaposed.

The refraction record section (Figure 4-15A) is a constant-offset (50-m or 164-ft) section. The appearance of such a section is counterintuitive. The first arrival times of a refractive event (i.e., the "first breaks" at the heavy line in Figure 4-15A) are a direct indicator of the refractive layer's *velocity* and not of its depth (Figure 4-16).

The data indicate that the high- and intermediate-velocity units lie at very shallow depths and slope parallel to the ground surface. This relationship is suggestive of a buried pediment surface. Granite crops out about 2,000 ft to the south of SNL-1 (Figure 4-16).

In the intermediate-velocity regime, the shale or mudstone is speculatively identified as the Permian Abo Formation; the Madera Group should lie below it. The boundary between the intermediate- and low-velocity regimes is interpreted to be the Sandia fault. At the surface, the velocity change at Record Station 125 coincides with a subtle but clear change in topographic slope, steepening to the west (Figure 4-14). This break in slope lines up with a line to the southwest that marks a change in surface drainage character. My examination of 1989 air photos (scale 1:9,600) revealed that as arroyos cross this NNE-trending line, they commonly make sharp course changes and tend to merge, decreasing the drainage density. The composite topographic-break/change-in-drainage line coincides with patterns on the aeromagnetic data (compare Figures 4-14 and 4-17). I interpret this composite lineament to be the trace of the Sandia fault.

The low-velocity regime west of Record Station 125 is interpreted to be a refractor within the shallow basin-fill alluvium. The specific identity of the refractor is unknown.

4.10.2 Reflection Data

The seismic reflection data are stacked in the computer by applying the estimated velocities to remove the effect of varying source-to-receiver distance and to maximize the signal-to-noise ratio, and then summing common-reflection point traces at their true source position in the subsurface. A typical reflection record section plots two-way time (vertical) against distance (horizontal). Geological Associates (2002) has taken the processing a step further and generated an interpreted depth section, to which I have added a geologic interpretation (Figure 4-15B). The section reveals three significant features. First, between Readings 30 and 125 at a depth of about

4,800 ft the data suggest angular truncation of units (red lines) below that depth. If the overlying units are Paleozoic formations, as interpreted, an angular unconformity below is unexpected and the reason for this appearance is presently unknown. This anomaly is noted here for future reference.

The second feature revealed by the reflection data is the near-horizontal attitude of bedding within the interpreted Santa Fe Group between Readings 125 and 300. This sharply contrasts with the third feature, the contortion of the Santa Fe Group west of Reading 300. I interpret the stylistic change at Reading 300 to be the West Sandia fault, which has no surface expression and likely dies out in the subsurface. The reflection data give no indication of depth to bedrock on the footwall block of the West Sandia fault.

4.11 Bedrock Structure

A small (40 by 75 ft) yet very significant outcrop of Madera limestone is located west of North Travertine Hill at a elevation of 5,480 ft (Plate III). The outcrop was first located by Krumhansl and McConnell (1994) and cited in Section 3.1. It consists of subhorizontal, gray, cherty limestone, a lithology most typical of the lower Madera Group, Gray Mesa Limestone (Kues 2001). It indicates that the eastern flank of the Albuquerque basin is deeply eroded at this point. Monitoring Well CWL-BW2, drilled about 3,500 ft WSW of the above outcrop, bottomed at a total depth of 998 ft (elevation 4,434 ft) in Santa Fe Group alluvium. The well indicates the highest possible elevation of bedrock at that location. Therefore, the Sandia fault, or an active strand of it, likely separates the two areas (Figure 4-18). The broad region sweeping from TA-III and TA-V northeastward appears to be a structural bench on the footwall block of the West Sandia fault, intermediate in depth (about 1,000 ft bgs) between the Manzano Base uplift and the deeper part of the Albuquerque basin.

The region west of the West Sandia fault is the hanging-wall block of the West Sandia fault (Figure 4-18). KAFB-11, a water-supply well located just north of the TAG area, bottomed at 1,327 ft bgs (elevation 4,099 ft) and indicates the highest possible elevation of bedrock on that part of the block.

The depth to bedrock elsewhere on this block is based entirely upon the seismic line discussed in Section 4.9. In the center of the line (SP 160 to SP 195), I pick the top of stratified bedrock (Paleozoic?) at the rather subtle increase in reflection continuity and amplitude, e.g., 0.86 sec at SP 190. Also in the center of the line, I interpret the Precambrian basement to occur at the abrupt downward loss of reflection continuity, e.g., 1.09 sec at SP 190 (Figure 3-2).

To the west, I tentatively agree with Dobecki (1985) and place a down-to-the-west normal fault at SP 195. I very tentatively pick the top of Precambrian at the downward decrease of reflection continuity, e.g., 1.10 sec at SP 210, but one could argue with equal conviction that cohesive reflections continue downward to as deep as 1.35 sec at SP 210. The picks chosen therefore suggest the seismic velocities shown in Table 4-2.

In sum, I interpret the top of subsurface bedrock at the base of the Santa Fe Group alluvium to be the stratigraphic top of the Madera Group (Figures 4-11 and 4-13). However, a much shallower bedrock pick (e.g., at 0.72 sec at SP 210), as Dobecki (1985) interpreted, cannot be ruled out based upon the data from one seismic line. The velocity contrast between Santa Fe Group alluvium and Permian or younger mudstone bedrock, if present, may not be sufficient to give a noticeable reflection event. Despite these reservations, and using reasonable estimates for seismic velocities within the Santa Fe Group alluvium (Table 4-2), the interpreted two-way seismic times to bedrock on the line can be converted to depth and elevation (Figure 4-18). The throw on the West Sandia fault may therefore be on the order of 1,600 ft down-to-the-west along the seismic line. Assuming that the fault is listric, this throw should diminish to zero at its southern and northern tips.

This page left intentionally blank.

5. Revision of Santa Fe Group Stratigraphy

5.1 Basic Relationships

The main elements of the Albuquerque basin stratigraphy were outlined during the SWHC Project of 1994 and 1995 (SNL/NM 1996). During the past seven years, new wells have been drilled and new insight has been gained about the architecture and geologic history of the basin. An array of cross sections supports the current stratigraphic ideas (Figure 5-1).

New drilling data have refined the interpreted distribution of the Ancestral Rio Grande (ARG) fluvial lithofacies, which was derived from source areas to the north, and the alluvial-fan lithofacies, which was derived from the uplands to the east. Both units belong to the upper Santa Fe Group, i.e., the latest units deposited before the onset of incision of the modern Rio Grande Valley. Cross sections strongly suggest that in the KAFB area the two units interfinger and are therefore coeval (Figures 5-2 and 5-3; SNL/NM 1996). The ARG has been subdivided into two mappable units: the lower, ARG "A", and the upper ARG (further subdivided into a "B" and a "C" in the SWHC [SNL/NM, 1996]). Through time, the eastern limit of the ARG retreated to the west (Figures 5-3 and 5-4).

5.2 Timing Issues

Two competing hypotheses are currently being hotly debated in the New Mexico geologic community concerning the stratigraphic relationship of the ARG and its flanking piedmont deposits, as well as important timing issues. The New Mexico Bureau of Geology and Mineral Resources (NMBG&MR) maintains that the ARG is coeval with the piedmont lithofacies from the east, but the USGS believes that the ARG is erosionally inset into the piedmont deposits and therefore younger. The interfingering relationship of the ARG with piedmont sediments seen at KAFB support the NMBG&MR position (Figures 5-2 and 5-3).

Geologists with the NMBG&MR believe that the ARG in this part of the Albuquerque basin ceased its aggradation somewhere between 1.0 and 0.7 Ma in the early Pleistocene, and then began to downcut into its earlier deposits in the late-early or middle Pleistocene, probably because of a major climate change (Love et al. 2001). The USGS maintains that incision began much earlier, perhaps as early as 2.5 Ma in the late Pliocene (Cole et al. 2001). Because the NMBG&MR geologists (particularly David Love and Sean Connell) have devoted more time and fieldwork to this issue, I provisionally lean toward their timing in this report.

5.3 Significance of Fine-Grained Alluvial Fan Unit

It is instructive to convert a structural cross section into a stratigraphic cross section, i.e., one artificially "hung" on a correlative datum (compare Figure 5-5 with Figure 5-3). The interfingering relationship of the ARG and a fine-grained alluvial-fan lithofacies becomes clearer.

To the west the top of the ARG appears to correlate to a widespread, high-resistivity marker bed on the geophysical logs in the western part of KAFB (SNL/NM 1996, Figure 3.1-19). Although the precise lithology of this thin bed is unknown it has the general log-character of a paleosol. The end of Santa Fe Group deposition, i.e., its top, in the Albuquerque basin consists of several discrete surfaces of variable ages (Connell et al. 2001). These surfaces consist of the Sunport surface (at the Albuquerque International Airport) developed on the top of the fluvial ARG, and a group of slightly younger surfaces collectively called the Llano de Manzano to the south and east, developed on alluvial-fan sediments prograded onto the abandoned Sunport surface. I therefore tentatively assume that the high-resistivity marker in the subsurface is a possible paleosol and that it is approximately equivalent to the top of the ARG, as shown on Figures 5-3 and 5-5.

Sample logs from the ARG's coeval fine-grained stratigraphic unit to the east (green in Figures 5-2, 5-3, and 5-5) indicate that this fine-grained alluvial-fan unit (FGU) is rich in clayey silt or silty clay. Laboratory calculation of saturated hydraulic conductivity (K_{sat}) in the FGU from the few wells with adequate core control (e.g., LWDS-MWI and MWL-MW4) revealed values generally in the 1×10^{-7} centimeters/sec range (SNL/NM 1996, v. 2). A split-spoon core sample taken in this zone from a depth of 400 ft bgs in MWL-MW5 consisted of plastic, brown clay.

The FGU is interpreted to be a relatively fine-grained piedmont deposit that grades into a more sandy lithofacies toward the eastern source areas. At first glance, it seems incongruous that a clay-rich, low-energy depositional environment could exist geographically between a vigorous braided-stream system on the west and an active alluvial-fan system on the east. It must be kept in mind that the present climate may be quite different from that which prevailed during deposition of this unit. A point in time, 800 Ka, is significant (Pazzaglia et al. 1999). Prior to the pre-middle Pleistocene, large-amplitude glacial-interglacial cycles had not yet begun. The more humid conditions resulted in deep weathering on the uplands and on the pediment east of the Sandia fault. The hillslopes were mantled with a thick soil that, for the most part, remained in place. Because drainage occurred via perennial streams, only fine-grained, clay-rich material reached the basin. By the middle Pleistocene, i.e., after 800 Ka, the climate became characterized by 100-ka glacial-interglacial climatic cycles. This promoted the removal of the soil mantle down to the corestone roots of the soil profile, and deposition of the material onto and across the pediment into the basin as alluvial fans. Steady removal of the soil favored overland flow in place of subsurface flow, and the development of ephemeral streams. The gradual exhumation of the soil profile produced a sedimentary deposit characterized by upwardcoarsening. The time of 800 Ka is also significant beyond the confines of the Albuquerque basin. Stratigraphic relationships determined by high-resolution seismic surveys in the Gulf of Mexico indicate a major drop in sea level at 800 Ka, which, in turn, was likely linked to a major climate change (Paleodata Inc. 1993; Figure 5-6). Such a change would be expected to profoundly alter hydrologic and sedimentation patterns over a wide area, including the Albuquerque basin.

It is quite conceivable that the interpreted paleosol in the subsurface of western KAFB and the top of the FGU roughly approximate this significant climatic event at 800 Ka. This date agrees reasonably well with the 1.0 Ma to 700 Ka time-constraint proposed by the NMBG&MR for the

climate change (Section 5.2). The change heralded the cessation of ARG aggradation (at least locally) and the beginning of fluvial incision of the modem Rio Grande Valley.

The top of the FGU can be correlated across an extensive area (Figures 5-2 and 5-3). Because the "contact" is likely a zone of interfingering between the coarser material above and the finer material below, rather than a true time line, the correlation is considered approximate. The part of the section containing this datum has evidently been subjected-to slight compression in post-FGU time, which caused gentle folding (Figures 4-15B and 5-7). Localized compressional forces can be produced within a hanging-wall block that has been down dropped along a listric fault. This re-focuses our attention to the West Sandia fault, which is interpreted to be concave-to-thewest in plan view. As stated in Section 4.10, the gentle folding suggests that the fault has indeed penetrated to some level above the FGU. It is not known whether this penetration has an influence on groundwater movement in the TAG area to the west (see Section 5.4).

5.4 TAG Flow Model

The new structural interpretations made in the Manzano Base West area have repercussions on the TAG area (Van Hart 2001). Most important is the interpretation that bedrock in the footwall block of the West Sandia fault lies at a depth of about 1,000 ft bgs, i.e., about 500 ft below the top of the regional groundwater table. If the fault penetrates the Santa Fe Group above, it could play a role in the TAG groundwater flow model. However, in the absence of compelling data, the fault is tentatively assumed to have no appreciable effect on the model. The geometry of the perched and regional groundwater systems in the TAG area can just as well be explained by variable stratigraphy within the Santa Fe Group.

Much of the groundwater under KAFB is contained within the FGU, and the upper part of the FGU is the aquifer that contains the perched groundwater in the TAG area. Neither the internal anisotropy that influences grpundwater movement in the perched zone in the TAG area nor the FGU's lateral variations in permeability are well understood.

In the TAG area, the regional groundwater elevations exhibit an anomalous pattern where the perched and regional systems merge (Figure 5-8). The unusually wide separation of the 4,920-ft and 4,930-ft contours is pronounced, but it is rather tightly constrained by monitoring wells and requires a geologic explanation. It may be no coincidence that the wide separation occurs in the area of interpreted merging of the perched and regional systems. A logical solution is to invoke a lithofacies change from the relatively impermeable FGU material supporting the perched system on the west to more permeable, mixed lithofacies to the east (Figure 5-7). Well logs from the easternmost wells in the TAG area, KAFB-0312 and KAFB-0314, are instructive. Descriptions of well-cuttings from these wells indicate that the stratigraphic interval laterally equivalent to the FGU consists largely of sand with only occasional clayey beds. Such a permeable sequence would probably not be capable of providing a basal aquitard for perched groundwater zones.

The wide contour spacing on the top of the regional groundwater table in this area is likely an indirect indicator of this lithofacies change and reflects the decrease in K_{sat} and the attendant increase in hydraulic gradient from east to west. At the point where the FGU loses its aquitard-

prone character toward the east, the perched groundwater migrates downward and merges with the regional system (Figures 5-9 and 5-10).

The final step in the TAG investigation is to step back and take a megascopic view of the geologic system (Figure 5-11A) and the hydrogeologic system (Figure 5-11B). Such a view is simplistic by design, but schematically illustrates the interpretation of the essential operative elements – stratigraphic, structural, and hydrogeologic – in the TAG area.

5.5 TA-V

The geology under TA-V has been analyzed previously (SNL/NM 1999, Figures 4.1.2-1 and 4.1.3-1). Since then, four wells have been added, including two relatively deep wells (TAV-MW7, total depth 644 ft bgs, and TA V-MW9, total depth 617 ft bgs). The earlier interpretation extended the ARG "A" east across TA-V to the AVN-l well based upon tenuous log correlation. The two wells, TAV-MW7 and TAV-MW9, contain deep stratigraphic sections similar to that of AVN-l and none contains ARG "A"-like material (Figure 5-12). The interpreted eastward limit of the ARG "A" has been accordingly shifted back to the west (Figures 5-3 and 5-4).

The upgradient well, TAV-MW3, has a log character quite different from the TA-V wells to the west and contains much more sand. At the time it was thought that a 300-ft interval (210 to 510 ft) in this sandy section contained small amounts of "pumice" (SNL/NM 1999, Figure 4.1.3-1). Pumice is light-colored, vesicular, glassy volcanic rock that typically floats on water. It is an index rock-type for the upper ARG. Based upon this one well, the upper ARG was interpreted to pass through that point and to somehow avoid most of TA-V. This required an acrobatic interpretation of the paleogeography. A reevaluation of the well has determined that pumice is probably not present at TAV-MW3. The upper ARG lithofacies map has been revised accordingly (contrast Figure 5-4 to SNL/NM 1999, Figure 4.1.3-1).

TAV-MW3 is relevant to the TAG area. The eastward change to more sandy lithofacies from TA-V to this well is thought to correlate to the interpreted lithofacies change in the eastern part. of the TAG area where the perched and regional groundwater systems merge. No perched system is known at TA-V; water discharged on the surface in the Liquid Waste Disposal System, just northwest of TA-V, has moved directly down through the FGU to the regional system and has caused slight mounding. The perching beds present within the FGU in the TAG area are evidently not developed in TA-V. The FGU clearly demonstrates that internal stratigraphic variation occurs between TA-V and the TAG area, and that the unit is far from monolithic.

5.6 New KAFB Wells

As this report was being finalized I acquired partial results of four new KAFB monitoring wells (Figure 5-13) drilled as part of KAFB's nitrate abatement investigation. Wells KAFB-0611 and KAFB-0612 were drilled just northwest of the Tijeras Arroyo Golf Club. They were completed as a regional groundwater and perched groundwater well, respectively. KAFB-0611 encountered sticky clay from 300 to 498 ft bgs, and gravel containing water from 498 to the total depth of 505 ft bgs. Weathered and rounded pumice was found mixed with clasts of limestone and granite at 498 ft bgs. The pumice indicates that the upper ARG fluvial lithofacies is present at that location,

farther east than expected. I have incorporated this incident into the lithofacies map of the upper Santa Fe Group (Figure 5-4).

Well KAFB-0615 was drilled very close to granite outcrops just west of the Manzano Base perimeter. The well encountered granite from 5 ft to the total depth of 322 ft bgs. Confined groundwater within the granite aquifer was logged at 300 ft bgs.

Well KAFB-0616 was drilled northeast of the golf course and encountered clean sand from the surface to gravel and water at 480 ft bgs. Total depth of this well is 505 ft bgs.

An additional two wells, KAFB-0613 and KAFB-0614, have been drilled as a closely-spaced pair at the south end of the Tijeras Arroyo Golf Course. Data from these were not available for inclusion in this report.

This page left intentionally blank.

6. Conclusions

The conclusions reached as a result of this investigation are as follows:

1. A paleochannel that has incised into bedrock below the Arroyo del Coyote in Lurance Canyon is clearly mappable from the Coyote Springs area on the west to the Burn Site on the east (Plates I and II).

2. Monitoring Well CTF-MW2, located on the western rim of the Hubbell bench, was drilled into a paleochannel cut into bedrock.

3. The "Travertine Block," so-called during the SWHC, is actually an early Tertiary, Laramide-age, pull-apart Travertine "basin" associated with the Tijeras/EOD right-lateral wrench-fault system.

4. The EOD Hills are collectively a Laramide-age, pop-up structure associated with the Tijeras/EOD right-lateral wrench-fault system.

5. The area of bedrock exposures of Triassic- through Pennsylvanian-age rocks near Hubbell Spring on the Isleta Pueblo Reservation, south of KAFB, is likely also a complex pop-up structure associated with the southern part of the Tijeras/EOD right-lateral wrench-fault system.

6. The position of the southern part of the Sandia fault is tightly constrained by the combination of surface geologic control, a ground-based magnetometer line run during the SWHC, and a group of boreholes drilled in 1998 in and around the CTA. The minimum throw on this down-to-the-west fault at the latter location is about 650 ft.

7. The Sandia fault north of the CTA is a segmented feature, rather than a simple, linear element, based upon USGS aeromagnetic data.

8. The northern part of the Sandia fault has a subtle surface expression consisting of changes in topographic slope and details of surface drainage.

9. The Sandia fault is detectable by modern seismic refraction surveys.

10. The West Sandia fault trends SW-NE and is concave to the west, based upon 2001 ground-based mag data, a 1984 reflection-seismic line, and a 2002 reflection-seismic line.

11. The depth to bedrock on the footwall block of the West Sandia fault is about 1,000 ft bgs based upon data from KAFB-10, a 1959 water-supply well in TA-V.

12. The throw on the West Sandia fault may be on the order of 1,600 ft down to the west, based upon the 1984 reflection seismic line.

13. The depth to bedrock in the hanging wall of the West Sandia fault may be on the order of 2,300 ft, based upon the 1984 seismic line, and likely consists of the top of the Pennsylvanian Madera Group. However, the presence of Permian Abo Formation mudstones lying above the Madera Group cannot be ruled out.

14. Given that the top of the regional groundwater in the TAG area is about 500 ft bgs, the top of bedrock in the footwall block of the West Sandia fault is about 500 ft deeper than the top of the regional groundwater (see Conclusion No. 11 above). Therefore, bedrock in the footwall block of the West Sandia fault likely plays little or no role in the conceptual groundwater flow model of the TAG area.

15. The gentle folding of the strata within the upper Santa Fe Group on the west side of the West Sandia fault in the TAG area suggests that the fault propagates upward from bedrock at least partially into the overlying Santa Fe Group. Downfaulting of the Santa Fe Group along this concave-to-the-west fault possibly created a space problem and the attendant local compression.

16. The merging of the perched groundwater with the regional system at the TAG area is explained by a lithofacies change within the upper Santa Fe Group, passing eastward from fine-grained aquitard-prone material to more permeable, mixed lithofacies. This lithofacies change causes the eastward disappearance of the aquitard that provides the base of the perched groundwater in the TAG area.

17. The fine-grained unit cited in Conclusion No. 16 is the depositional product of a more humid, early Pleistocene climate. A major, regional climate change at the beginning of the middle Pleistocene, c.a. 800 Ka, heralded the beginning of predominantly coarse-grained sedimentation as ephemeral streams rapidly stripped the thick soil from the uplands to the east. The climate change possibly played a role in the cessation of fluvial aggradation by the ARG and the beginning of the incision of the modern Rio Grande Valley.

18. At TA-V, two new, relatively deep wells drilled during 2001 (TAV-MW7 and TAV-MW9) constrain the interpreted eastward limit of the fluvial ARG lithofacies. The wells show that the upper part of the ARG "A" pinches out near the west side of TA-V. If more deeply buried parts of the ARG "A" extend across the area, these must lie at depths below the deepest wells. The pumice-bearing upper ARG, which normally occurs above the ARG "A," is absent at TA-V.

19. The abrupt lithofacies change eastward from fine-grained upper Santa Fe Group under TA-V to the more porous sediments in the easternmost, upgradient well just outside of the area (TAV-MW3) is equated to the same lithofacies change proposed for the TAG area (noted above in Conclusion No. 16).

7. References

Abbott, J.C., and L.B. Goodwin, 1995, "A Spectacular Exposure of the Tijeras Fault, with Evidence for Quaternary Motion," in *Geology of the Santa Fe Region, Albuquerque Country, New Mexico Geological Society 46th Annual Field Conference Guidebook*, pp. 117–125.

AGI, see American Geological Institute.

Aksu, A.E., T.J. Calon, and R.N. Hiscoss, 2000, "Anatomy of the North Anatolian Fault Zone in the Marmara Sea, Western Turkey—Extensional Basins Above a Continental Transform," *GSA Today*, pp. 3–7, June 2000.

American Geological Institute (AGI), 1987, *Glossary of Geology*, 3rd ed.; R.L. Bates, and J.A. Jackson, eds., American Geological Institute, Alexandria, Virginia.

Cather, S.M., 1992, "Suggested Revisions to the Tertiary Tectonic History of North-Central New Mexico," in *San Juan Basin IV, New Mexico Geological Society 43rd Annual Field Conference Guidebook*, pp. 109–122.

Cole, J.C., B.D. Stone, R.R. Shroba, and D.P. Dethier, 2001, "Pliocene Incision of the Rio Grande in Northern New Mexico," *Geological Society of America*, Abstracts with Programs, p. A-48.

Connell, S.D., D.W. Love, F. Maldonado, P.B. Jackson, W.C. McIntosh, and M.C. Eppes, 2001, "Is the Top of the Upper Santa Fe Group Diachronous in the Albuquerque Basin?" in *U.S. Geological Survey Middle Rio Grande Basin Study*, Proceedings of the Fourth Annual Workshop, Albuquerque, New Mexico, February 15–16, 2000, U.S. Geological Society Open-File Report 00-488, pp. 18–20.

Cooke, R., A. Warren, and A. Goudie, 1993, *Desert Geomorphology*, UCL Press, London.

Dobecki, T.L., 1985, *Geoconsultant's Report, Seismic Reflection Survey on Kirtland Air Force Base, New Mexico*, prepared for Sigma Geoservices, Inc., Englewood, Colorado.

Dooley, T., and K. McClay, 1997, "Analog Modeling of Pull-Apart Basins," *American Association of Petroleum Geologists Bulletin*, v. 81/11, pp. 1804–26.

Fritts, J.E., and D. Van Hart, 1997, *Sandia North Geologic Investigation Project Report*, Environmental Restoration Project, Sandia National Laboratories, Albuquerque, New Mexico, March 31, 1997.

Geological Associates, 2002, *Final Report, Shallow Seismic Line SNL-1, Sandia National Laboratories*, Geological Associates, Albuquerque, New Mexico, November 15, 2002.

Grant, P.R., 1981, *Geothermal Potential on Kirtland Air Force Base*, SAND Report SAND81-7141, Sandia National Laboratories, Albuquerque, New Mexico.

Grant, P.R., 1982, "Geothermal Potential in the Albuquerque Area, New Mexico," in *Albuquerque Country II, New Mexico Geological Society 33rd Annual Field Conference Guidebook*, pp. 325–331.

Grauch, V.J.S., C.L. Gillispie, and G.R. Keller, 1999, "Discussion of New Gravity Maps for the Albuquerque Basin Area," in *Albuquerque Geology, New Mexico Geological Society 50th Annual Field Conference Guidebook*, pp. 119–124.

Harding, T.P., 1973, "Newport-Inglewood Trend, California—An Example of Wrenching Style of Deformation," *American Association of Petroleum Geologists Bulletin*, v. 57/1, pp. 97–116.

Hayden, N., 1991, "Dextral Oblique-Slip Deformation Along the Montosa Fault Zone at Abo Pass, Valencia and Socorro Counties, New Mexico," *New Mexico Geology*, v. 13/3, p. 64.

Heywood, C.E., 1992, *Isostatic Residual Gravity Anomalies of New Mexico*, U.S. Geological Survey Water-Resources Investigations Report 91-4065.

Hyndman, D.A., 1995, *Seismic and Magnetic Investigations, Arroyo del Coyote and Adjacent Areas, Kirtland Air Force Base, New Mexico, prepared for Site-Wide Hydrogeologic Characterization Project*, Sandia National Laboratories, Albuquerque, New Mexico.

Hyndman, D.A., and S.S. Brandwein, 2002, *Geophysical Investigation on the West Flank of Manzano Base, Kirtland Air Force Base, Albuquerque, New Mexico*, Sandia National Laboratories, Albuquerque, New Mexico, April 2002.

IT, see IT Corporation.

IT Corporation (IT), 1993, *A Surface Gravity Survey for Fault Delineation and Hydrogeologic Characterization: Draft Report Prepared for Site-Wide Hydrogeologic Characterization Project*, Environmental Restoration Project, Sandia National Laboratories, Albuquerque, New Mexico.

KAFB, see Kirtland Air Force Base.

Karlstrom, K.E., S.D. Connell, C.A. Ferguson, A.S. Read, G.R. Osburn, E. Kirby, J. Abbott, C. Hitchcock, K. Kelson, J. Noller, T. Sawyer, S. Ralser, D.W. Love, M. Nyman, and P.W. Bauer, 1999a, *Geology of Tijeras Quadrangle, Bernalillo County, New Mexico*, New Mexico Bureau of Mines and Mineral Resources Open-File Digital Map Series, OF-DM-4, geologic map scale 1:24,000, New Mexico Bureau of Mines and Mineral Resources, Socorro, New Mexico.

Karlstrom, K.E., S.M. Cather, S.A. Kelley, M.T. Heizler, F.J. Pazzaglia, and M. Roy, 1999b, "Sandia Mountains and Rio Grande Rift–Ancestry of Structures and History of Deformation," in *Albuquerque Geology, New Mexico Geological Society 50th Annual Field Conference Guidebook*, pp. 155–165.

Kelley, V.C., 1975, *Geology of Sandia Mountains and Vicinity*, New Mexico Bureau of Mines and Mineral Resources Memoir 29, New Mexico Bureau of Mines and Mineral Resources, Socorro, New Mexico, 135 p.

Kelley, V.C., 1977, *Geology of the Albuquerque Basin, New Mexico*, New Mexico Bureau of Mines and Mineral Resources Memoir 33, New Mexico Bureau of Mines and Mineral Resources, Socorro, New Mexico, 60 p.

Kelson, K.I., C.S. Hitchcock, and B.J. Harrison, 1999, "Paleoseismology of the Tijeras Fault Near Golden, New Mexico," in *Albuquerque Geology, New Mexico Geological Society 50th Annual Field Conference Guidebook*, pp. 201–209.

Kirtland Air Force Base (KAFB), 1993, *U.S. Air Force ER Program Work Plan, Stage "2B,"* Kirtland Air Force Base, Albuquerque, New Mexico.

Krumhansl, J.L., and V.S. McConnell, 1994, *Geology of the Travertine Hills Area, Kirtland Air Force Base*, Sandia National Laboratories, Albuquerque, New Mexico, revised November 15, 1994.

Kues, B.S., 2001, "The Pennsylvanian System in New Mexico—Overview with Suggestions for Revision of Stratigraphic Nomenclature," *New Mexico Geology*, v. 23/4, pp. 103–122.

Lisenbee, A.L., L.A. Woodward, and J.R. Connolly, 1979, "Tjieras-Cañoncito Fault System—A Major Zone of Recurrent Movement in North-Central New Mexico," in *Santa Fe Country, New Mexico Geological Society 30th Annual Field Conference Guidebook*, pp. 89–99.

Love, D.W., C. Hitchcock, E. Thomas, K. Kelson, D. Van Hart, S. Cather, R. Chamberlin, O. Anderson, J. Hawley, J. Gillentine, W. White, J. Noler, T. Sawyer, M. Nyman, B. Harrison, and R. Colpitts, 1996, *Geology of the Hubbell Spring 7.5-min Quadrangle, Bernalillo and Valencia Counties, New Mexico*, New Mexico Bureau of Mines and Mineral Resources, Open-File Digital Map DM-13, scale 1:12,000, New Mexico Bureau of Mines and Mineral Resources, Socorro, New Mexico.

Love, D.W., S.D. Connel, R.M. Chamberlin, S.M. Cather, W.C. McIntosh, N. Dunbar, G.A. Smith, and S.G. Lucas, 2001, *Constraints on the Age of Extensive Fluvial Facies of the Upper Santa Fe Group, Albuquerque and Socorro Basins, Central New Mexico*, Geological Society of America, Abstracts with Programs, p. A-48.

Macbeth, 1992, *Munsell Soil Color Charts*, revised edition, Kollmorgen Instruments Corporation, New York.

Machette, M.N., 1985, "Calcic Soils of the Southwestern United States," in *Soil and Quaternary Geology of the Southwestern United States*," Geological Society of America, Special Paper 230, pp. 1–42.

Magnavita, L.P., and H.T.F. da Silva, 1995, "Rift Border System: The Interplay Between Tectonics and Sedimentation in the Recôncavo Basin, Northeastern Brazil," *American Association of Petroleum Geologists Bulletin*, v. 79/11, pp. 1590–1607.

Maldonado, F., S.D. Connell, D.W. Love, V.J.S. Grauch, J.L. Slate, W.C. McIntosh, P.B. Jackson, and F.M. Byers, Jr., 1999, "Neogene Geology of the Isleta Reservation and Vicinity, Albuquerque Basin, Central New Mexico," in *Albuquerque Geology, New Mexico Geological Society 50th Annual Field Conference Guidebook*, pp. 175–188.

May, S.J., S.A. Kelley, and L.R. Russell, 1994, "Footwall Unloading and Rift Shoulder Uplifts in the Albuquerque Basin—Their Relation to Syn-Rift Fanglomerates and Apatite Fission-Track Ages," in G.R. Keller and S.M. Cather, eds., *Basins of the Rio Grande Rift, Structure, Stratigraphy, and Tectonic Setting*, Geological Society of America, Special Paper 291, pp. 125–134.

MICROPALEO (Micropaleo Consultants, Inc.), 1993, Palynologic Analysis-Five Samples from Shallow Wells, Kirkland [sic] Air Force Base: Contractor Report Prepared for GRAM, Inc., August 2, 1993.

Moss, J.D., 1977, "The Formation of Pediments—Scarp Backwearing or Surface Downwasting?" in D.O. Doehring, ed., *Geomorphology in Arid Regions*, Proceedings Volume of the 8th Annual Geomorphology Symposium at State University of New York, George Allen and Unwin, London.

Myers, D.A., 1982, "Stratigraphic Summary of Pennsylvanian and Lower Permian Rocks, Manzano Mountains, New Mexico," in *Albuquerque Country, New Mexico Geological Society 33rd Annual Field Conference Guidebook*, pp. 233–237.

Myers, D.A., and E.J. McKay, 1970, *Geologic Map of the Mount Washington Quadrangle, Bernalillo and Valencia Counties, New Mexico*, U.S. Geological Survey, Map GQ-886, scale 1:24,000.

Myers, D.A., and E.J. McKay, 1976, *Four Hills Manzano Base Area Map.*

Paleodata Inc., 1993, *Gulf of Mexico Chronostratigraphic Correlation Chart*, Schlumberger/Geco-Prakla, Houston, Texas.

Pazzaglia, F.J., L.A. Woodward, S.G. Lucas, O.J. Anderson, K.W. Wegmann, and J.W. Estep, 1999, "Phanerozoic Geologic Evolution of the Albuquerque Area," in *Albuquerque Geology, New Mexico Geological Society 50th Annual Field Conference Guidebook*, pp. 97–114.

Personius, S.F., M.N. Machette, and K. Kelson, 1999, "Quaternary Faults in the Albuquerque Area–An Update," in *Albuquerque Geology, New Mexico Geological Society 50th Annual Field Conference Guidebook*, pp. 189–200.

Reiche, P., 1949, "Geology of the Manzanita and North Manzano Mountains, New Mexico," *Geological Society of America Bulletin*, v. 60, pp. 1183–1212.

Reynolds, C.B., 2002, Personal communication regarding Excavation of Solar Tower Foundation.

Riddle, L., and P.R. Grant, 1981, *Geothermal Studies at Kirtland Air Force Base, Albuquerque, New Mexico*, SAND Report SAND81-0852, Sandia National Laboratories, Albuquerque, New Mexico.

Sigma Geoservices, Inc., 1984, "Seismic Reflection Survey on Kirtland Air Force Base, New Mexico," Sigma Geoservices, Inc., Englewood, Colorado.

Sandia National Laboratories/New Mexico (SNL/NM), 1996, *Site-Wide Hydrogeologic Characterization Project, Annual Report*, Calendar Year 1995, Annex: Conceptual Geologic Model of the Sandia National Laboratories and Kirtland Air Force Base, prepared by GRAM, Inc. and W. Lettis and Associates, Inc., Environmental Restoration Project, Sandia National Laboratories, Albuquerque, New Mexico.

Sandia National Laboratories/New Mexico (SNL/NM), 1999, "Summary Report of Groundwater Investigations at Technical Area V, Operable Units 1306 and 1307," Sandia National Laboratories, Albuquerque, New Mexico, March 1999.

SNL/NM, see Sandia National Laboratories/New Mexico.

USAF, see U.S. Air Force.

U.S. Air Force (USAF), 1989, *Aerial Photographs of Kirtland Air Force Base*, USAF-35 00 06-106 29 25, nos. 3-25-1 and 6-15-17, scale 1:4800, taken March 23, 1989.

U.S. Geological Survey (USGS), 1998, *Digital Data from the Isleta/Kirtland Aeromagnetic Survey Collected South of Albuquerque, New Mexico*, U.S. Geological Survey, Open-File Report 98-341.

USGS, see U.S. Geological Survey.

Van Hart, D., 2001, *Shallow Groundwater System Investigation: Tijeras Arroyo and Vicinity*, Environmental Restoration Project, Sandia National Laboratories, Albuquerque, New Mexico, June 2001

Van Hart, D., D.A. Hyndman, and S.S. Brandwein, 1999, *Analysis of the USGS Isleta/Kirtland Air Force Base Aeromagnetic Survey*, Groundwater Protection Program, Environmental Restoration Project, Sandia National Laboratories, Albuquerque, New Mexico, October 1999.

Wilcox, R.E., T.P. Harding, and D.R. Seely, 1973, "Basic Wrench Tectonics," *American Association of Petroleum Geologists Bulletin*, v. 57/1, pp. 74–96.

8. Glossary

Ancestral Rio Grande "A"	Lower part of stratigraphic sequence deposited by Ancestral Rio Grande fluvial system of the upper Santa Fe Group.
Apatite fission-track data	An analytical method of dating the thermal history of a crustal block. Continuous spontaneous decay of trace amounts of ^{238}U in the mineral apatite leaves fission tracks in the mineral. The tracks are annealed at a rate controlled by temperature. At high temperatures, the annealing rate exceeds the track production rate and no tracks are preserved. As the mineral cools during uplift and passes through a temperature range of 75-125 degrees Celsius (°C) the partially annealed tracks are preserved. Finally, at lower temperatures the fission tracks produced are fully preserved and annealing is minor. Therefore the partially annealed and fully retained tracks are used to calculate the time the mineral passed (i.e., was uplifted) through the approximate 100°C isotherm.
Caliche	Calcareous material formed near the surface during soil-forming processes in sandy or gravelly sediments of the arid Southwest. A more accepted term is *calcic soil*.
Corestone	An ellipsoidal or rectangular block of granite formed by subsurface weathering.
Footwall (fault) block	The fault block on the underside of a normal fault.
Formline	Line on a map drawn from an aerial photograph, depicting the surface configuration of a bed boundary in a sedimentary sequence.
Granite	An igneous rock composed mainly of visible grains of quartz and feldspar.
Grus	The fragmented products of in-situ granular disintegration of granite.
Half graben	A downdropped fault block bounded on one side by a listric fault.
Hanging-wall block	The fault block on the upside of a normal fault.
Hubbell bench	An extensive area underlain by shallow bedrock generally located between the Manzanita and Manzano Mountains to the east and the Albuquerque basin to the west.
Igneous rocks	Rocks formed by solidification of molten or partly molten material.

Laramide	A period of major compressive deformation affecting New Mexico during the early Tertiary (Paleocene and Eocene).
Left-lateral fault	A strike-slip fault on which the side opposite the observer has been displaced to the left.
Lithofacies	A lateral, mappable subdivision of a stratigraphic unit distinguishable from adjacent subdivisions on the basis of lithology.
Listric fault	A curved, downward-flattening, generally concave upwards normal fault.
Lithology	The physical characteristics of a rock, i.e., color, mineralogy, and texture.
Manzanita Mountains	A relatively low-lying segment of the uplifted eastern shoulder of the Albuquerque basin, located between the Sandia Mountains to the north and the Manzano Mountains to the south.
Manzano Base	A secured area encompassing the uplift of Precambrian rocks known as Four Hills.
Manzano Base West	The eastern portion of the Albuquerque basin on the western piedmont of Manzano Base.
Metamorphic rocks	Rocks derived from pre-existing rocks by recrystallization or deformation in response to significant changes in temperature, pressure, and/or shearing stress.
Normal fault	A fault on which the hanging wall is displaced downward relative to the footwall.
Paleosol	A buried soil horizon.
Palynology	Study of pollen from seed plants and spores from other plants with embryos, and the age-dating of these materials.
Pediment	A broad, gently-sloping rock-floored surface developed in an arid or semiarid region at the foot of an abrupt and receding mountain front.
Pedogenic	Pertaining to soil formation.

Pedogenic carbonate morphology	Refers to sequence of development of secondary calcium carbonate emplaced during soil forming processes. Sequence is divided into six stages of increasing carbonate content and structural development through time, i.e., Stages I through VI.
Pleistocene	A geologic-age term that refers to an epoch of time within the Quaternary Period, beginning somewhere from 1.8 to 1.65 Ma (the exact beginning is currently the subject of debate) and ending 10,000 years ago. It also refers to the sediments deposited during this time.
Plio-Pleistocene	A combination geologic-age term referring to the Pliocene Epoch of the Tertiary Period and the Pleistocene Epoch of the Quaternary Period.
Pluton	An igneous intrusion, usually of great size.
Pop-up structure	A structural uplift associated with a major strike-slip fault zone and caused by localized compression.
Pull-apart basin	A basin associated with a major strike-slip fault zone and caused by localized extension.
Pumice	A light-colored, highly porous, glassy igneous rock produced by violent volcanic eruption that typically floats on water.
Quartzite	A metamorphic rock consisting of quartz and formed by recrystallization and fusing of grains.
Reflection seismic survey	A seismic survey based upon the measurement of the travel times of compression waves produced by an artificial source (explosives, vibration, impact), propagated downward, and reflected back from subsurface boundaries having elastic-wave velocity contrasts. The reflected waves are recorded by instruments at the surface and processed by a computer.
Releasing bend	A bend in a strike-slip fault that results in crustal extension in the vicinity of the bend.
Refraction seismic survey	A seismic survey based upon the measurement of the travel times of compression waves produced by an artificial source (explosives, impact), propagated downward that travel parallel to a high-velocity layer while emitting compression waves upwards. The emitted waves are recorded by instruments at the surface and processed by a computer.

Reverse fault	A fault on which the hanging wall is displaced upward relative to the footwall.
Right-lateral fault	A strike-slip fault on which the side opposite the observer has been displaced to the right.
Rio Grande rift	A linear trough bounded by normal faults.
Seismic survey	A method of geophysical prospecting in which elastic waves are artificially produced in the Earth.
Split-spoon (sampler)	A borehole coring device, consisting of two half-cylinders, that is percussion-driven ahead of a drill bit and from which a core sample is retrieved by separating the two halves.
Strike-slip fault	A fault along which the relative movement is horizontal and parallel to the fault's trace on the surface.
Syntectonic	A geologic event occurring during tectonic activity.
Thrust fault	A type of reverse fault with a dip 45° or less on which the hanging wall is displaced upward relative to the footwall.
Transpression	A stage of crustal deformation intermediate to compression and strike-slip faulting.
Travertine	Dense, finely-crystalline or concretionary limestone formed by rapid chemical precipitation of $CaCO_3$ from solution in the surface-water and groundwater via agitation of stream water or by evaporation around the mouth or in the conduit of a spring, especially a hot spring.
Upper Ancestral Rio Grande	Upper part of stratigraphic sequence deposited by the Ancestral Rio Grande fluvial system of the upper Santa Fe Group.
Wrench fault	A type of strike-slip fault which is vertical or subvertical.
Wrench-fault basin	A structural depression associated with a major strike-slip fault zone.

FIGURES

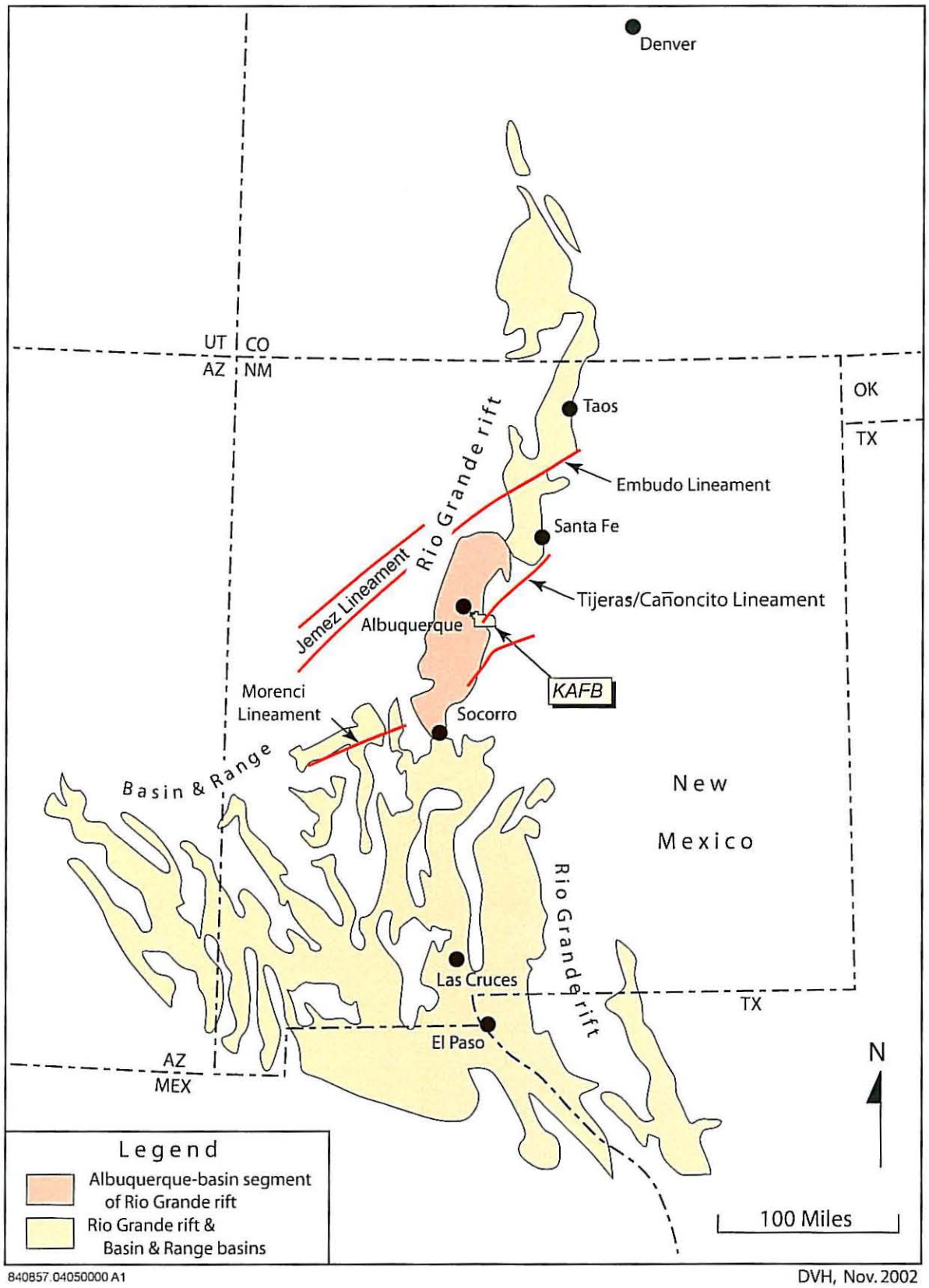

Figure 1-1 Location of Rio Grande Rift, Albuquerque Basin, and Select Precambrian Lineaments (in Red)
(Modified from Karlstrom et al., 1999b, and Pazzaglia et al., 1999)

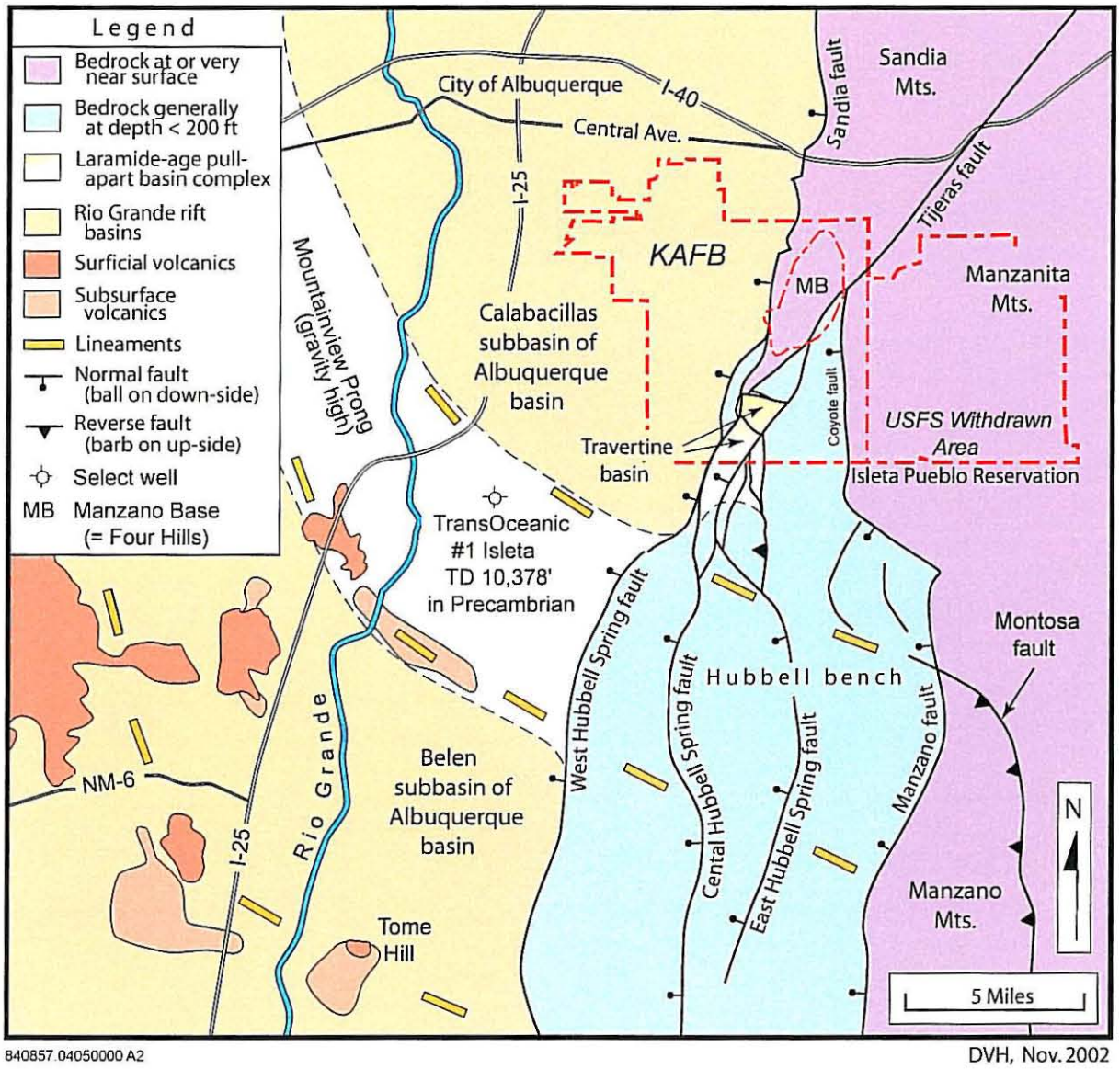

Figure 1-2 Structural Provinces of Kirtland Air Force Base (KAFB) and Vicinity

(Modified in part from Grauch et al., 1999, and Maldonado et al., 1999)

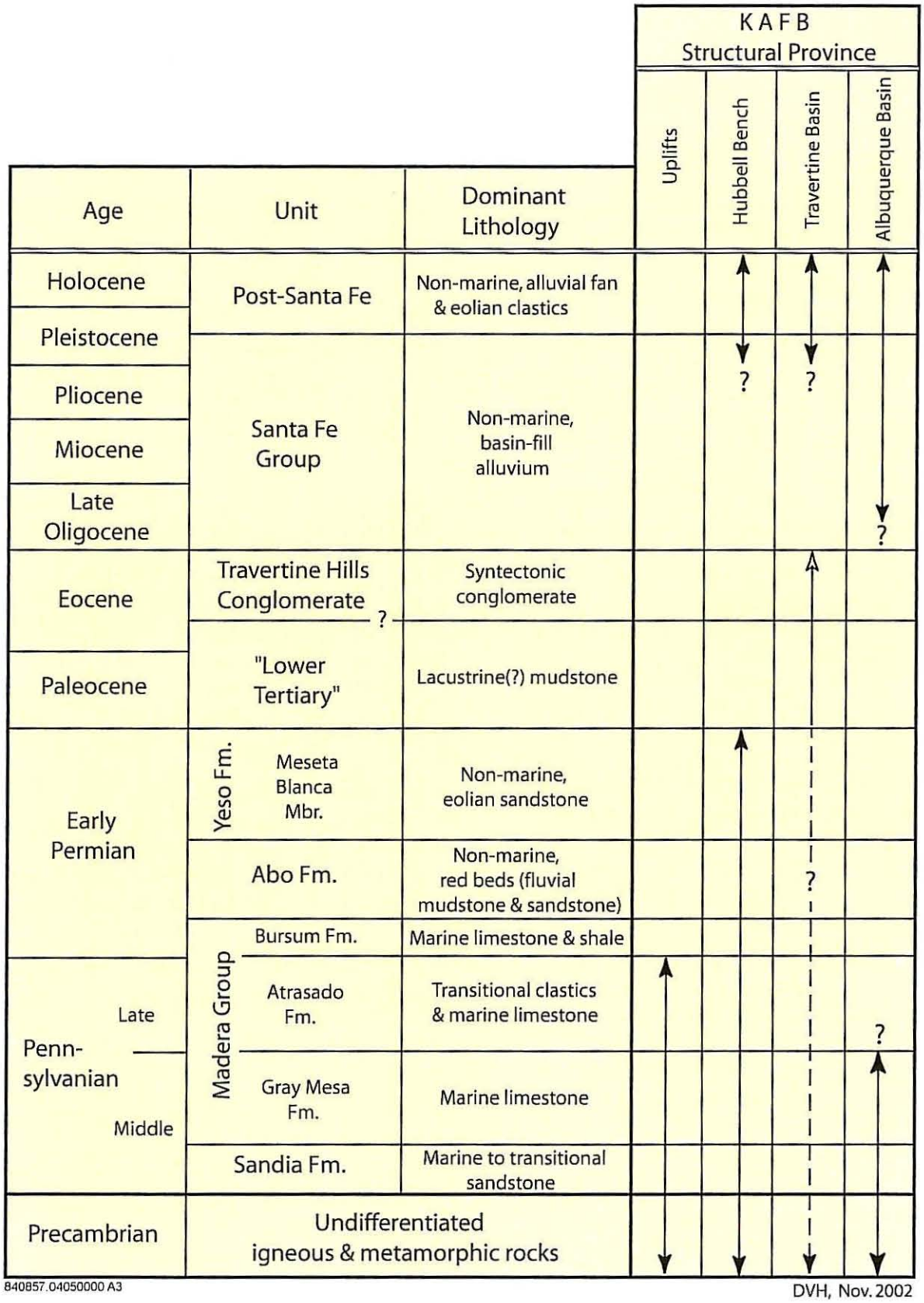

Figure 1-3 Stratigraphic Section on Kirtland Air Force Base (KAFB)

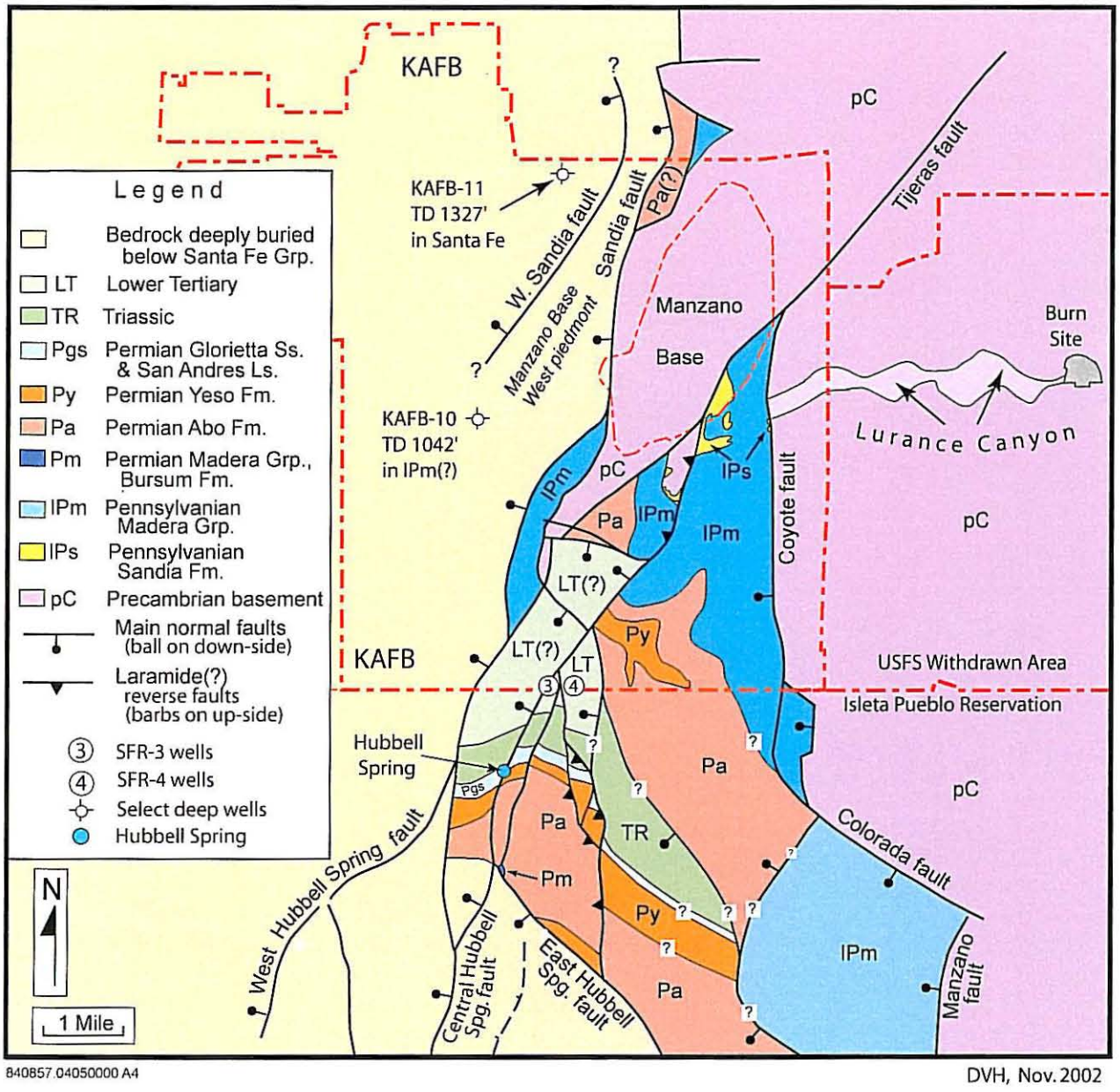

840857.04050000 A4

DVH, Nov. 2002

Figure 1-4 Fault Systems and Interpreted Bedrock Geology of Kirtland Air Force Base (KAFB) and Vicinity
(Modified from Love et al., 1996, and Van Hart et al., 1999)

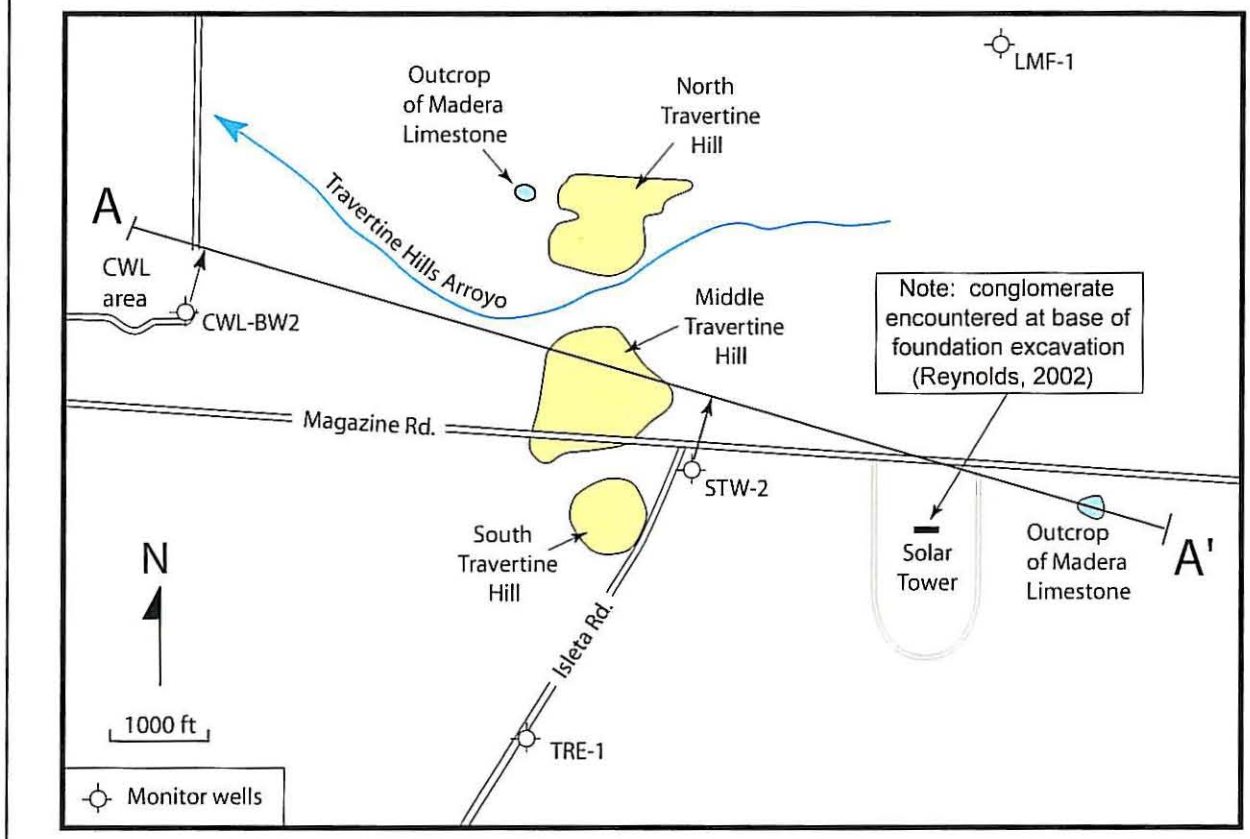

A. Location Map of Cross Section A-A'

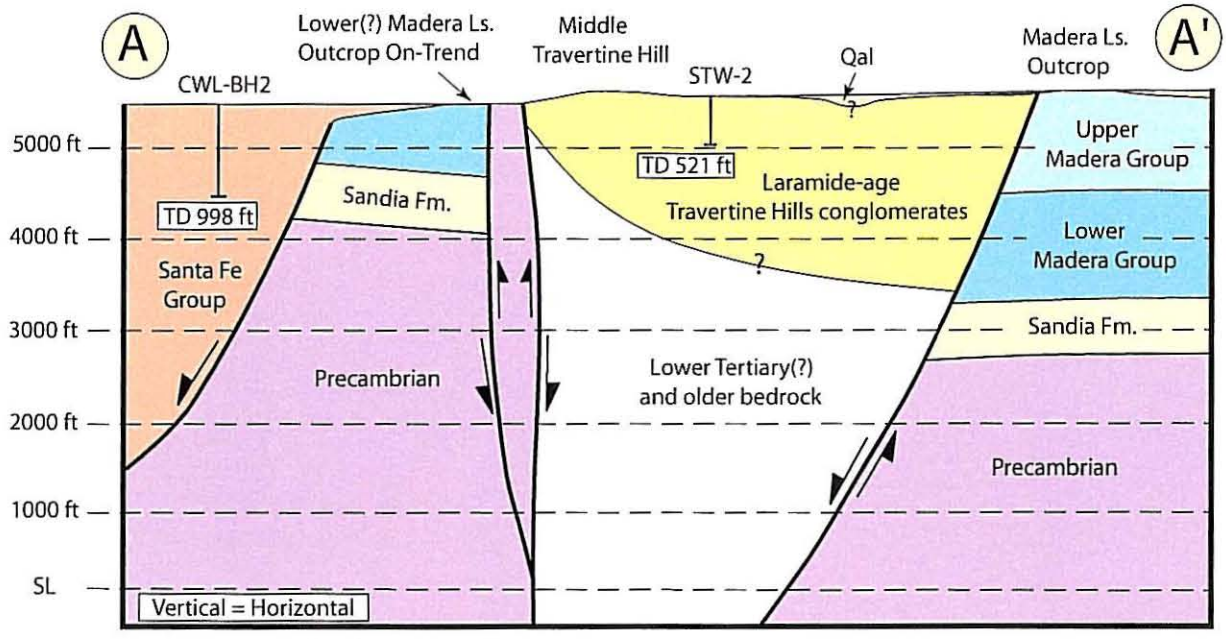

B. Cross section A-A' Across Travertine Basin

840857.04050000 A5

DVH, Nov. 2002

Figure 3-1 Travertine Basin

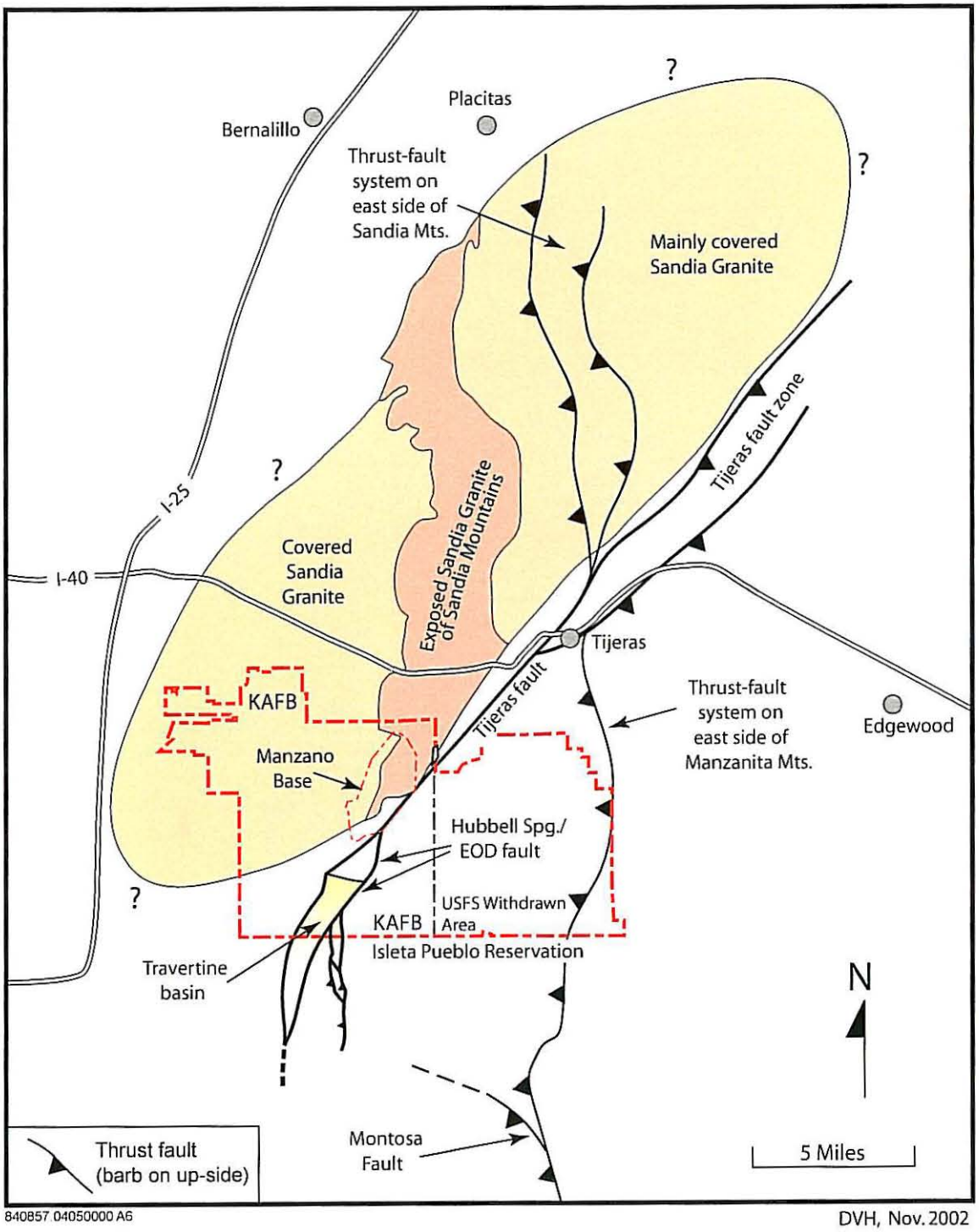

Figure 3-2 Laramide Structures and Location of Precambrian Sandia Granite Pluton
(Modified from Karlstrom et al., 1999b)

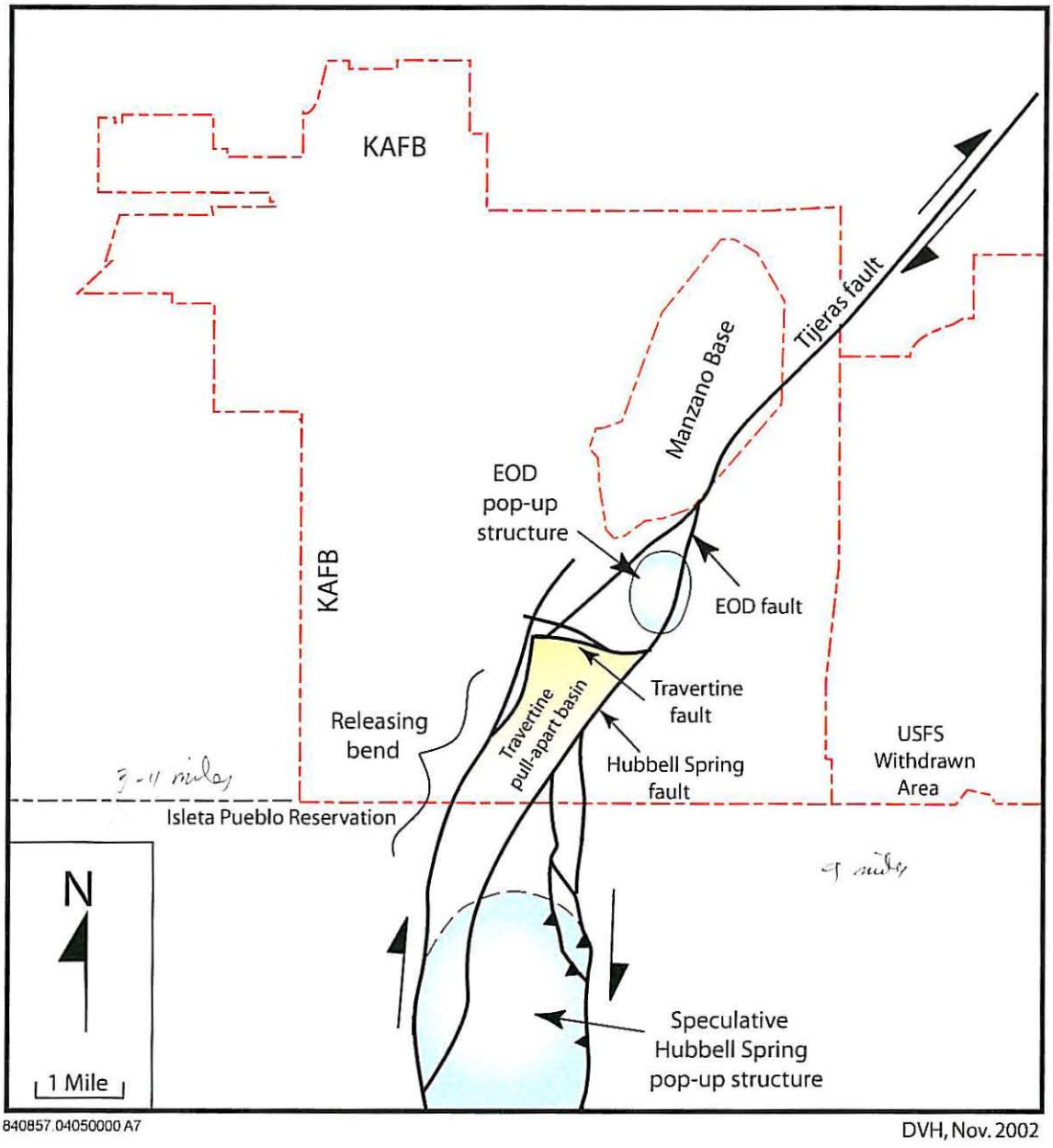

Figure 3-3 Laramide-Age Tijeras Wrench-Fault System

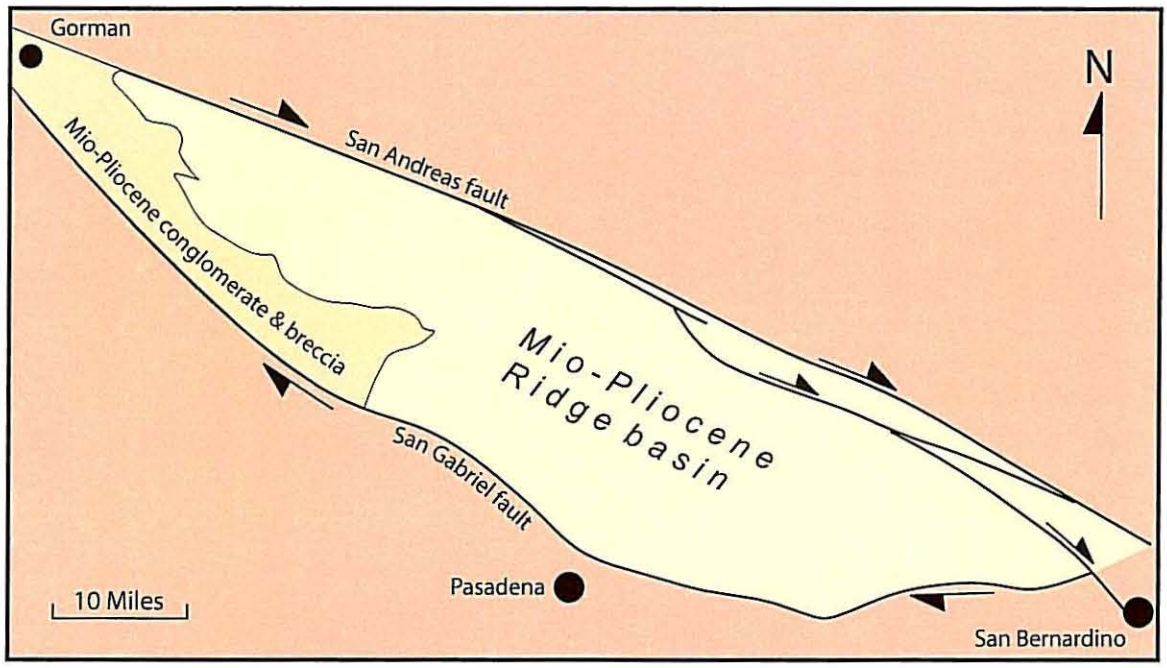

A. Ridge Basin, Southern California
(Modified from Wilcox et al., 1973)

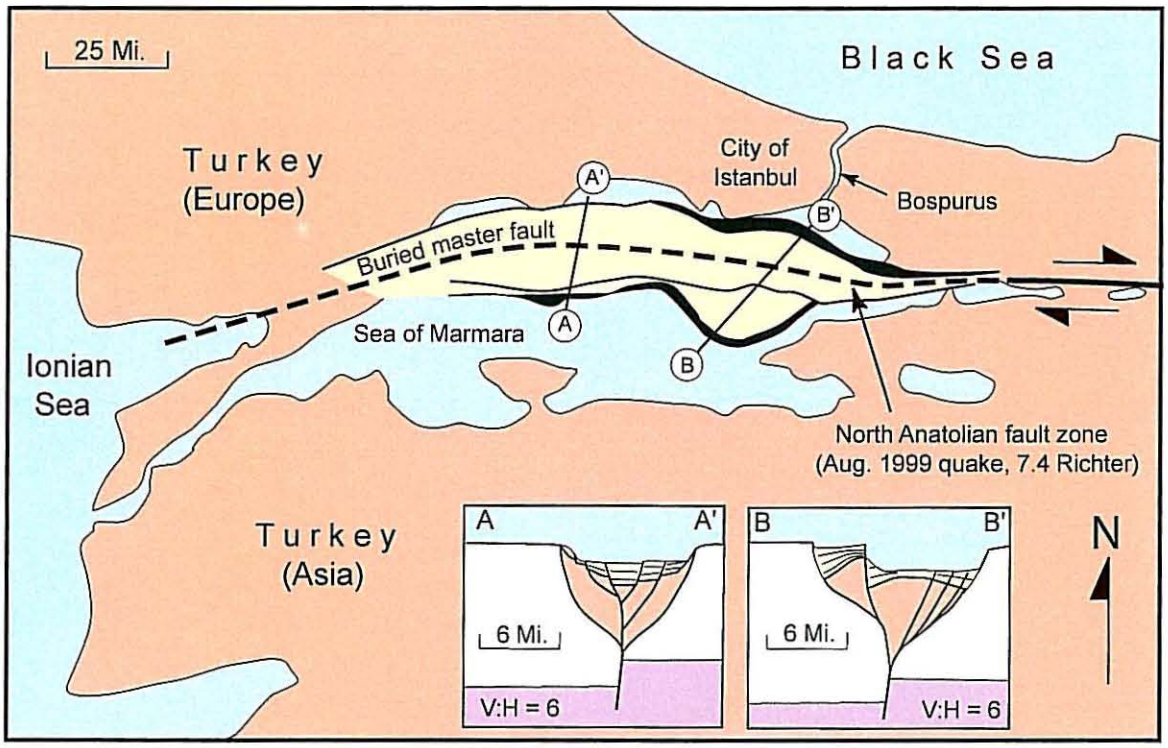

B. Sea of Marmara (Turkey) Wrench-Fault Basin Along North Anatolian Fault
(Modified from Aksu et al., 2000)

840857.04050000 AB

DVH, Nov. 2002

Figure 3-4 Examples of Basins Along Wrench Faults

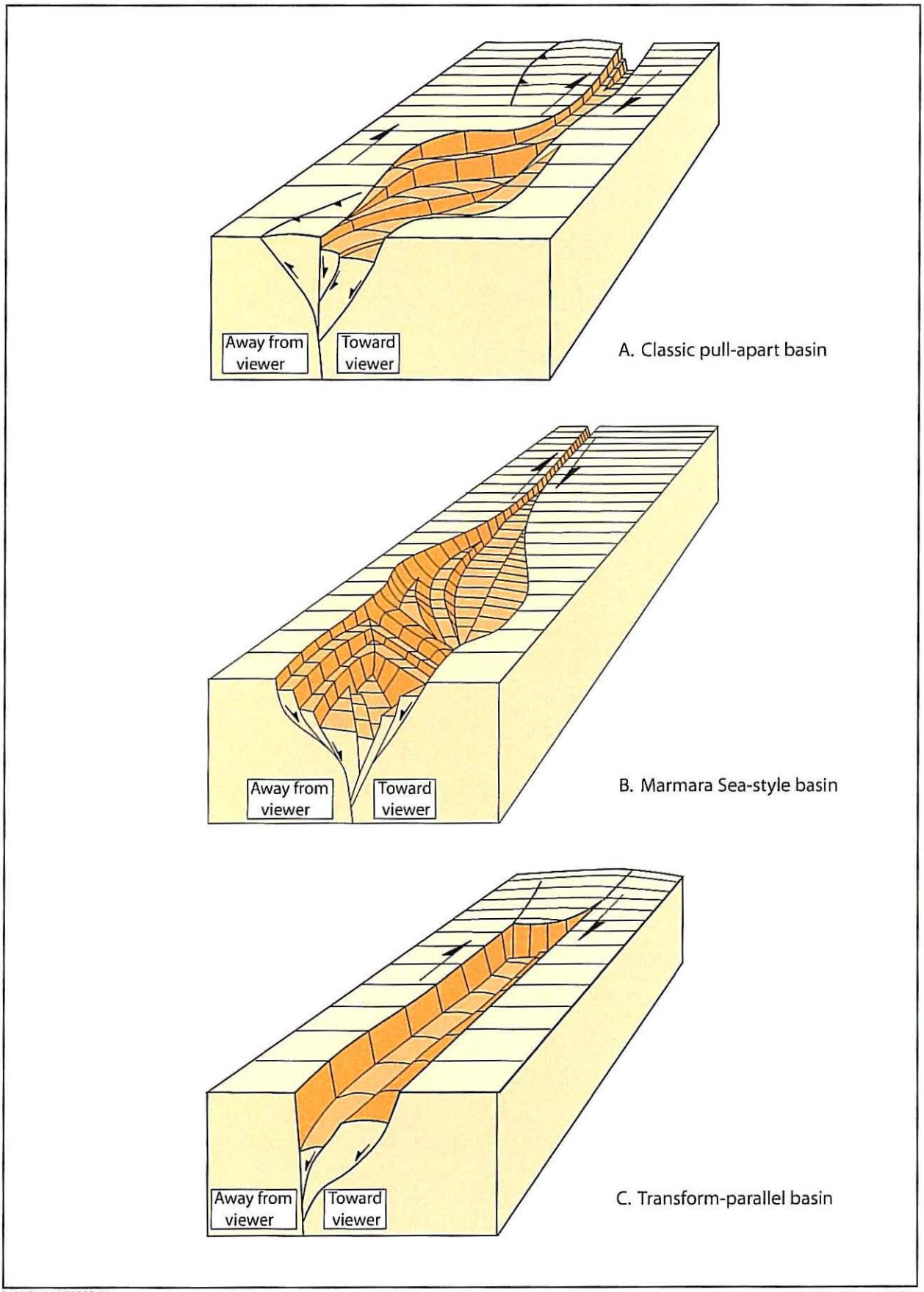

840857.04050000.A9

DVH, Nov. 2002

Figure 3-5 Geometric Variations of Basins in Right-Lateral Wrench-Fault Systems
(Modified from Aksu et al., 2000)

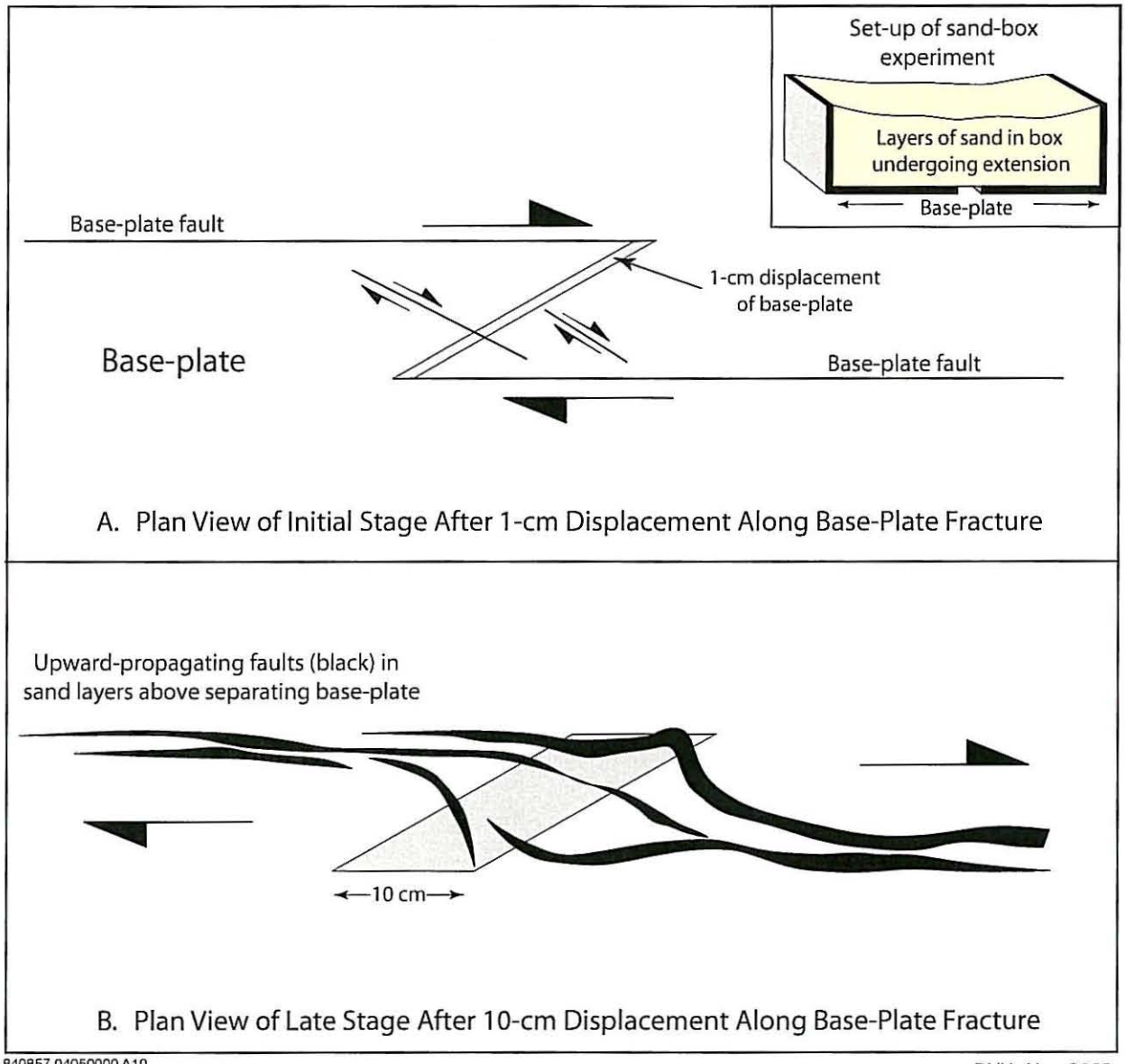

840857.04050000 A10

DVH, Nov. 2002

Figure 3-6 Development of Pull-Apart Basin in Sand Box Experiment
(Modified from Dooley and McClay, 1997)

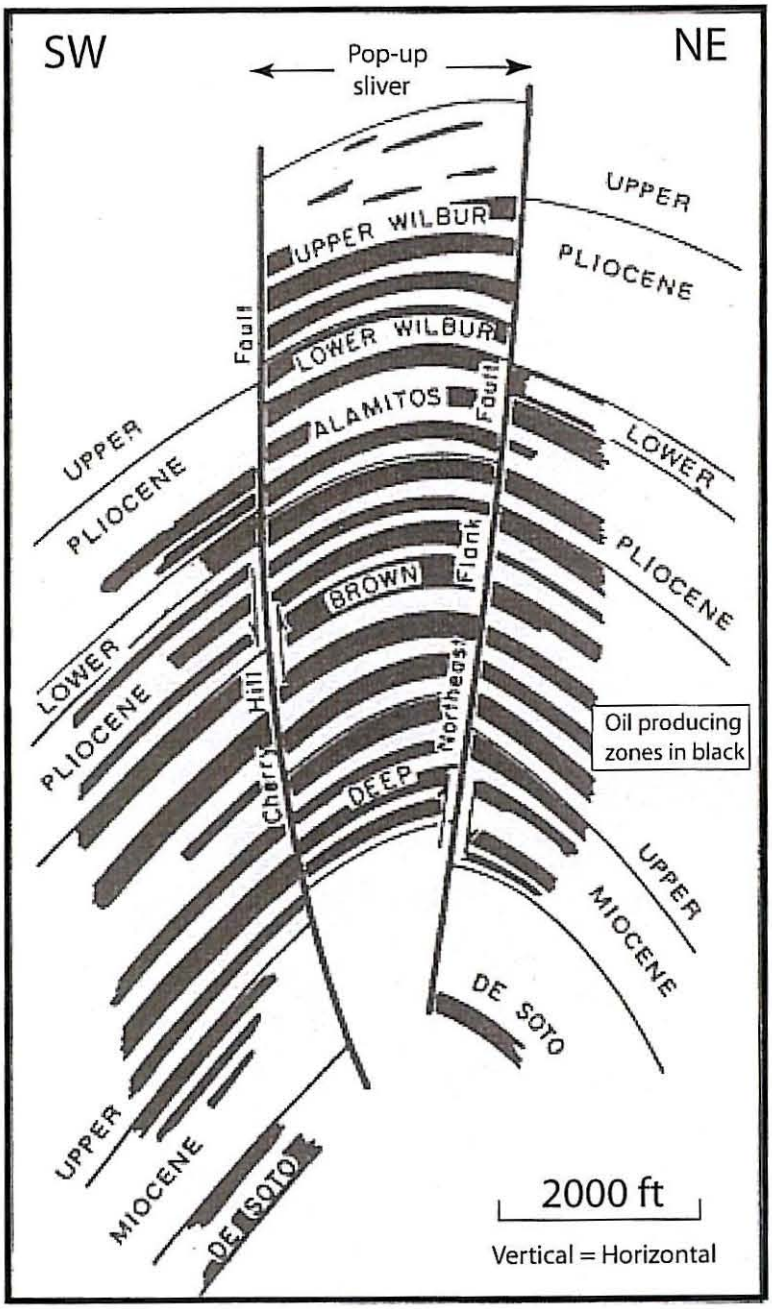

Figure 3-7 Example of Pop-Up Sliver in Wrench-Fault System, Cross Section of Long Beach Oil Field, California
(Modified from Harding, 1973)

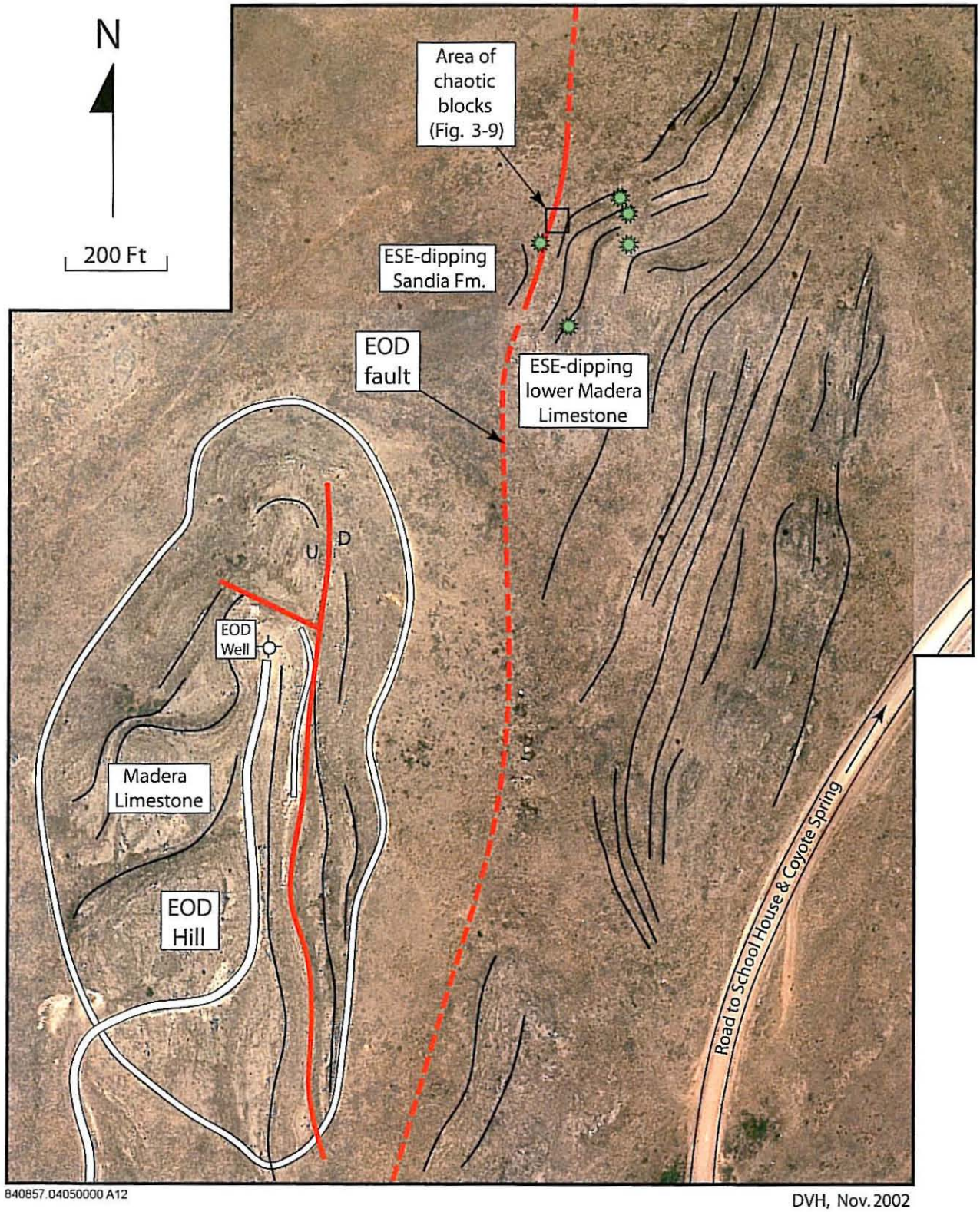

Figure 3-8 Eastern Portion of EOD Hills and EOD Fault
(Shown are reference juniper trees in green and select formlines;
air photo by USAF, 1989, scale 1:4800)

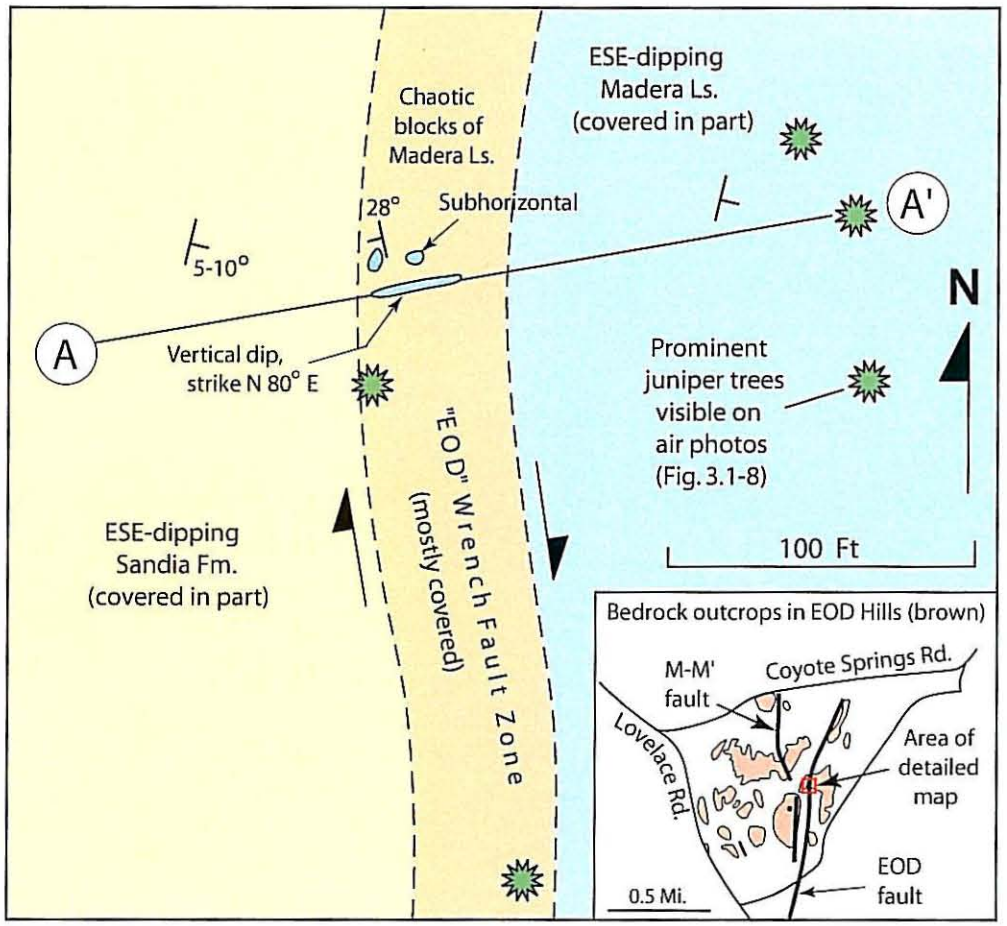

A. Sketch Map

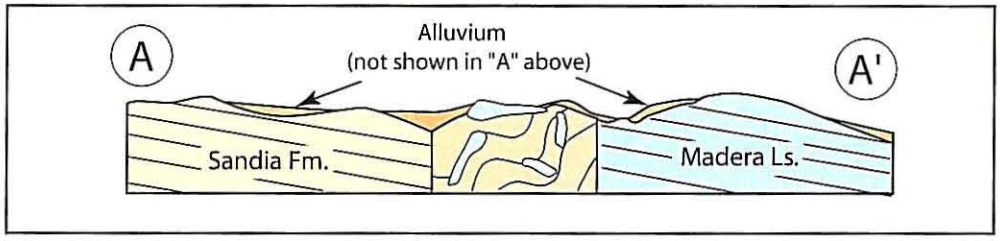

B. Schematic Cross Section

840857.04050000 A13

DVH, Nov. 2002

Figure 3-9 EOD Fault Zone on East Side of EOD Hills

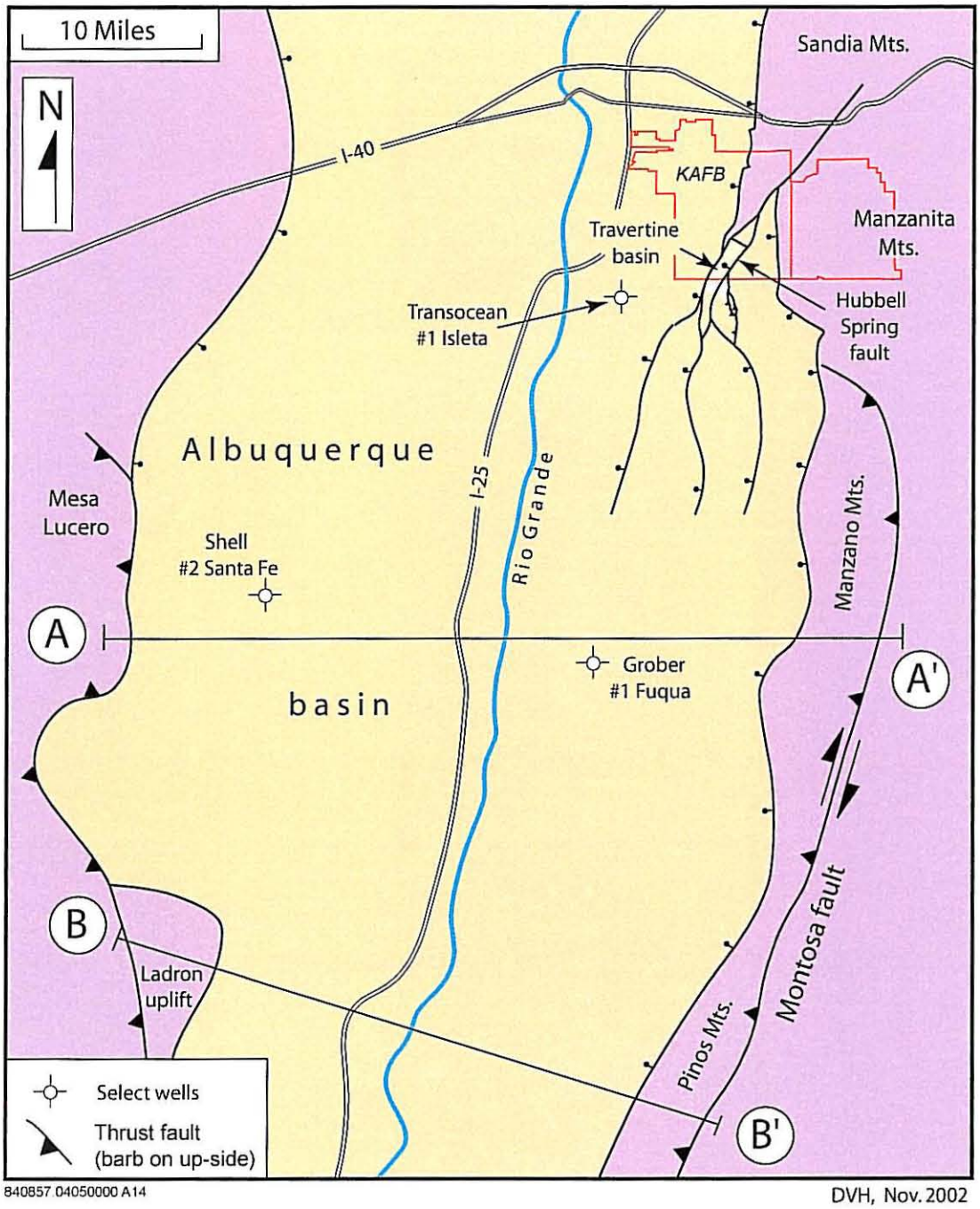

Figure 3-10 Simplified Map of Southern Albuquerque Basin Showing Uplifts (purple), Montosa Fault, and Cross Sections Depicted in Figure 3-11

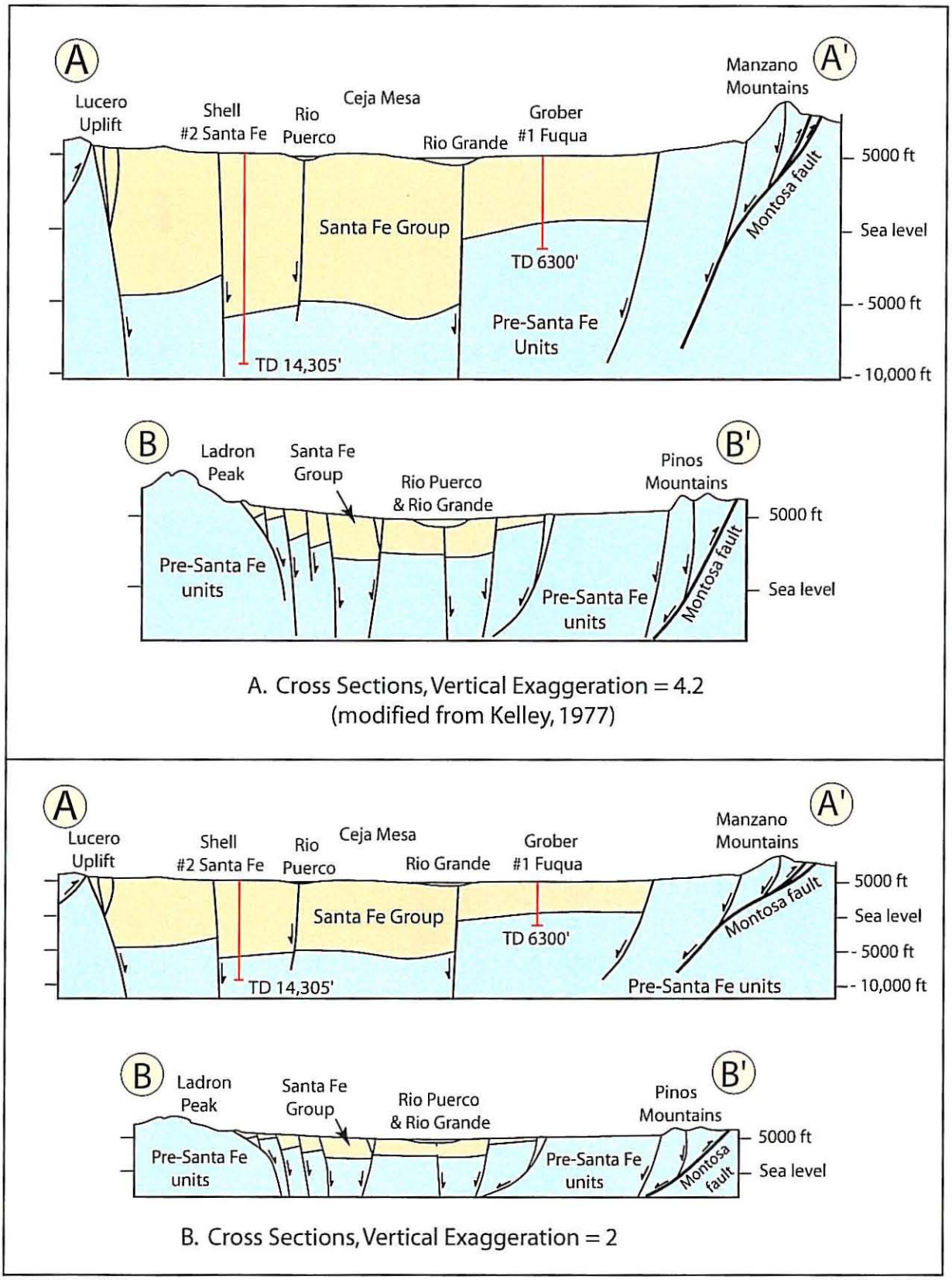

840857.04050000 A15

DVH, Nov. 2002

Figure 3-11 Cross Sections Across Southern Albuquerque Basin
(Showing reactivated Laramide-age Montosa thrust fault;
see Figure 3-10 for location)

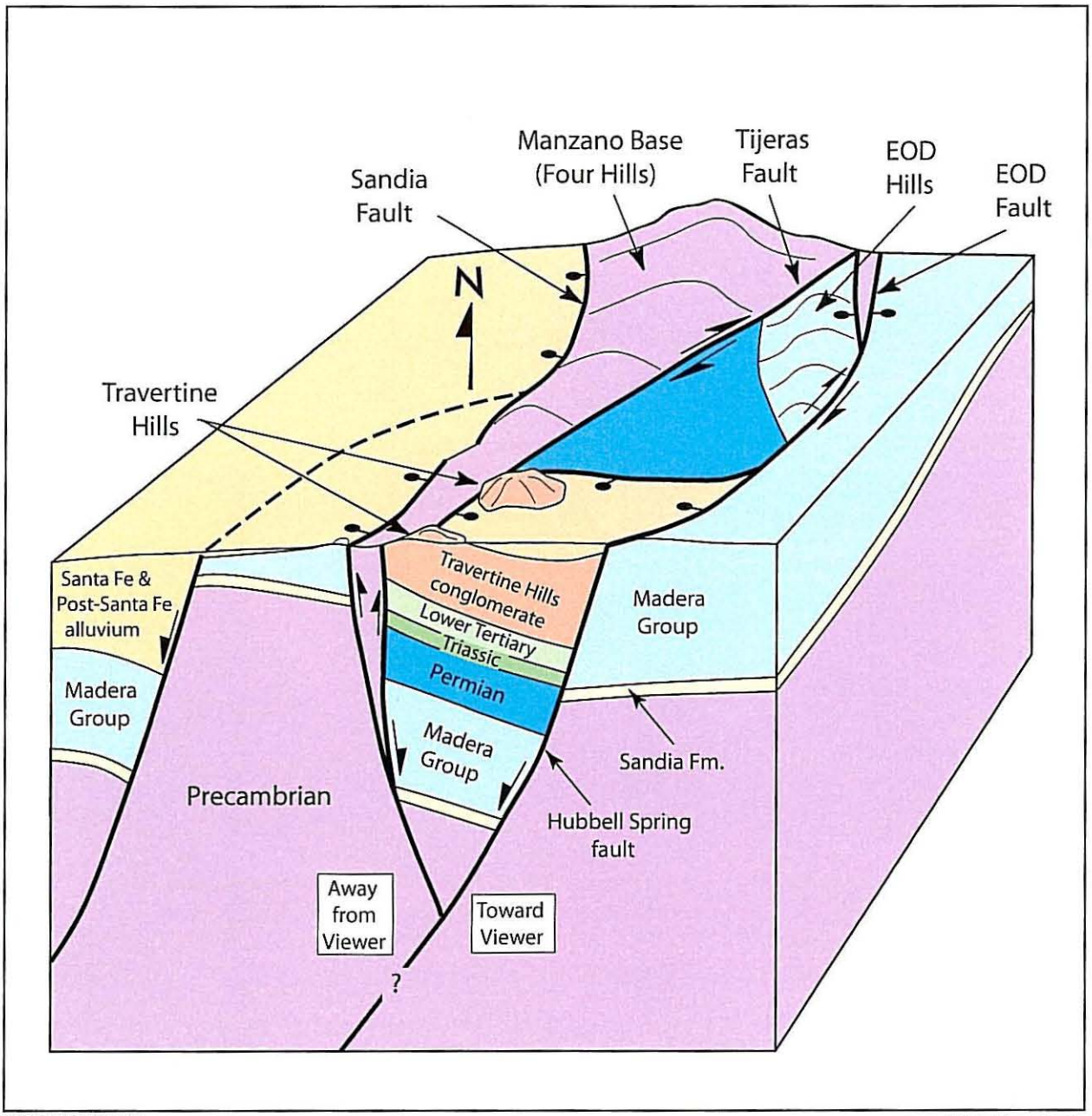

840857.04050000 A16

DVH, Nov. 2002

Figure 3-12 Schematic Block Diagram of Travertine Hills/EOD Hills Area
(Arrows show early Tertiary, Laramide-age relative movement)

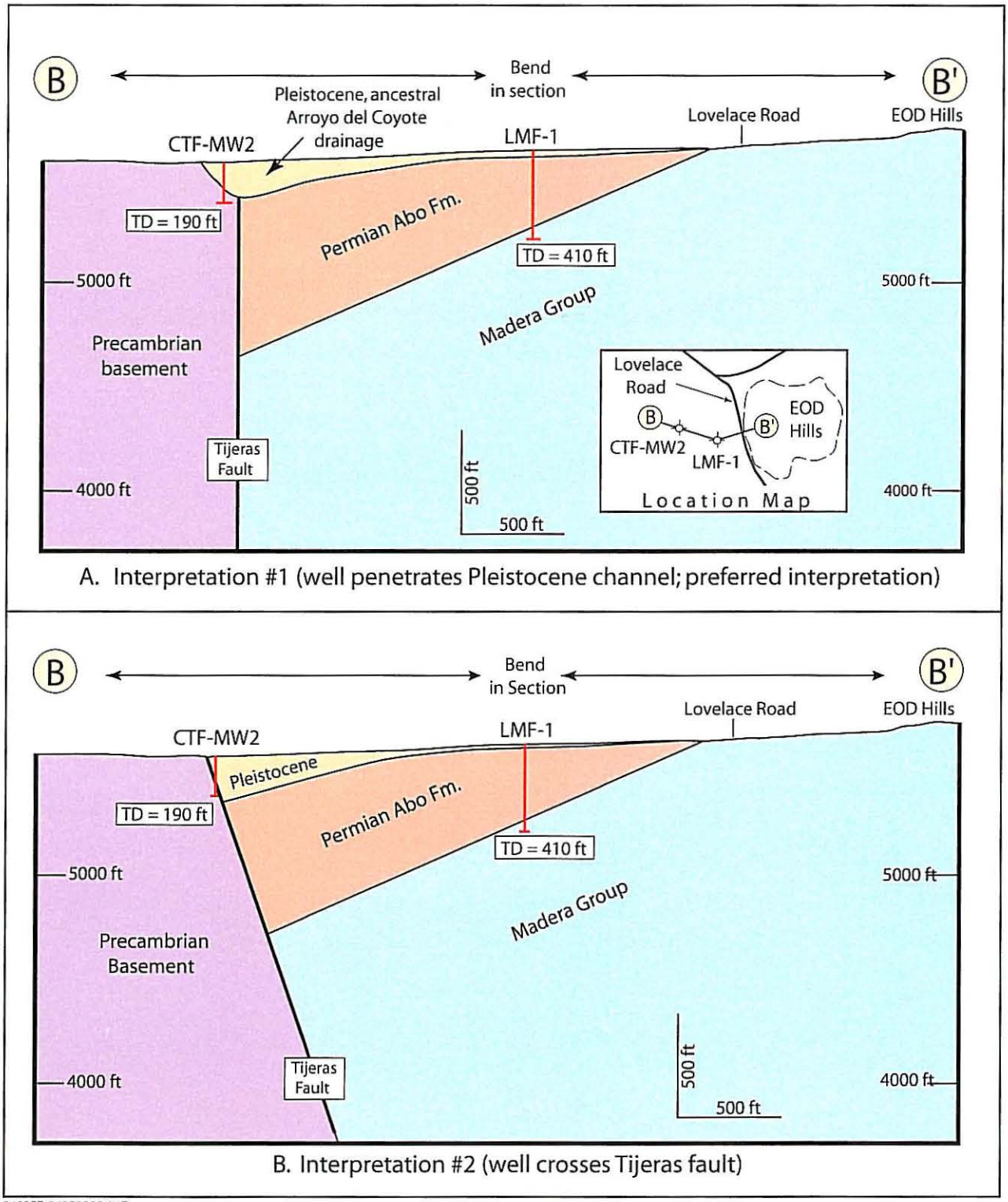

Figure 3-13 Cross Section B-B' Showing Alternative Interpretations of Well CTF-MW2

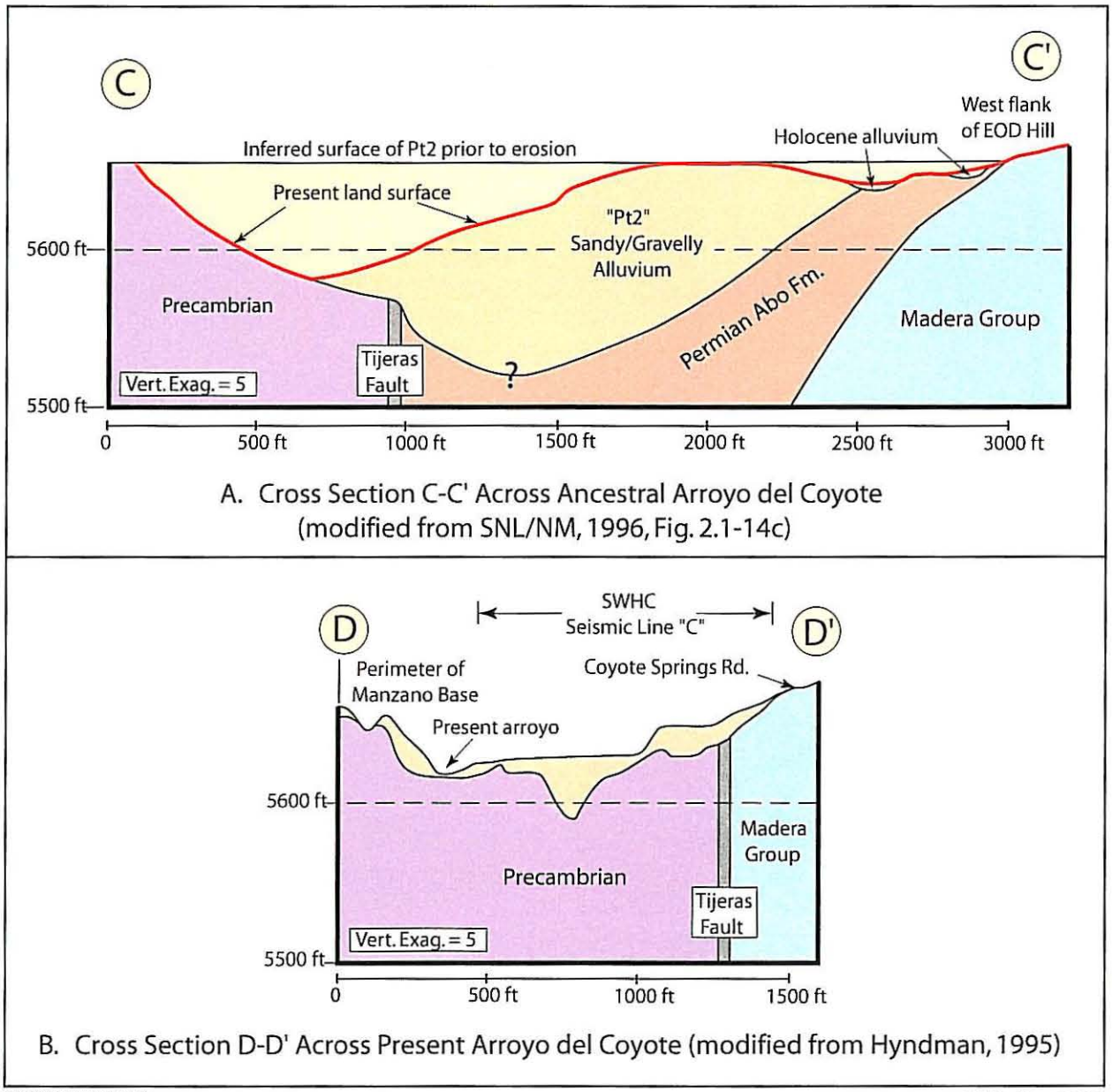

840857.04050000.A18

DVH, Nov. 2002

Figure 3-14 Cross Sections Across Ancestral and Present Arroyo del Coyote
(Locations on Plate III)

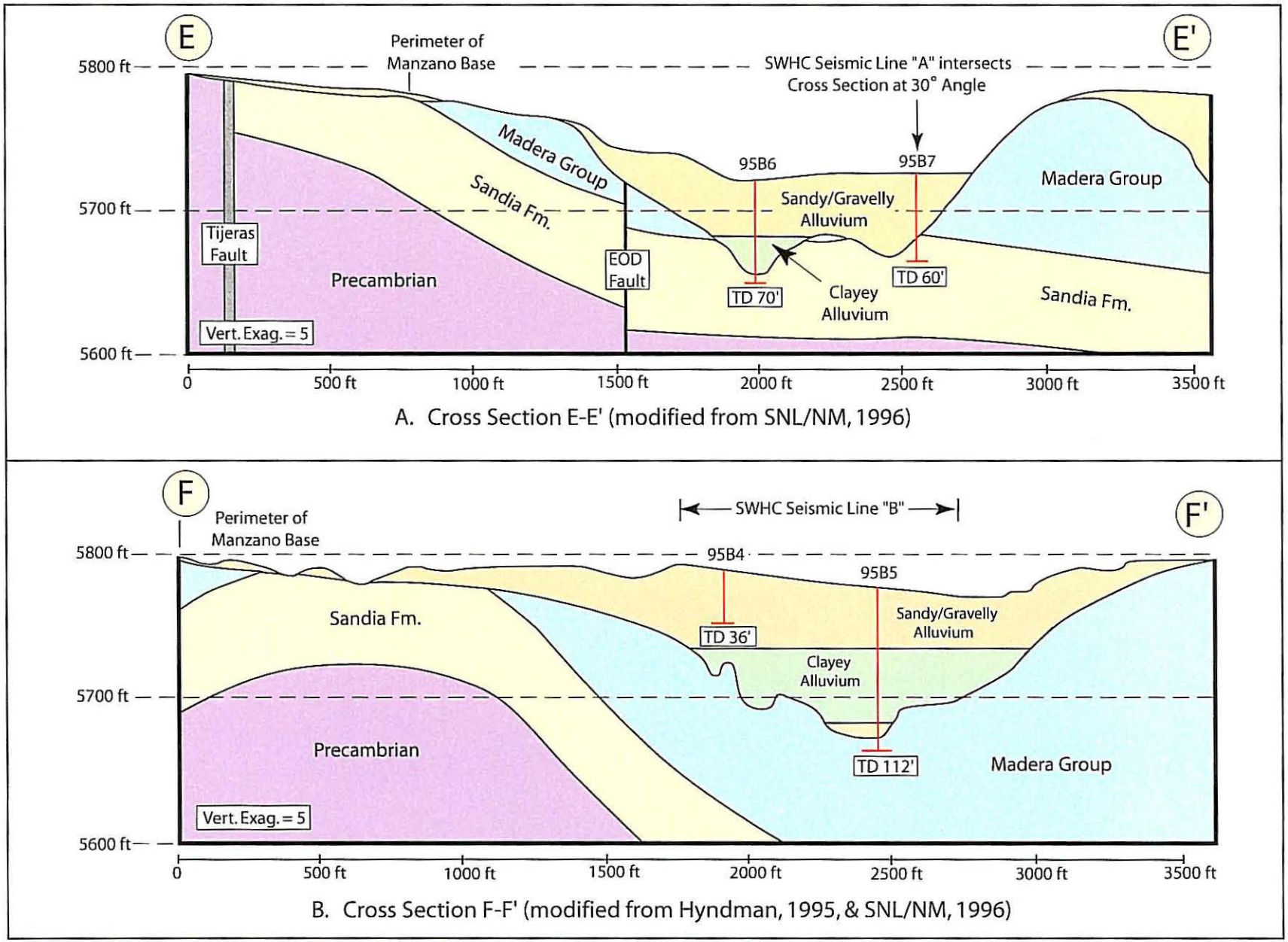

840857.04050000.A19

DVH, Nov. 2002

Figure 3-15 Cross Sections Across Arroyo del Coyote
(Locations on Plate III)

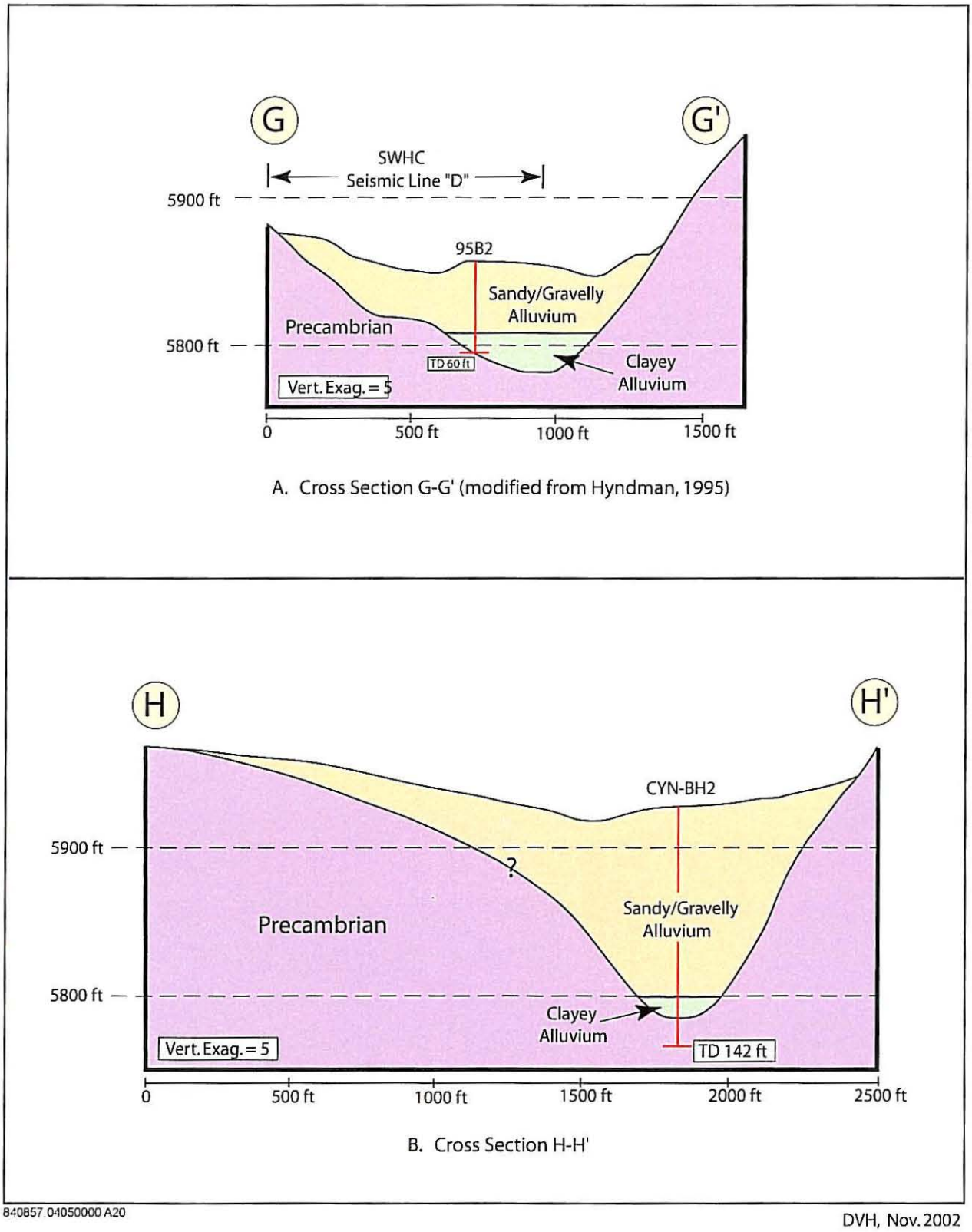

Figure 3-16 Cross Sections Across Arroyo del Coyote
(Locations on Plate III)

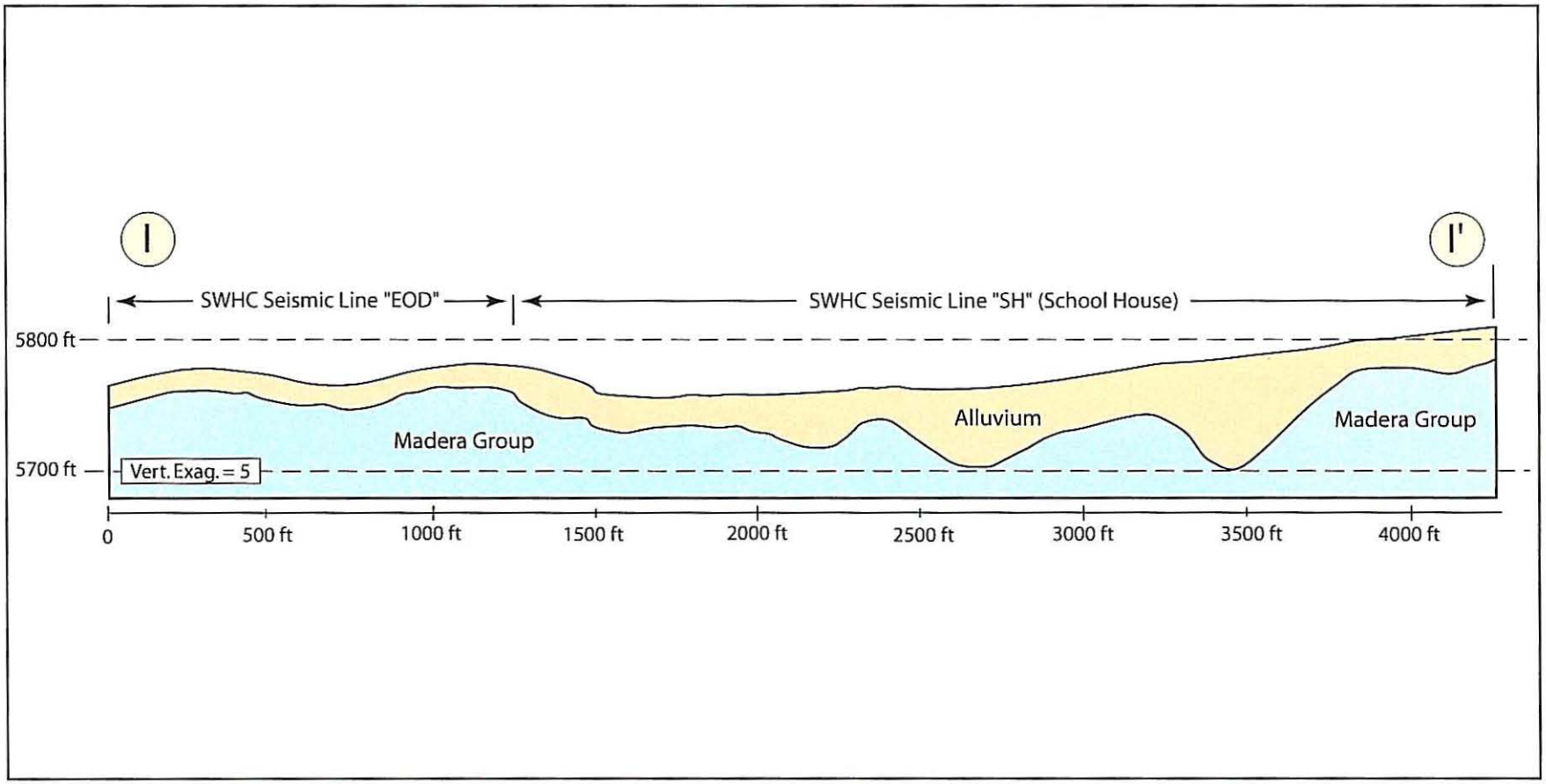

840857.04050000 A21

DVH, Nov. 2002

Figure 3-17 Cross Section I-I' Across Ancestral Arroyo del Coyote
(Modified from Hyndman, 1995; location on Plate III)

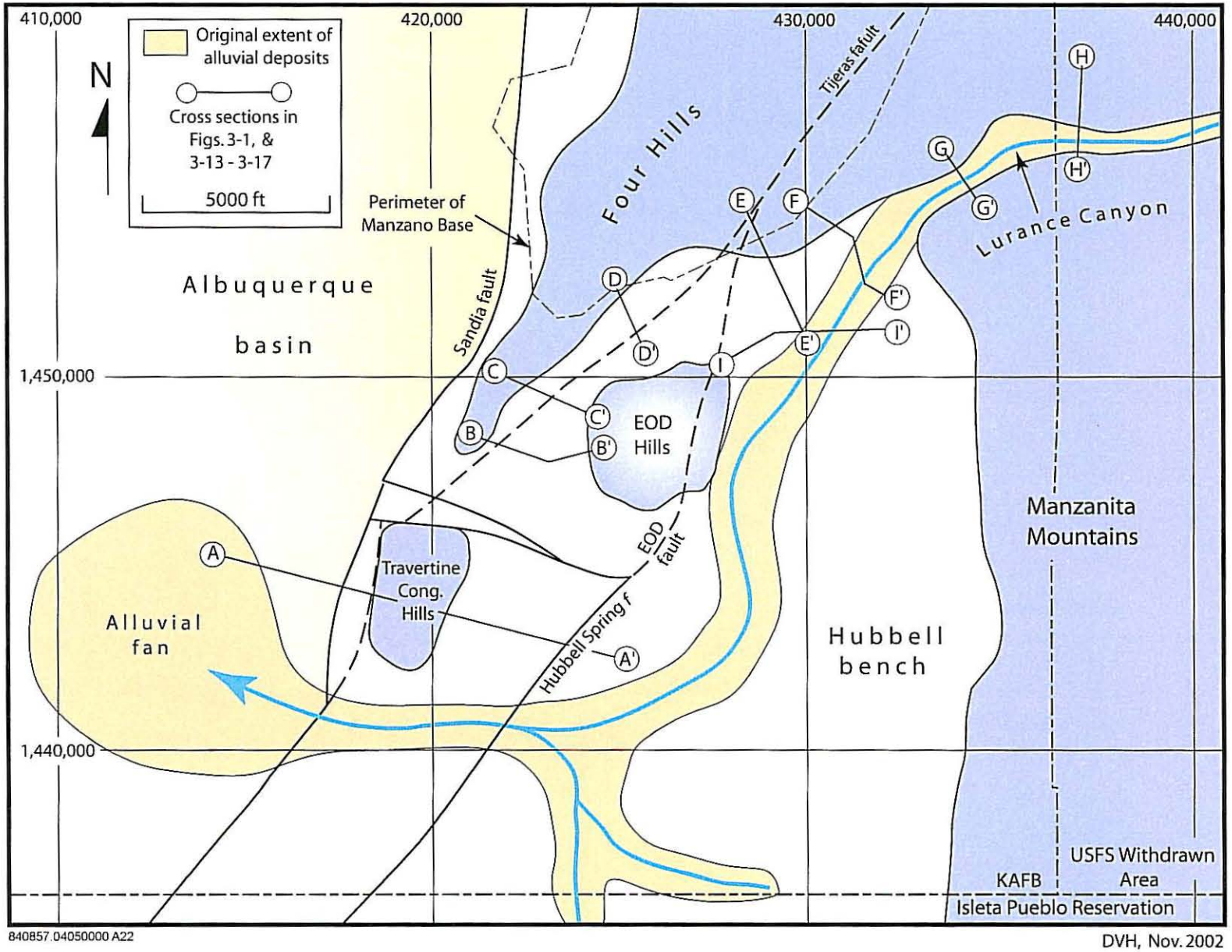

Figure 3-18 Paleodrainage I: Late Pliocene(?) to Early(?) Pleistocene
(Modified from SNL/NM, 1996)

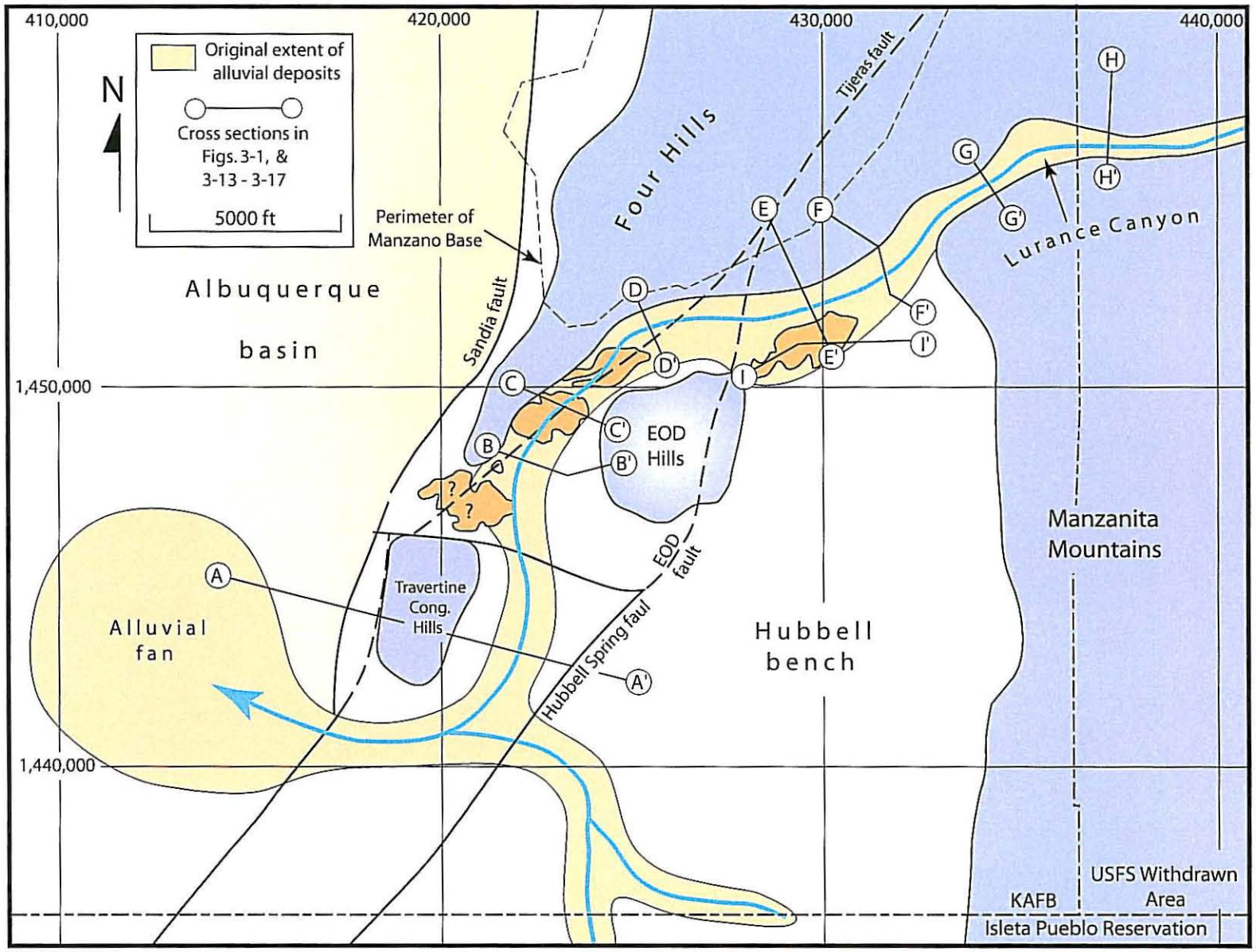

Figure 3-19 Paleodrainage II: Middle Pleistocene
(Modified from SNL/NM, 1996)

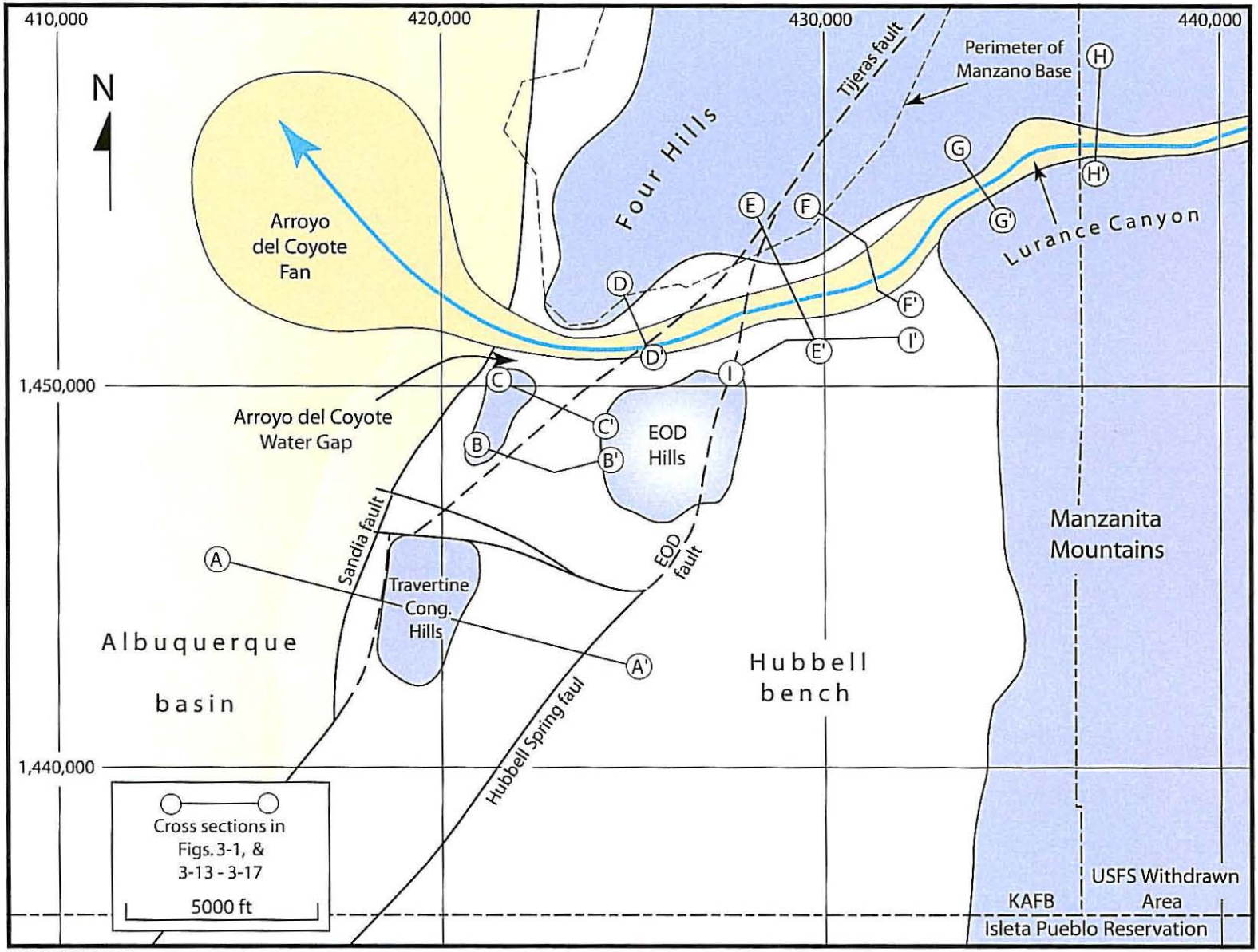

Figure 3-20 Paleodrainage III: Middle to Late Pleistocene
(Modified from SNL/NM, 1996)

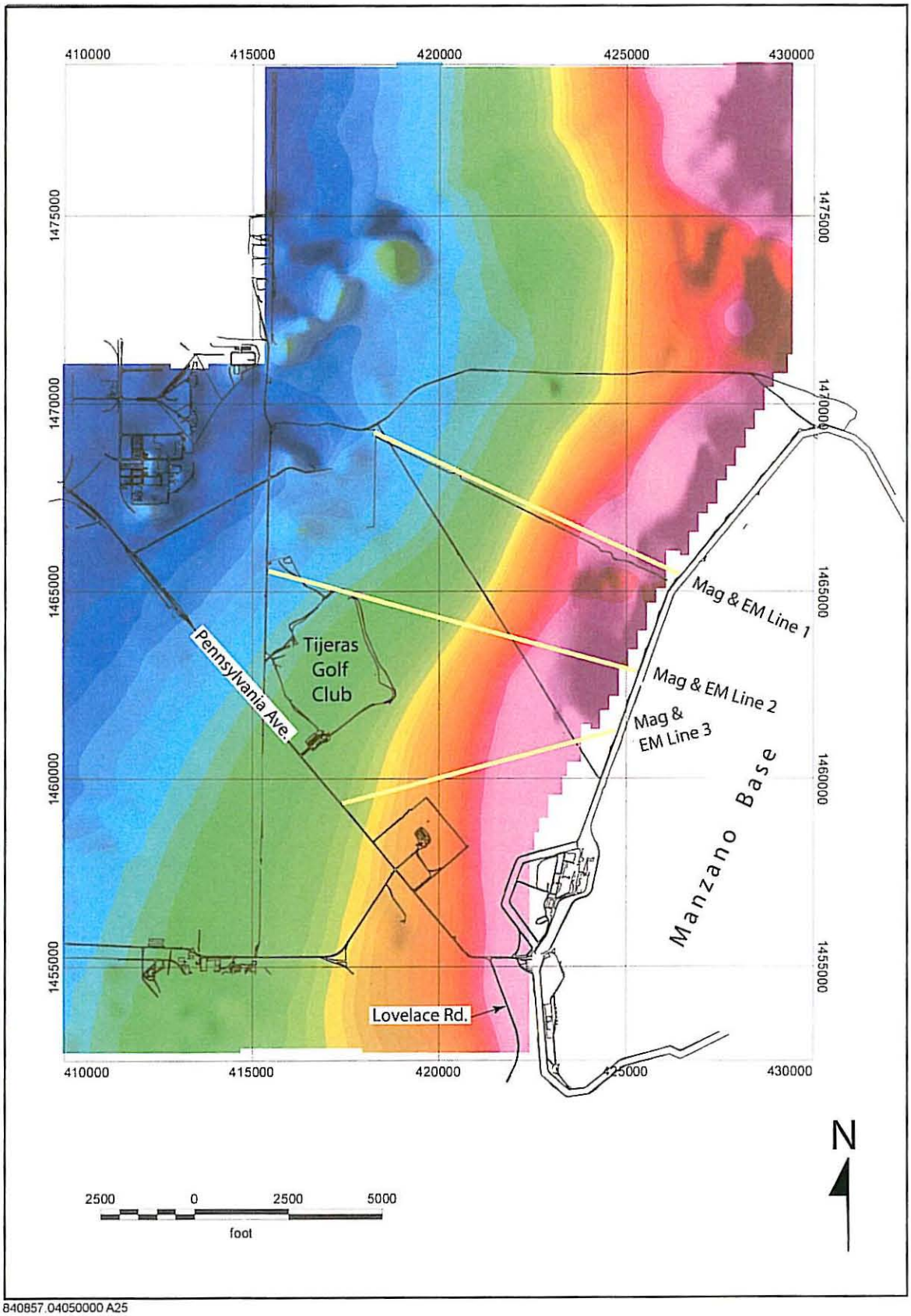

840857.04050000 A25

Figure 4-1 Total Magnetic Field (USGS 1997) and Location of 2001 Ground-Based Magnetometer (Mag) Lines
(Modified from Hyndman & Brandwein, 2002)

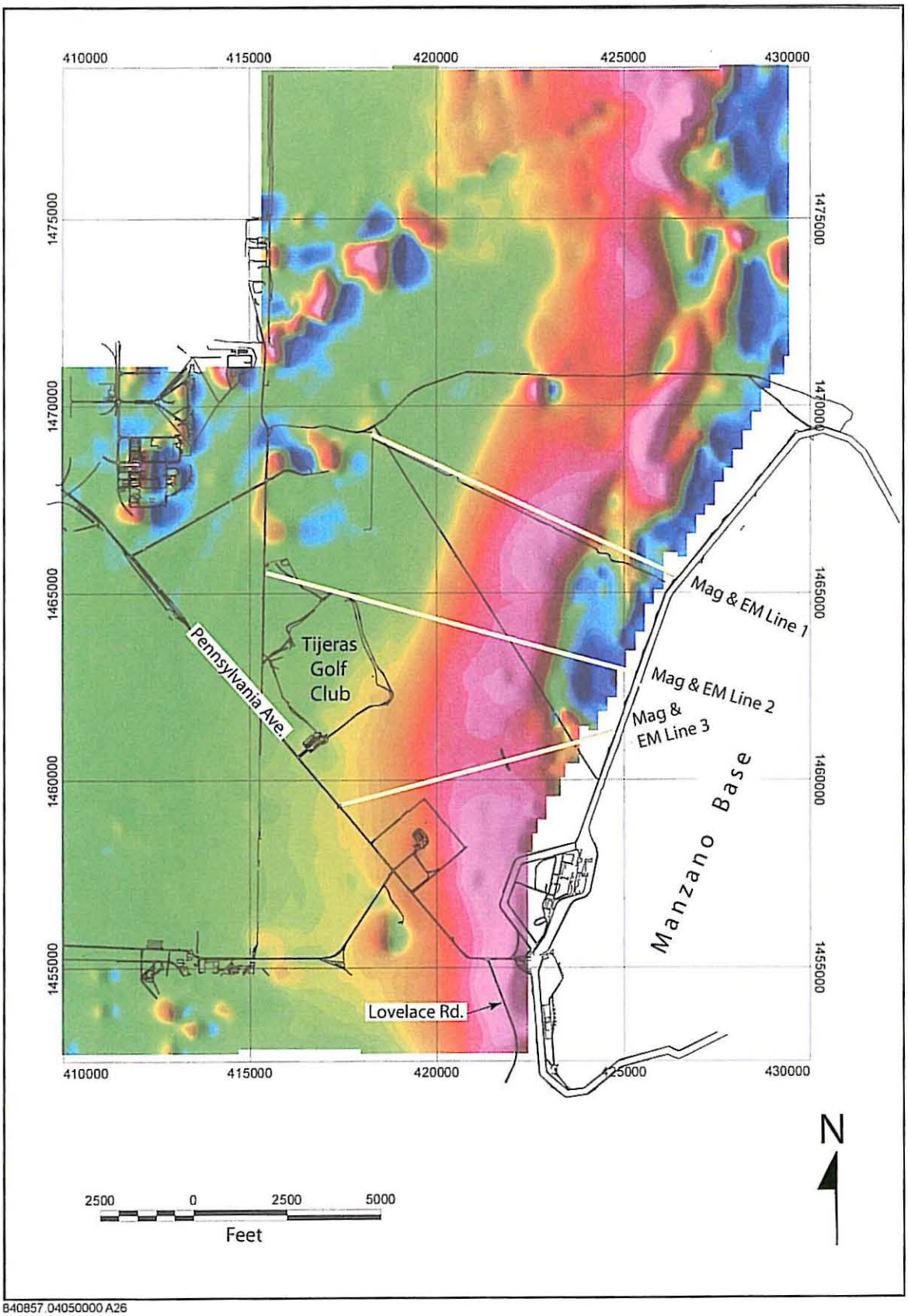

840857.04050000.A26

Figure 4-2 Horizontal Magnetic Gradient (USGS 1997) and Location of 2001 Ground-Based Magnetometer (Mag) Lines
(Modified from Hyndman & Brandwein, 2002)

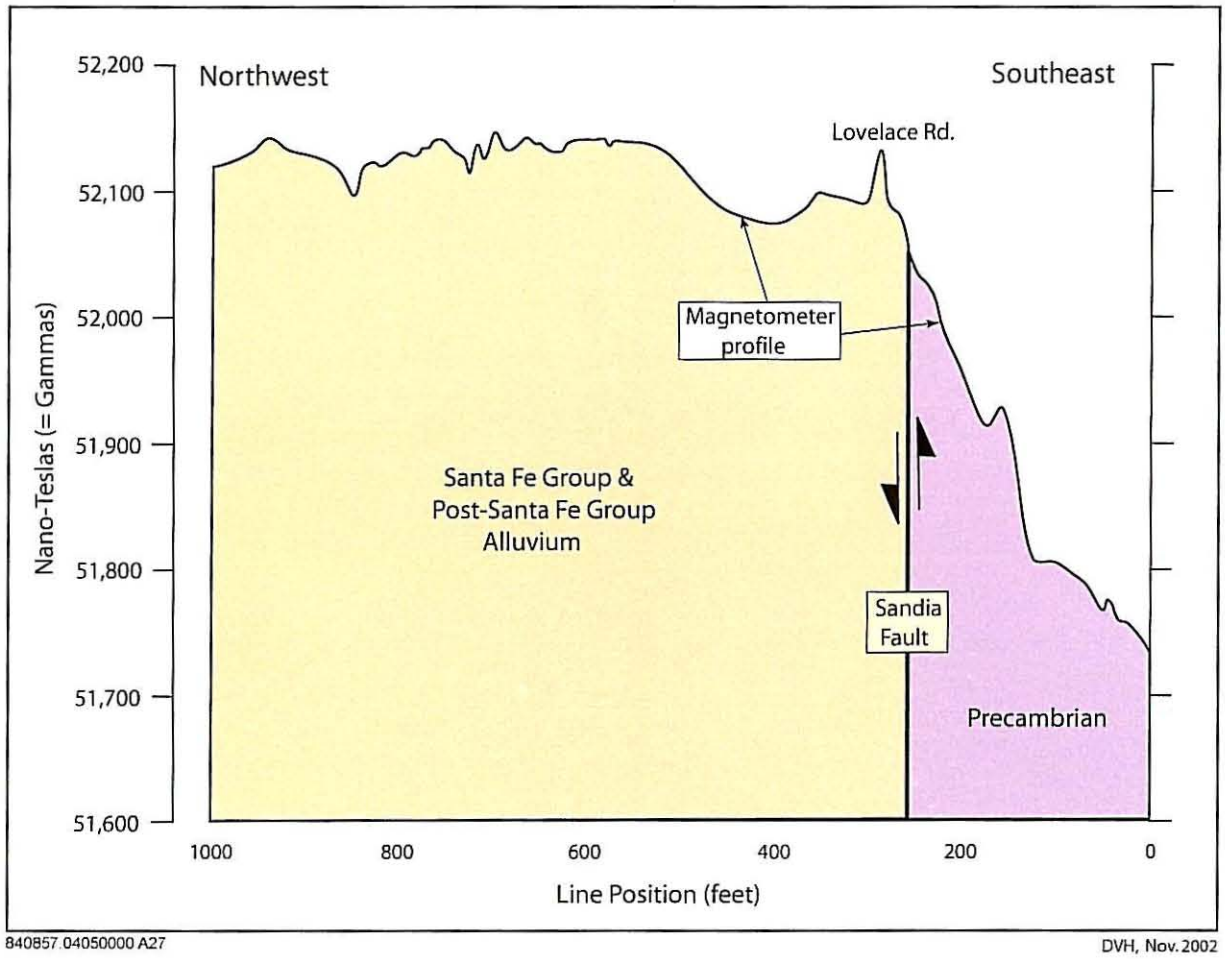

Figure 4-3 Ground-Based Magnetometer Line "E"
(Modified from Hyndman, 1995; location on Plates III & IV)

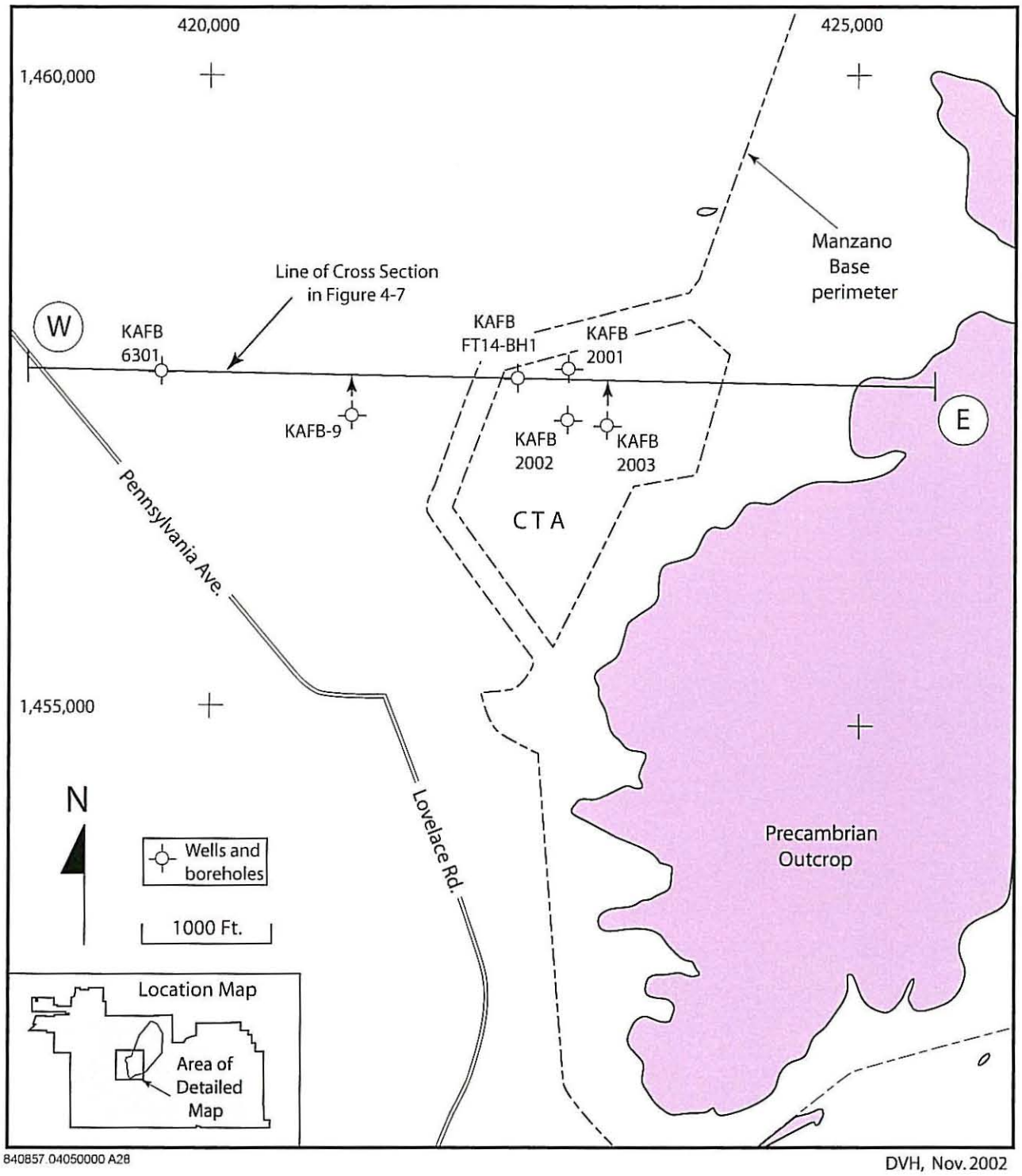

Figure 4-4 Location Map, Manzano Base and Central Training Academy (CTA)

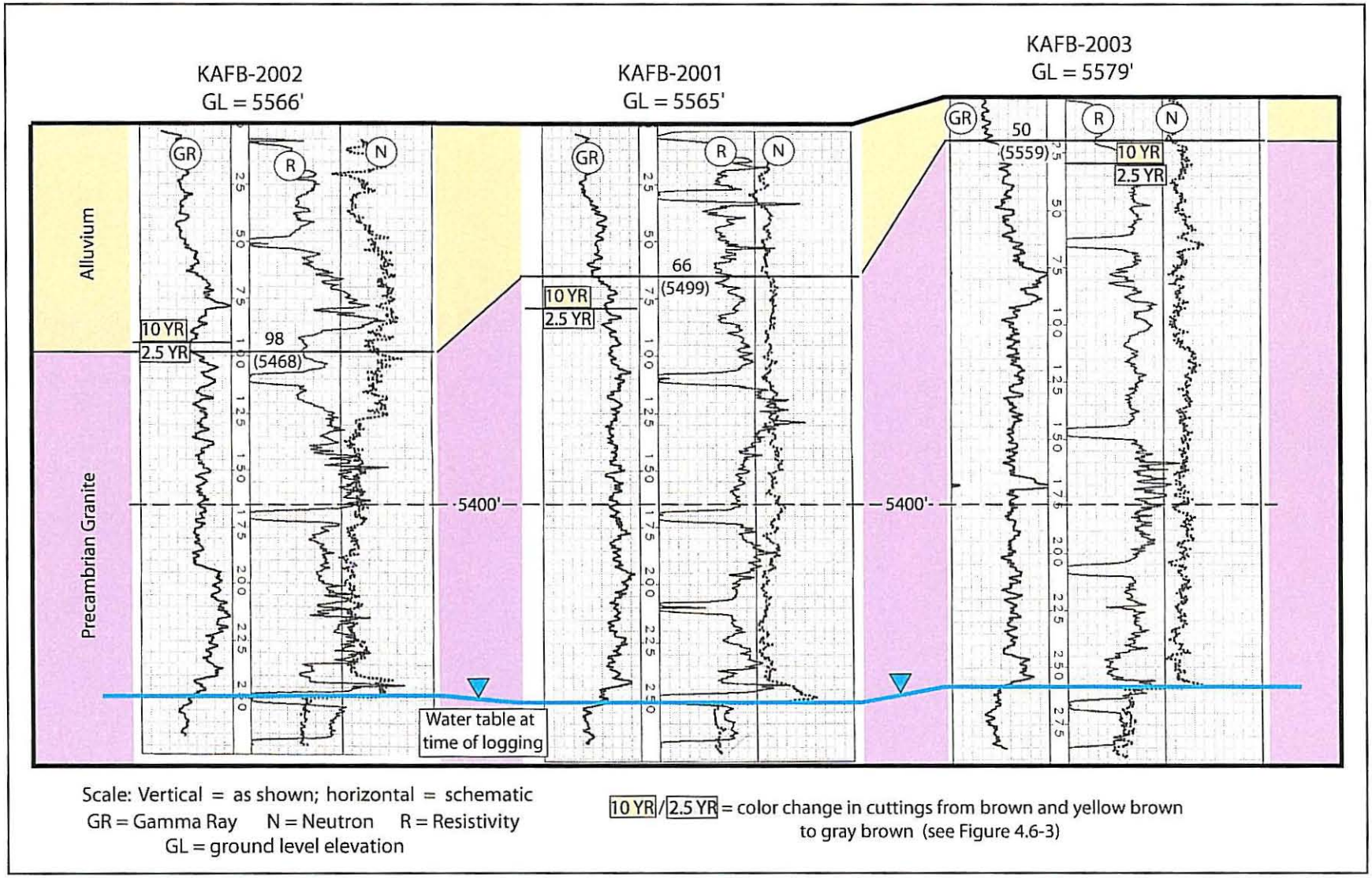

DVH, Nov. 2002

Figure 4-5 Well-Log Correlation Section Across Central Training Academy
(Well locations in Figure 4-4)

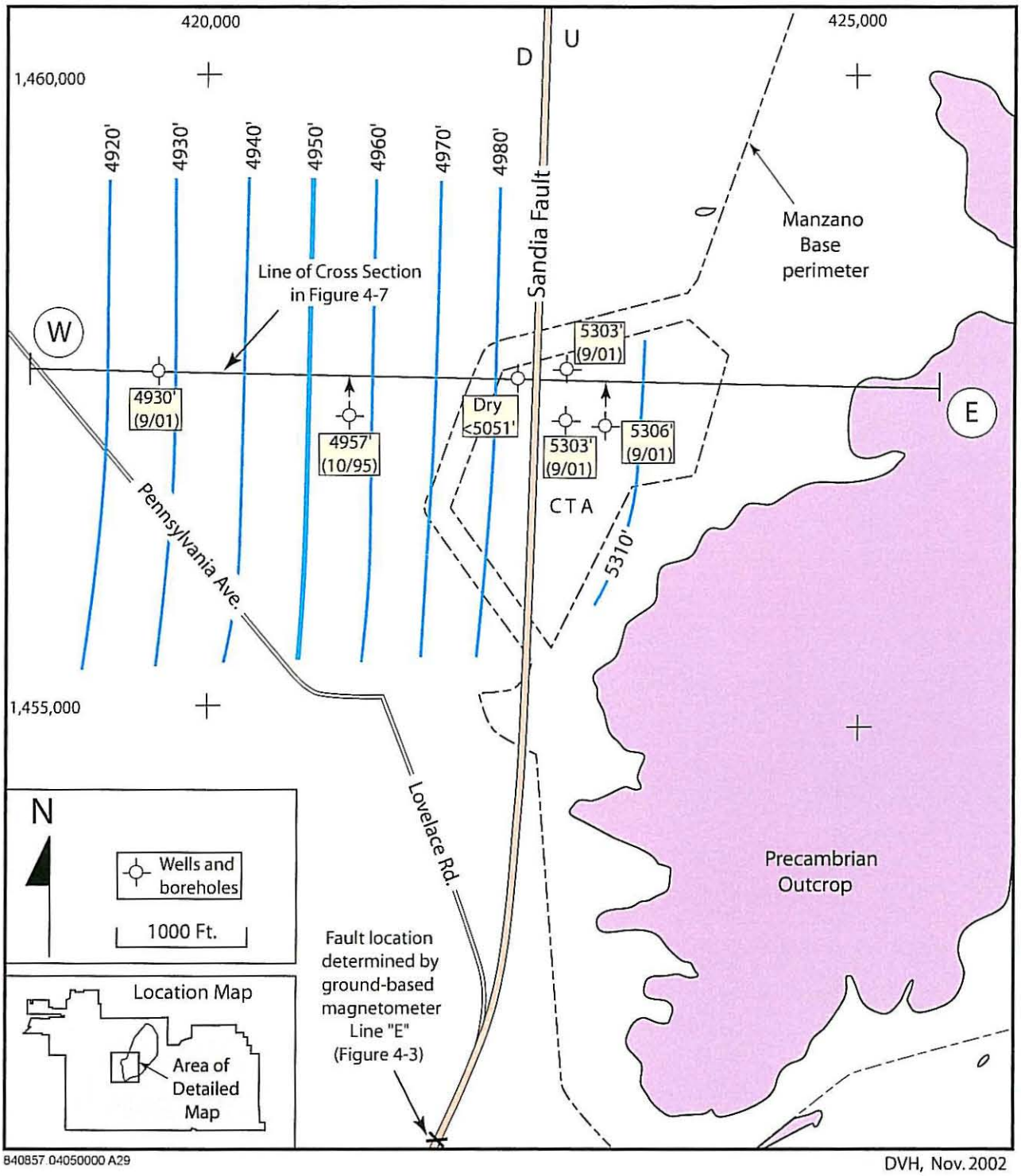

Figure 4-6 Elevation of Top of Regional Water Table, Manzano Base and Central Training Academy (CTA) (CI = 10 ft)

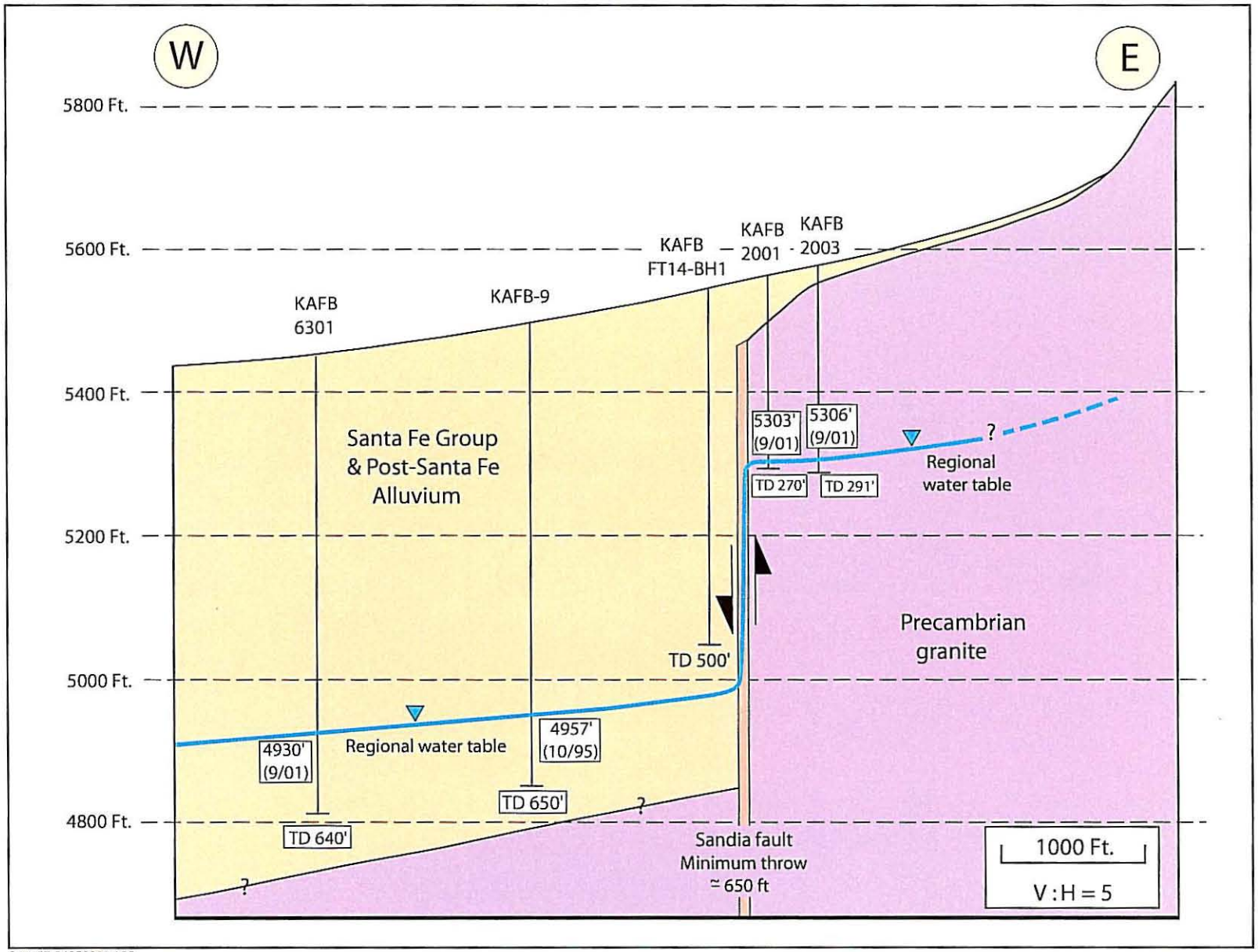

Figure 4-7 West-East Cross Section Across Manzano Base and Central Training Academy
(Location in Figure 4-4)

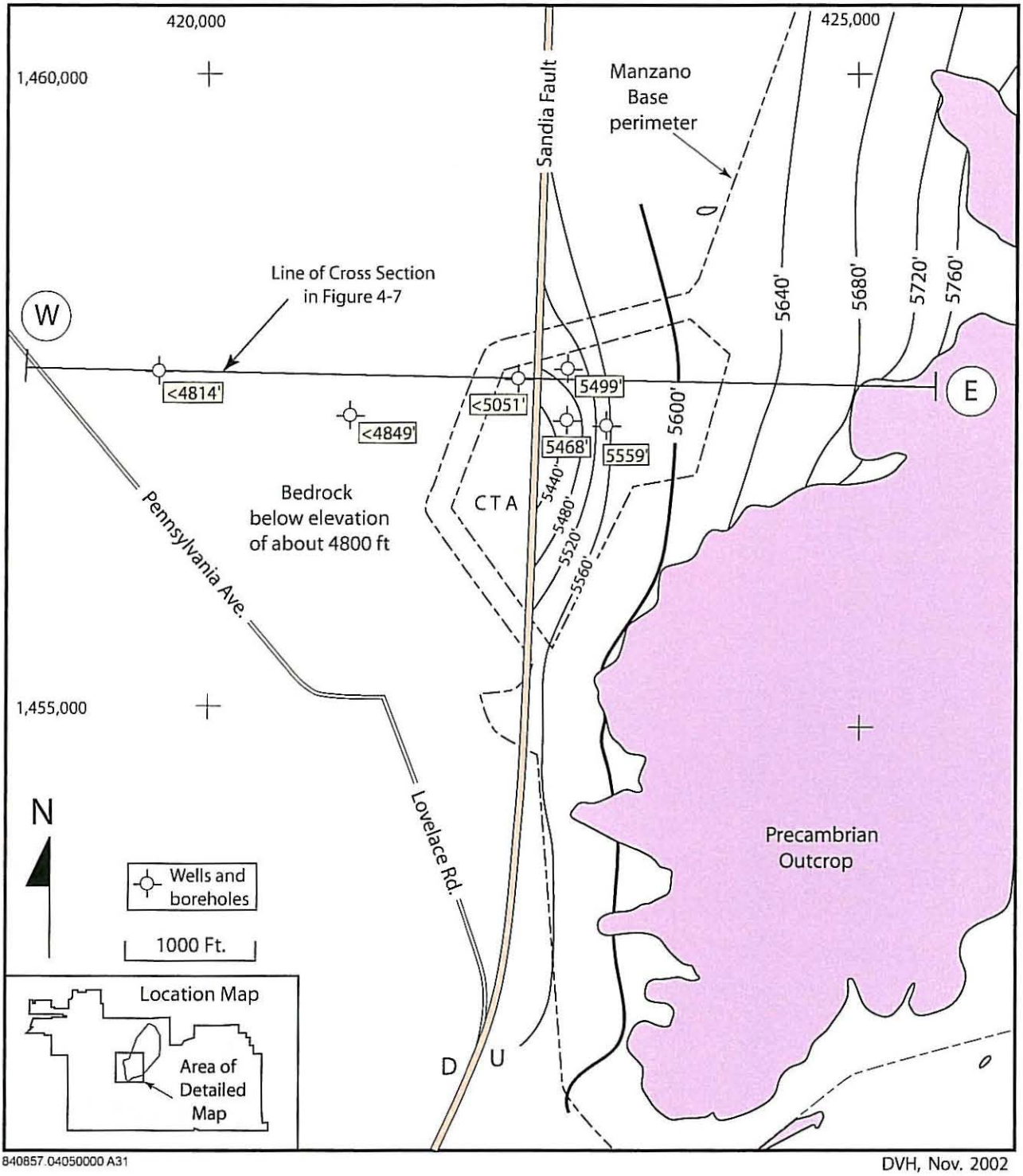

Figure 4-8 Elevation of Top Subsurface Bedrock, Manzano Base and Central Training Academy (CTA) (CI = 40 ft)

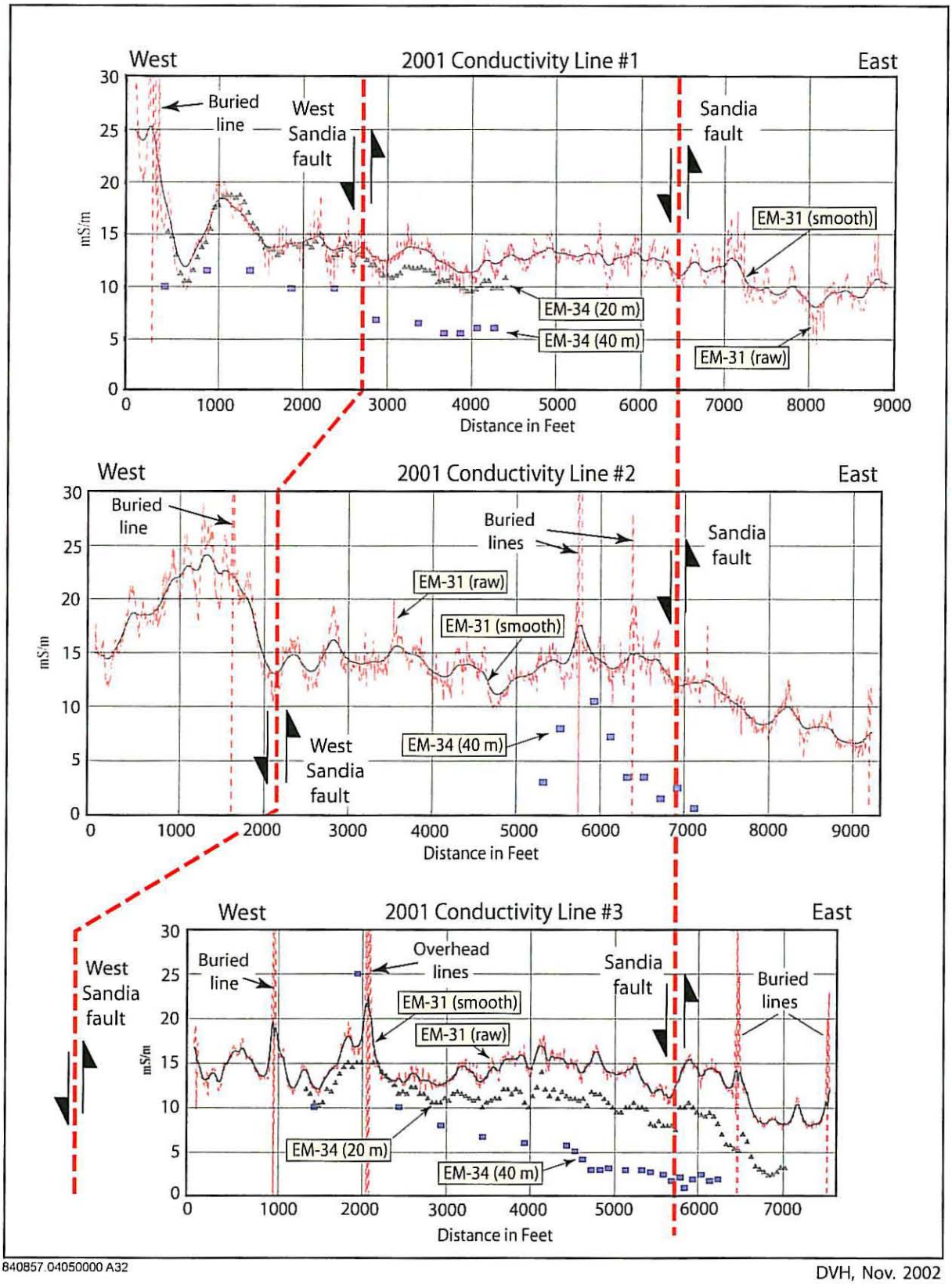

840857.04050000 A32

DVH, Nov. 2002

Figure 4-9 2001 Electromagnetic Ground Conductivity Data, Manzano Base West Area

(Modified from Hyndman and Brandwein, 2002; location of lines in Figures 4-1 and 4-2)

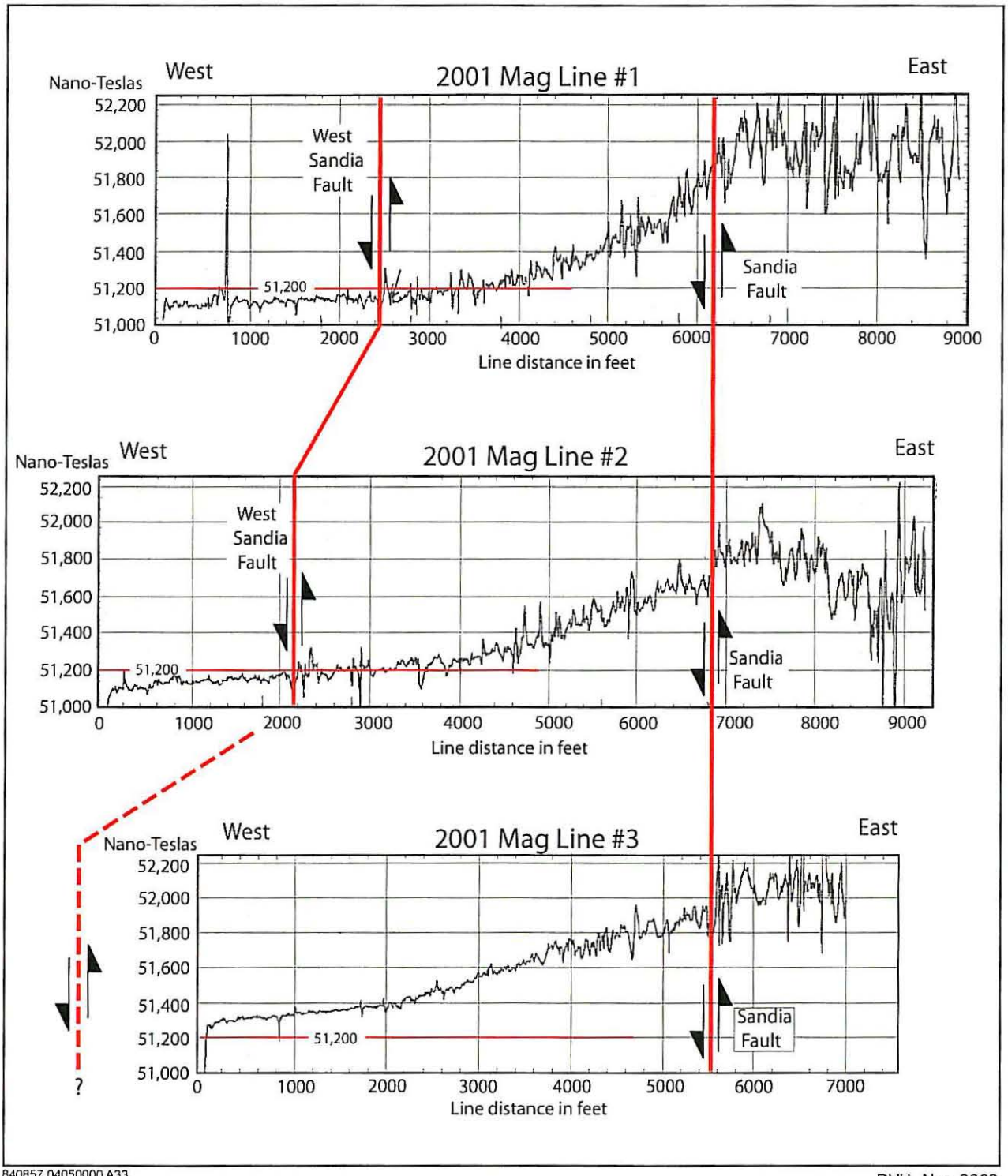

Figure 4-10 2001 Ground-Based Magnetometer Data, Manzano Base West Area
(Draft versions modified from Hyndman & Brandwein, 2002;
location of lines in Figures 4-1 and 4-2)

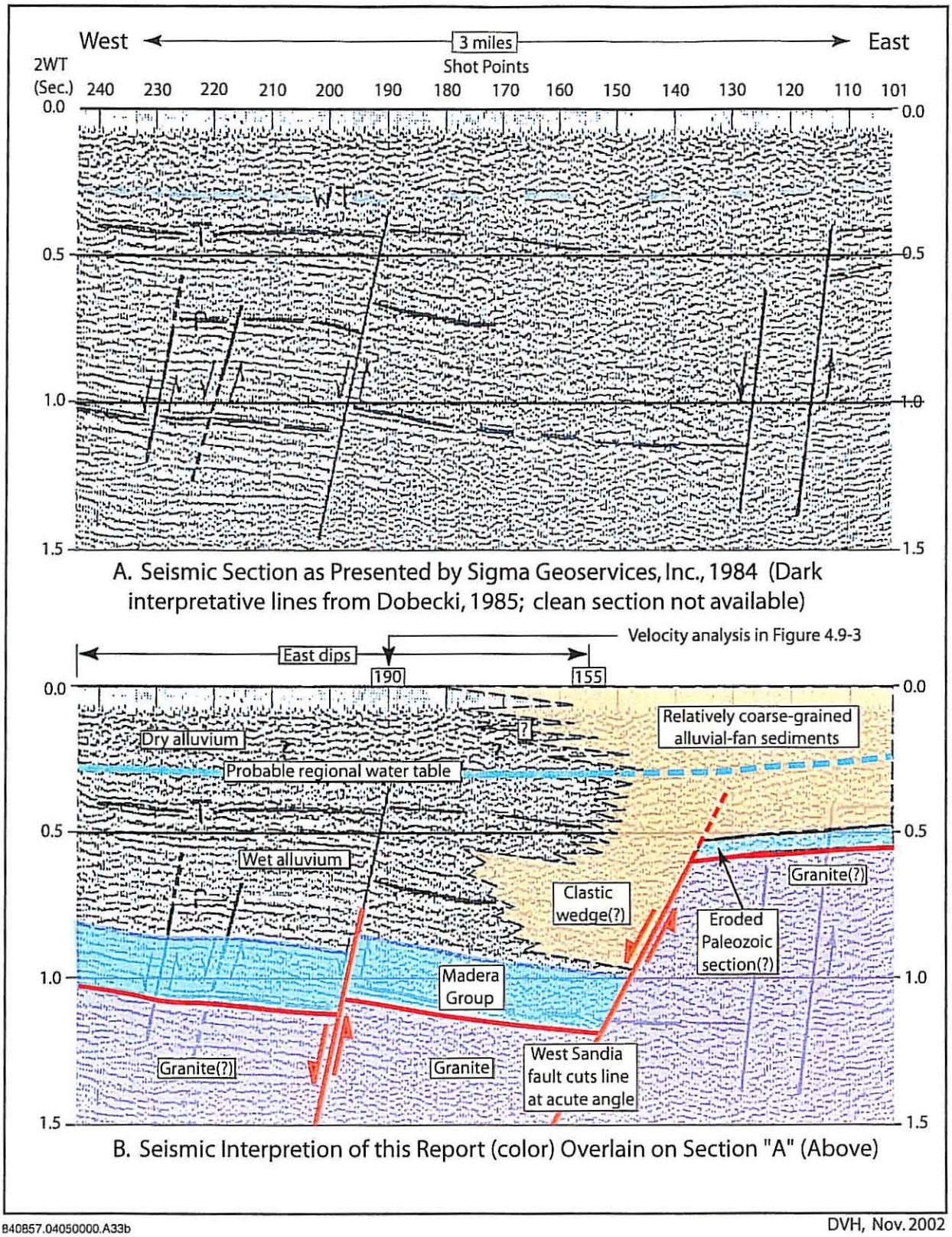

840857.04050000.A33b

DVH, Nov. 2002

Figure 4-11 Reflection Seismic Record Section, Manzano Base West Area
(Modified from Sigma Geoservices, Inc., 1984)

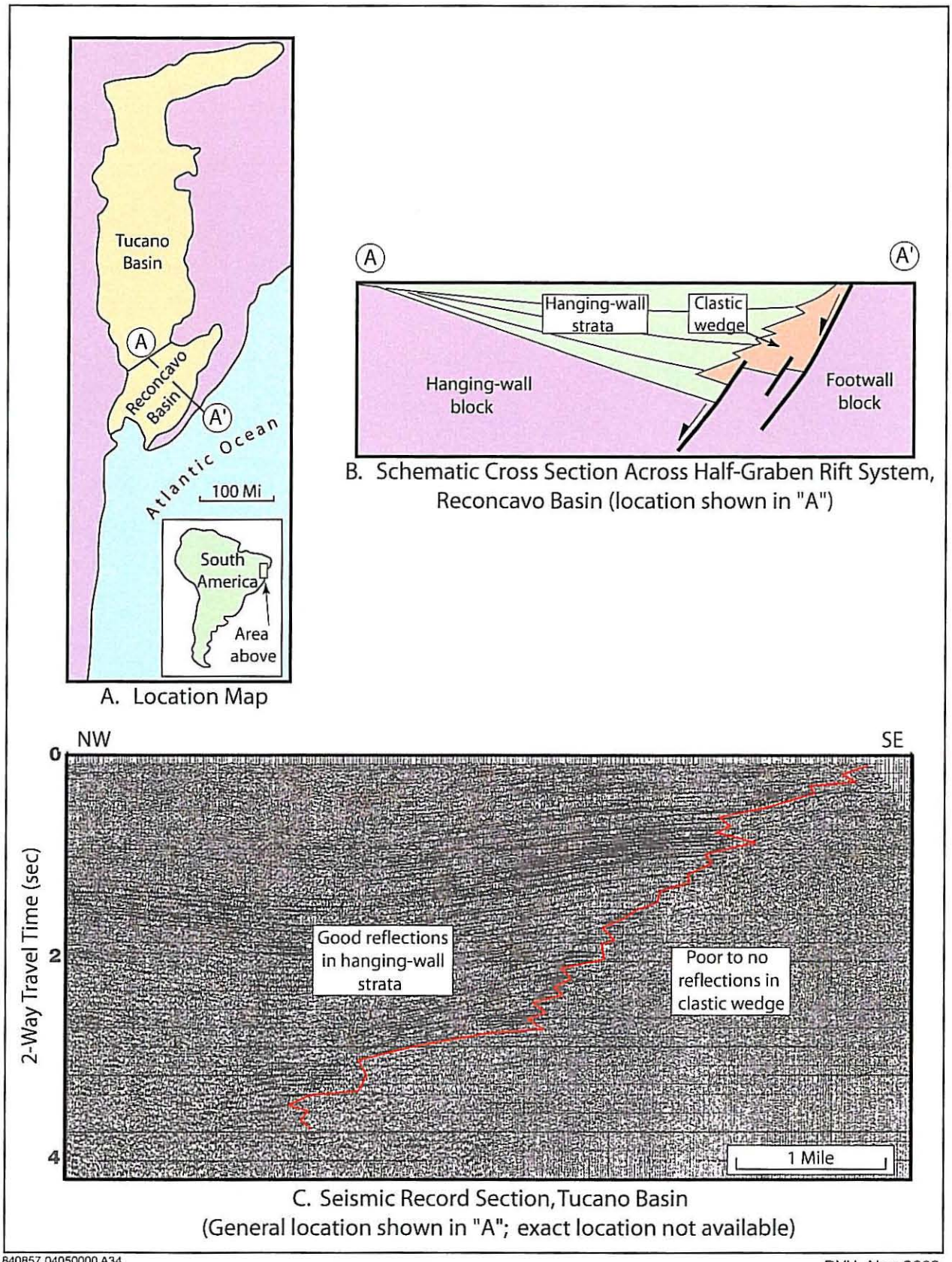

840857.04050000 A34

DVH, Nov. 2002

Figure 4-12 Example of Effect of Clastic Wedge on Seismic Records, Atlantic Coast of Brazil

(Modified from Magnavita and da Silva, 1995)

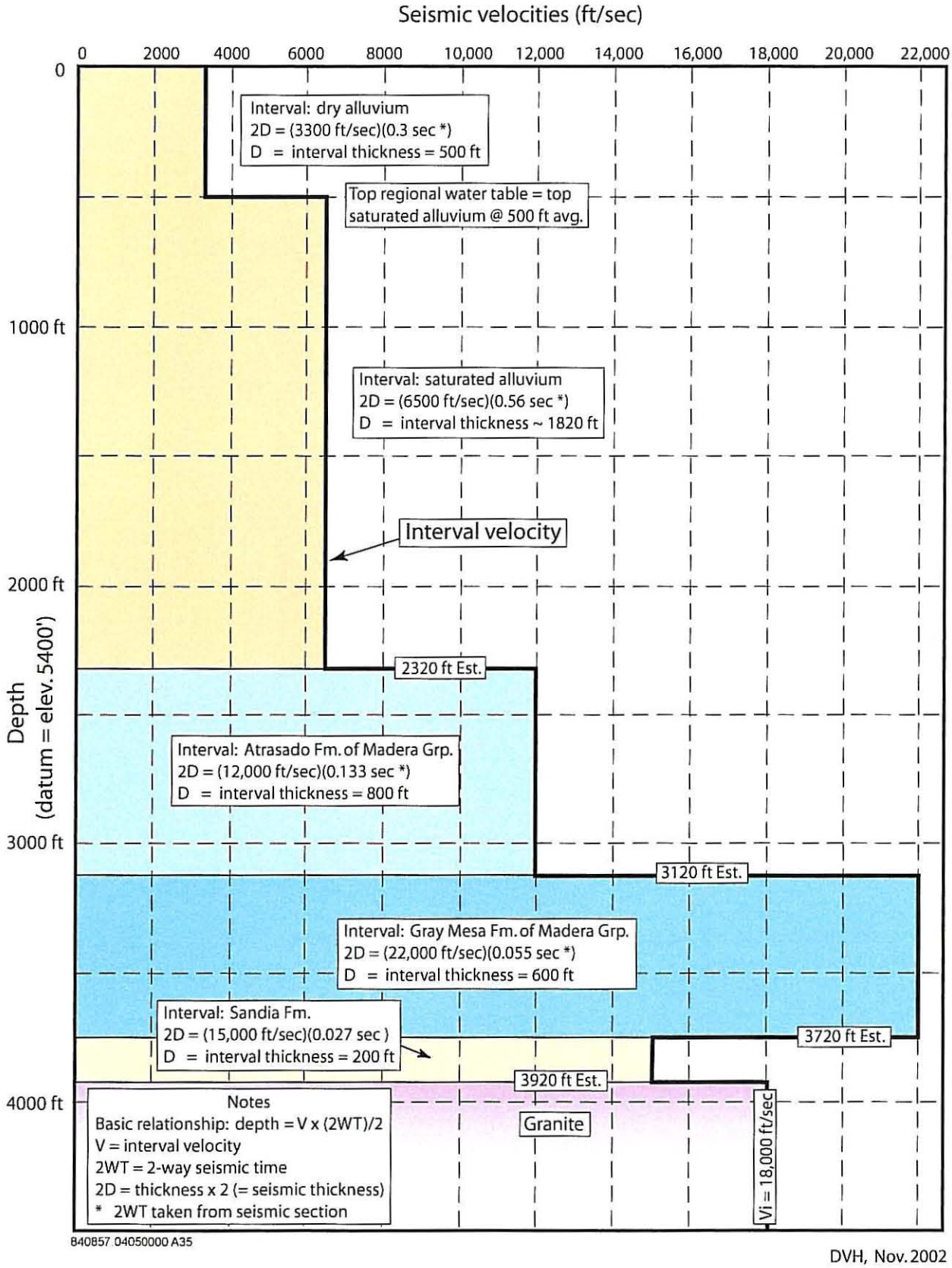

Figure 4-13 Provisional Velocity Profile, Manzano Base West Area
(Analysis at SP 190, Figure 4-11)

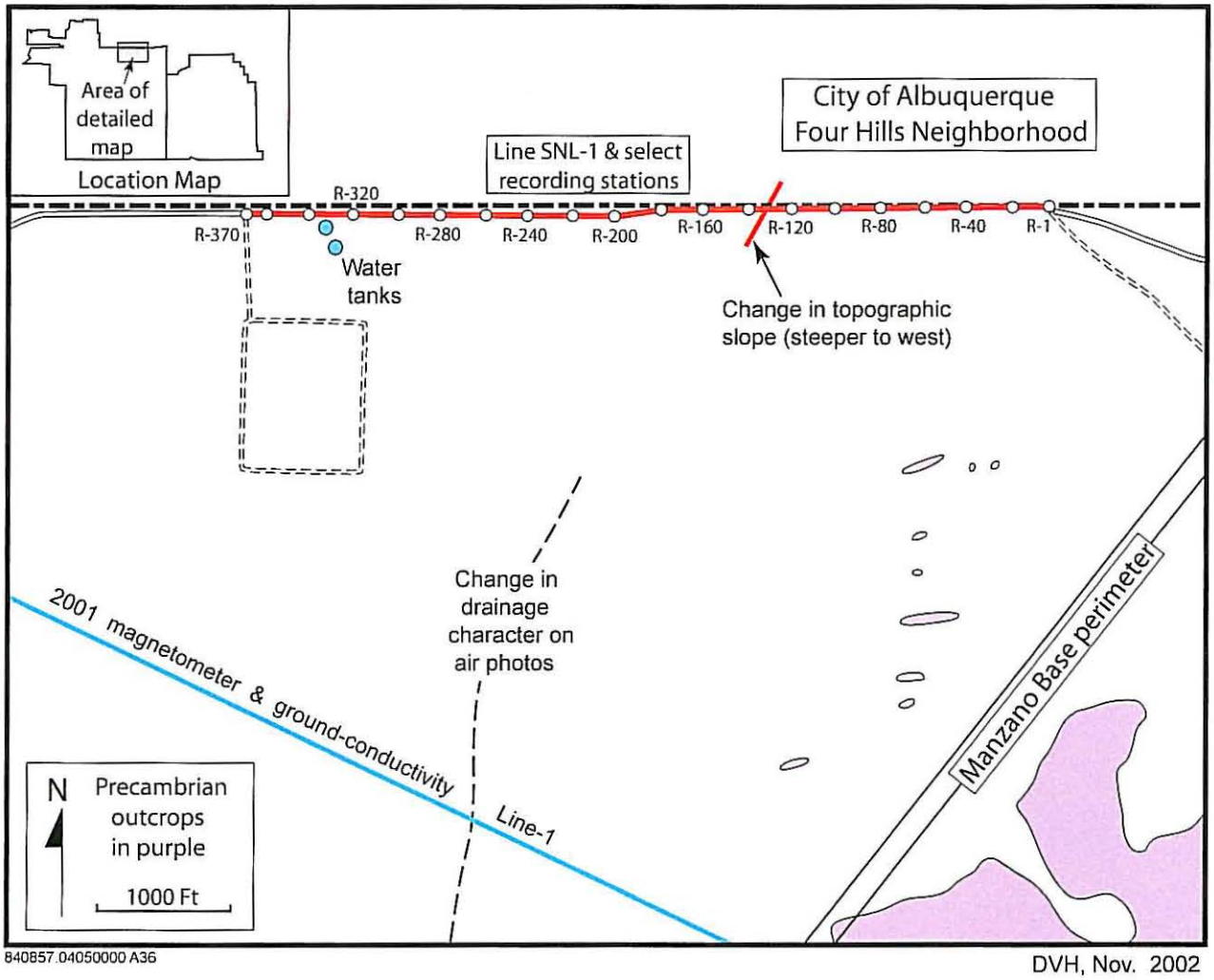

Figure 4-14 Location of 2002 Seismic Line SNL-1

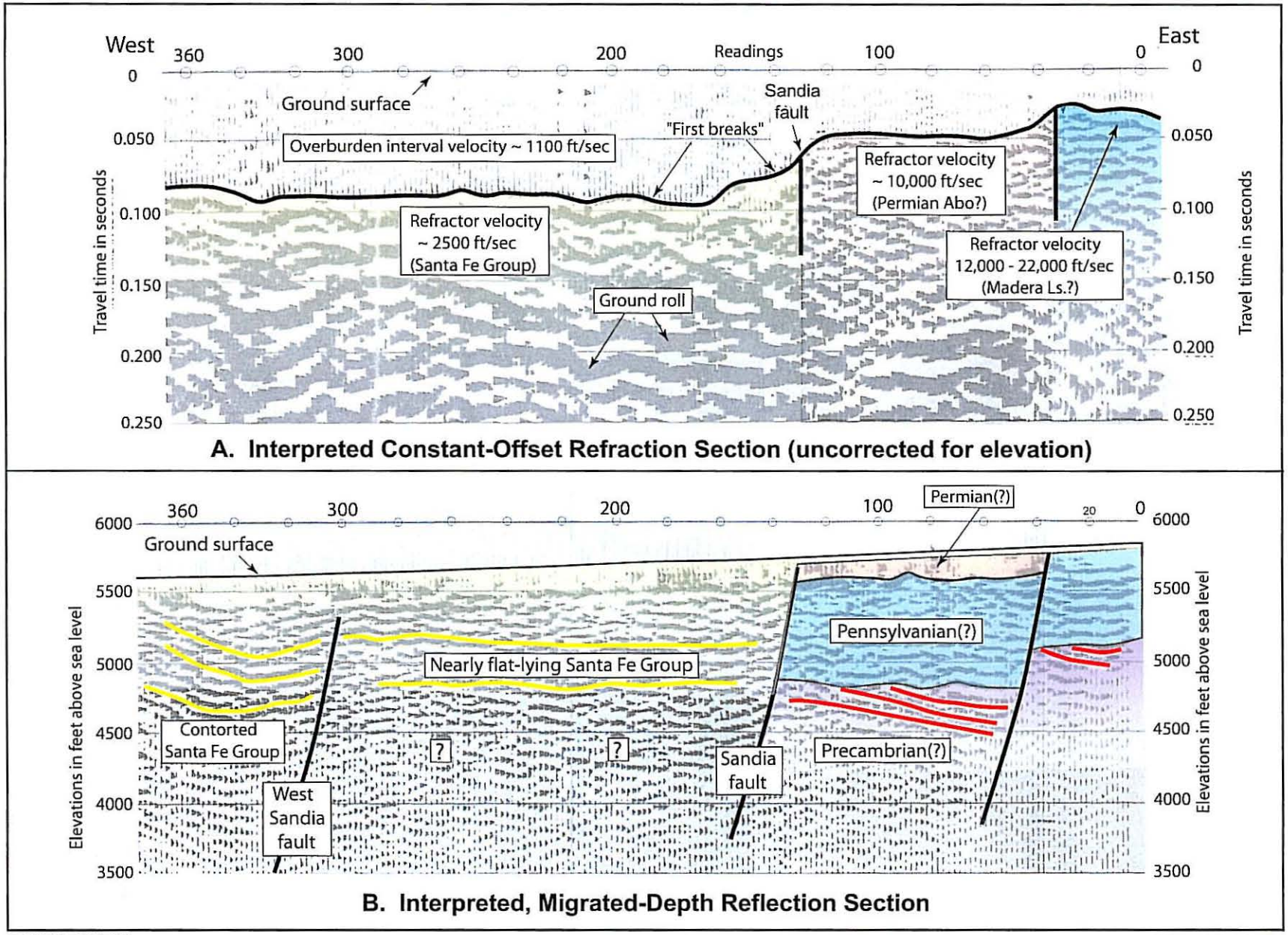

840857.04050000 A37

DVH, Nov. 2002

Figure 4-15 Record Sections, Seismic Line SNL-1
(Modified from Geological Associates, 2002)

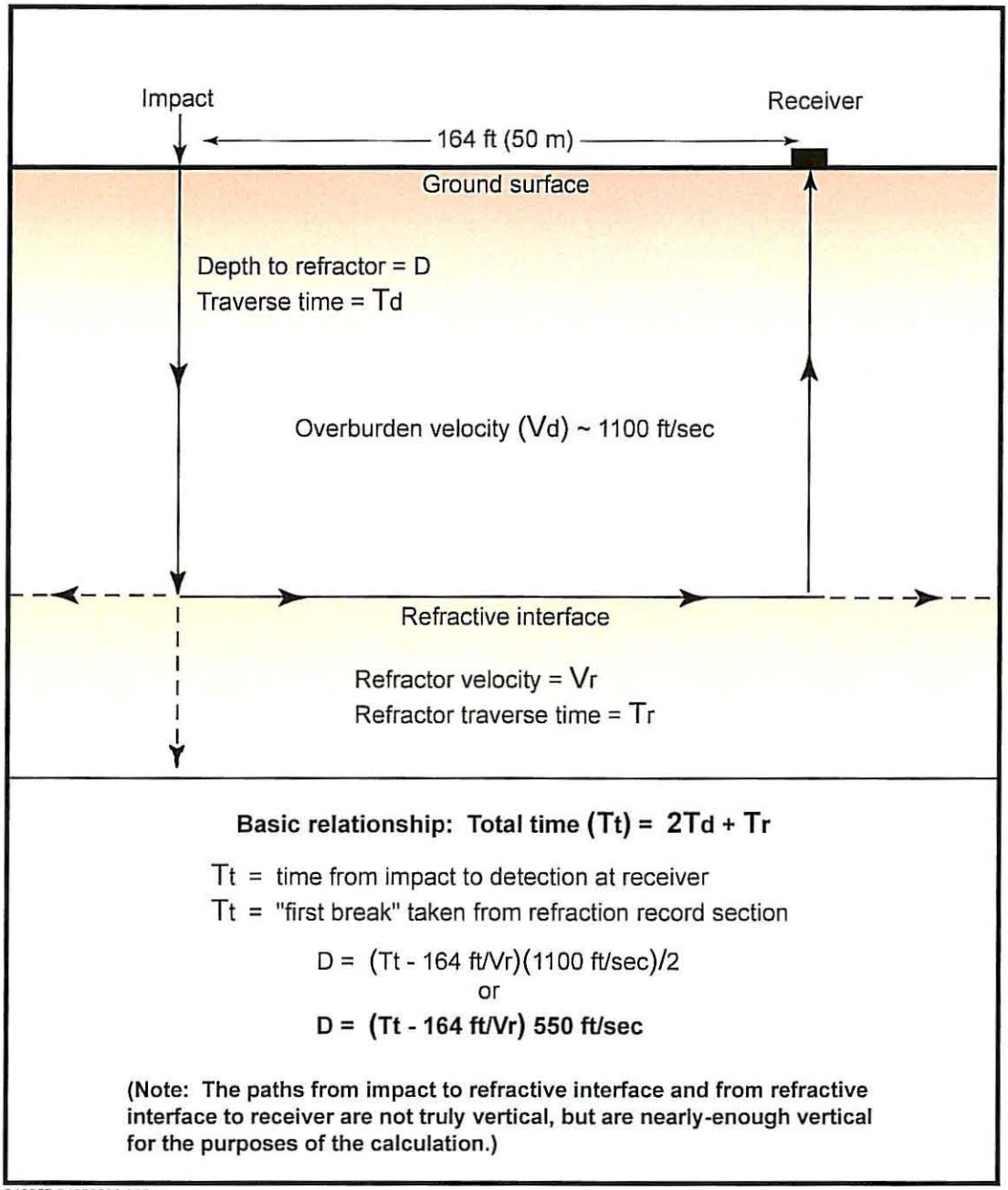

840857.04050000 A38

DVH, Nov. 2002

Figure 4-16 Seismic Refraction Principles for Line SNL-1

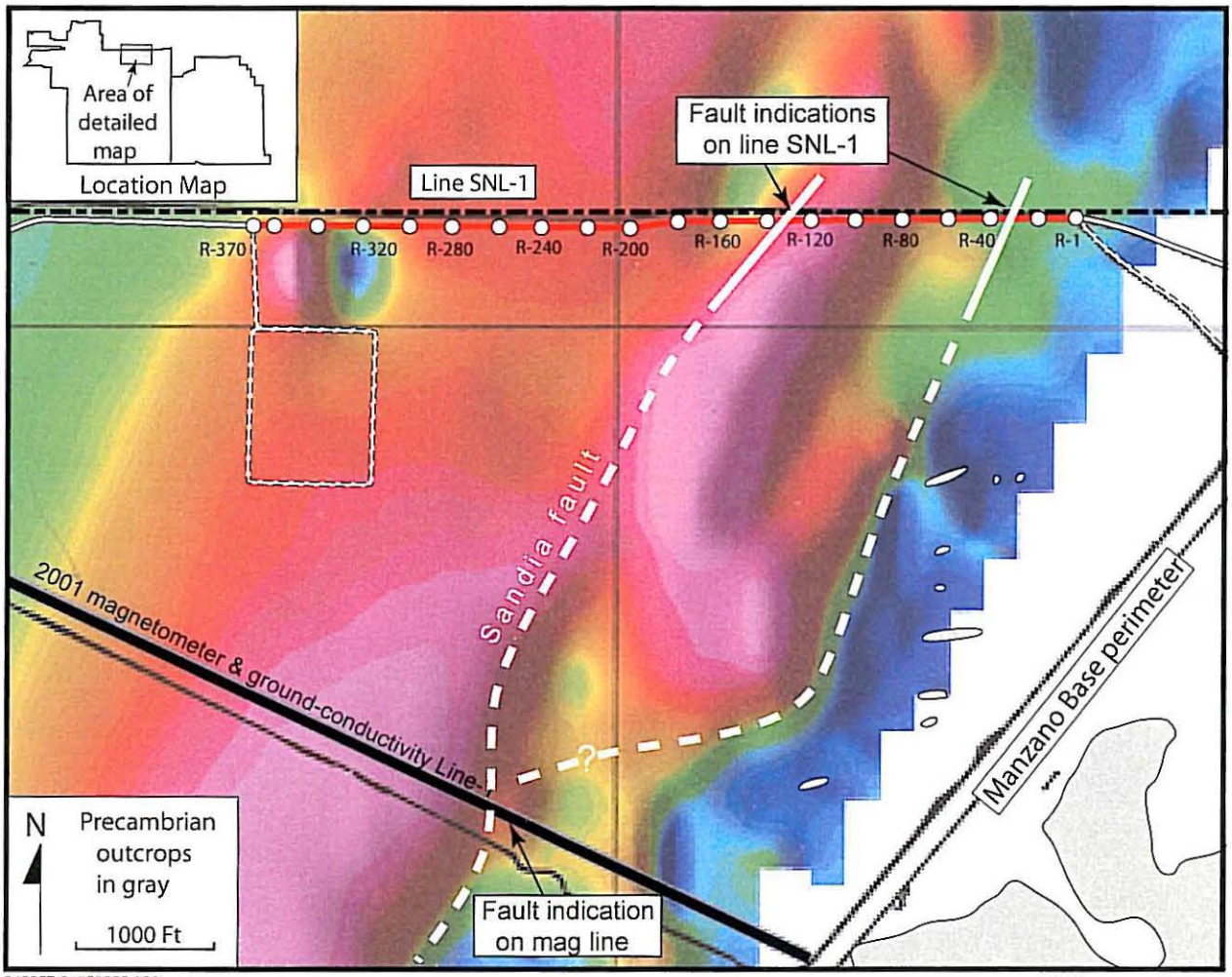

Figure 4-17 Seismic Line SNL-1 Refraction-Data Fault Cuts Compared to USGS Aeromagnetic Data (color)

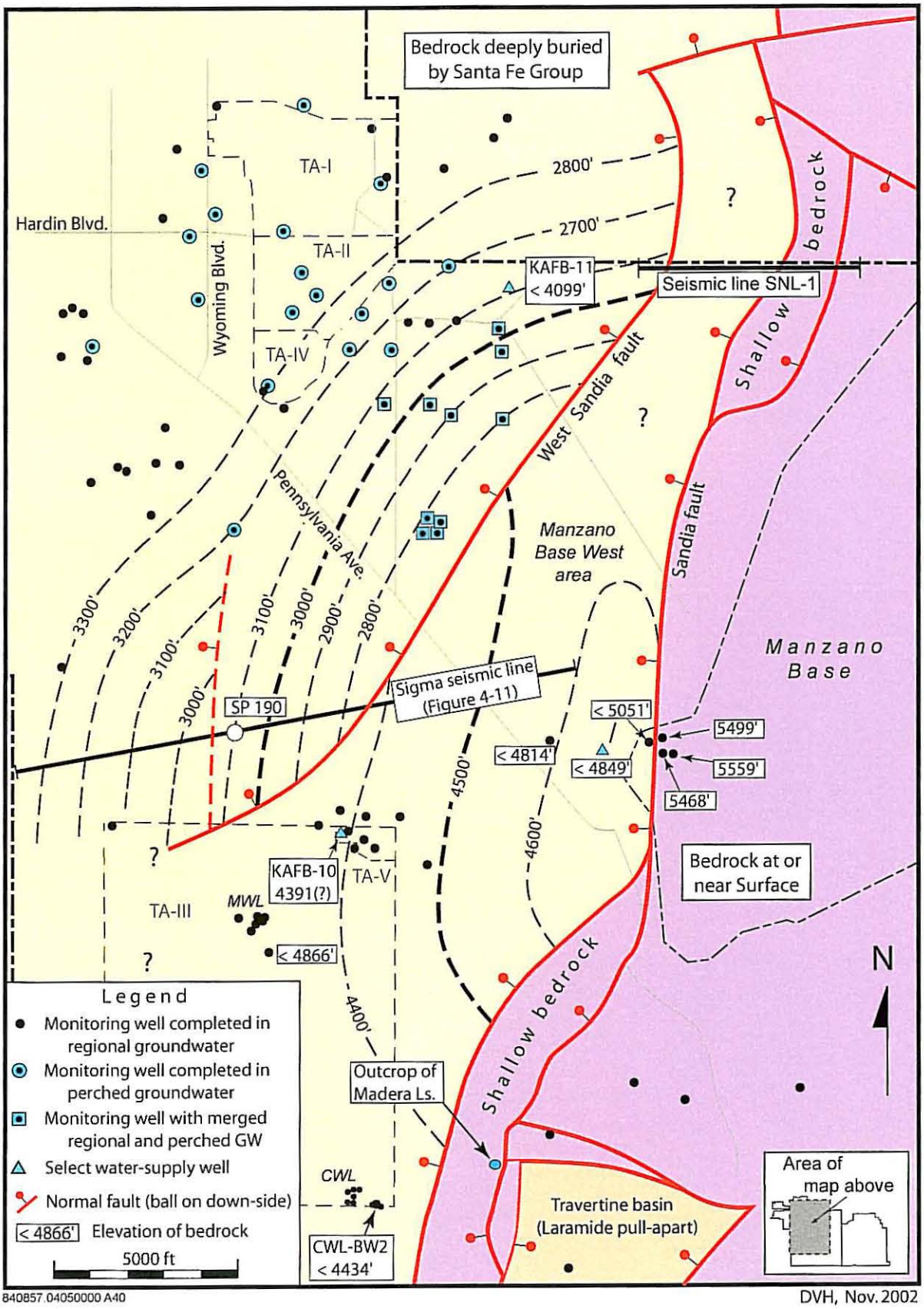

840857.04050000 A40

DVH, Nov. 2002

Figure 4-18 Speculative Subsurface Structure Map on Top Bedrock (CI = 100 ft)

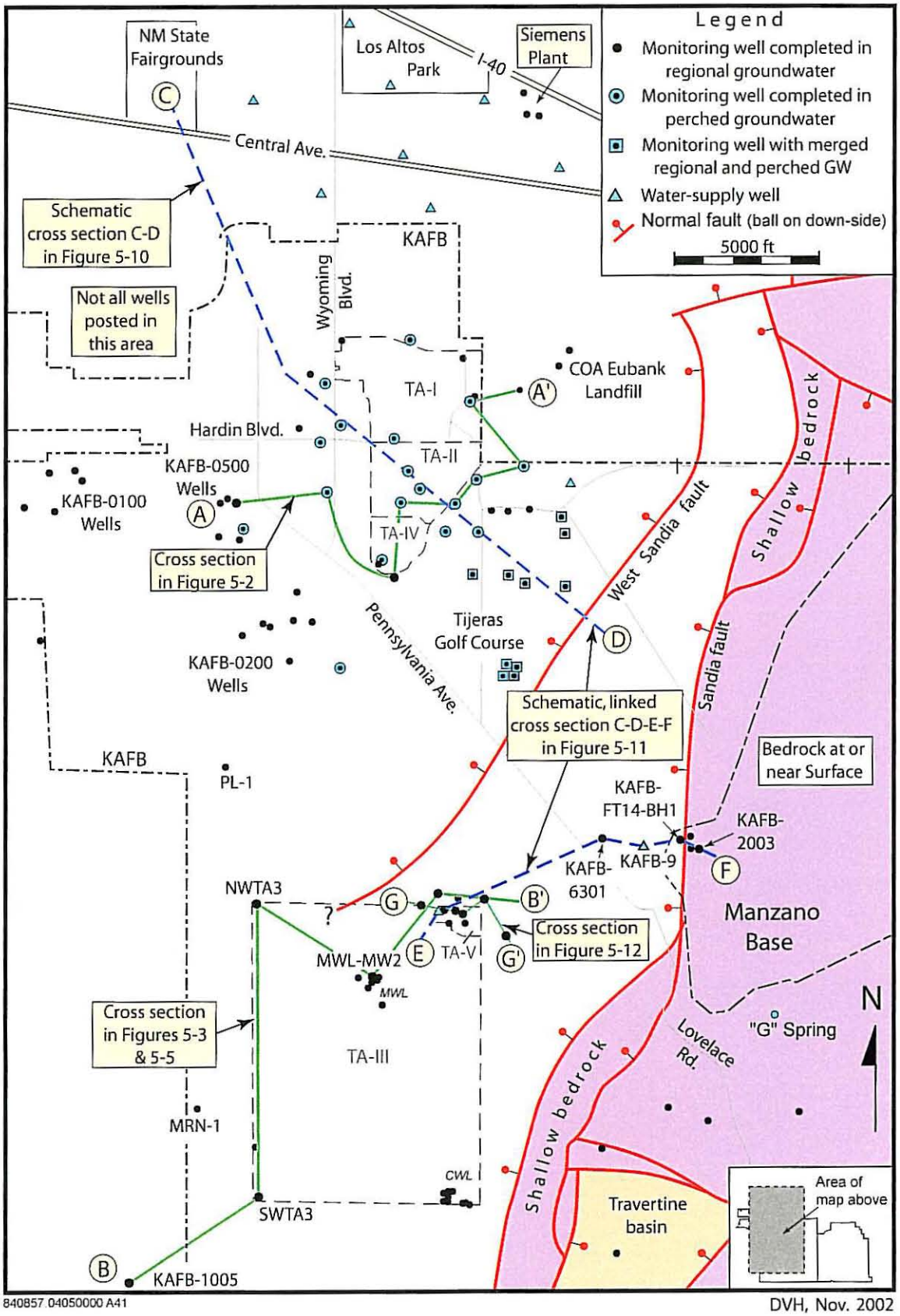

Figure 5-1 Cross Section Location Map, Western Portion of Kirtland Air Force Base (KAFB)

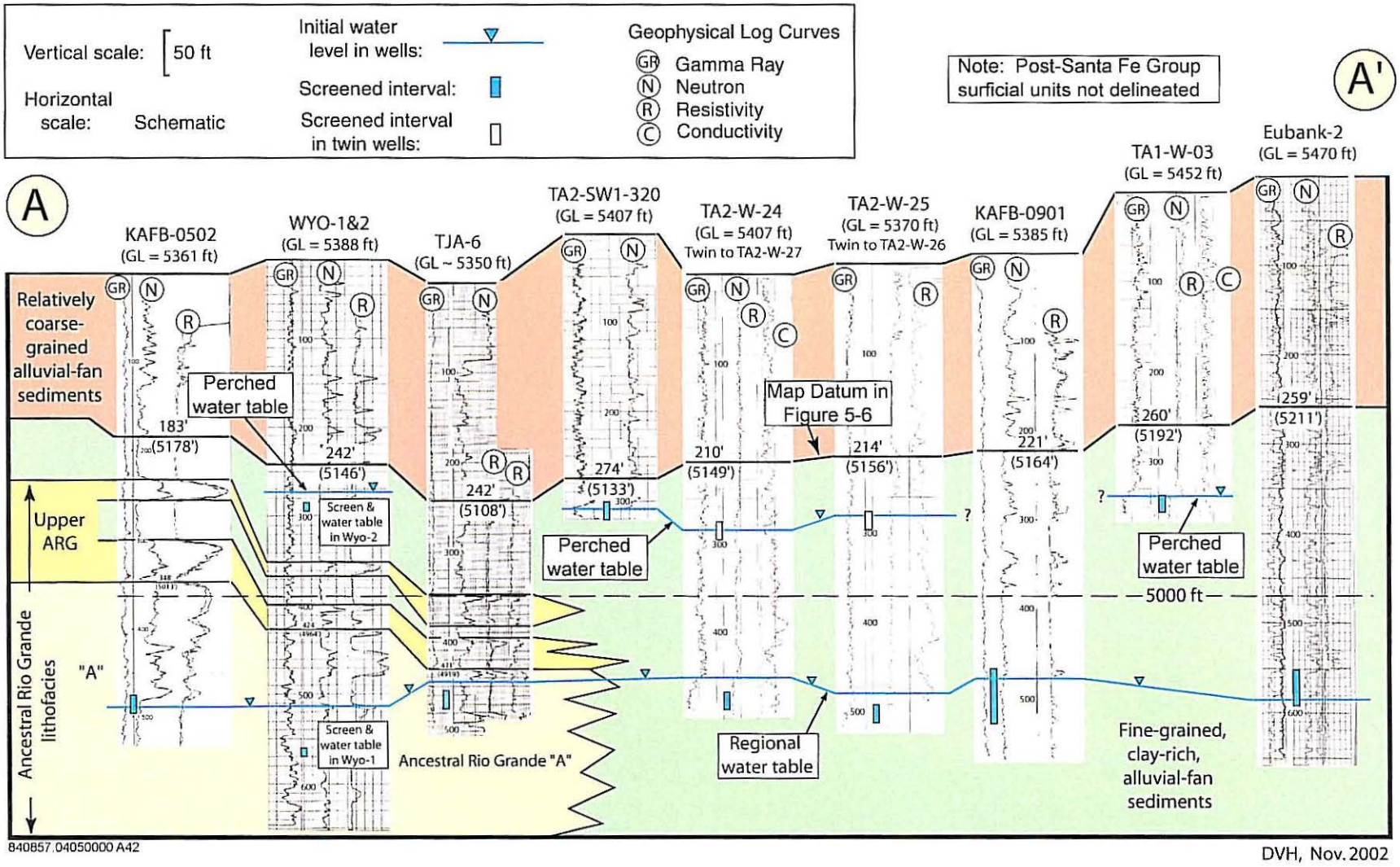

Figure 5-2 Geophysical-Log Correlation Section A-A' , Tijeras Arroyo Groundwater (TAG) Area
(Location in Figure 5-1)

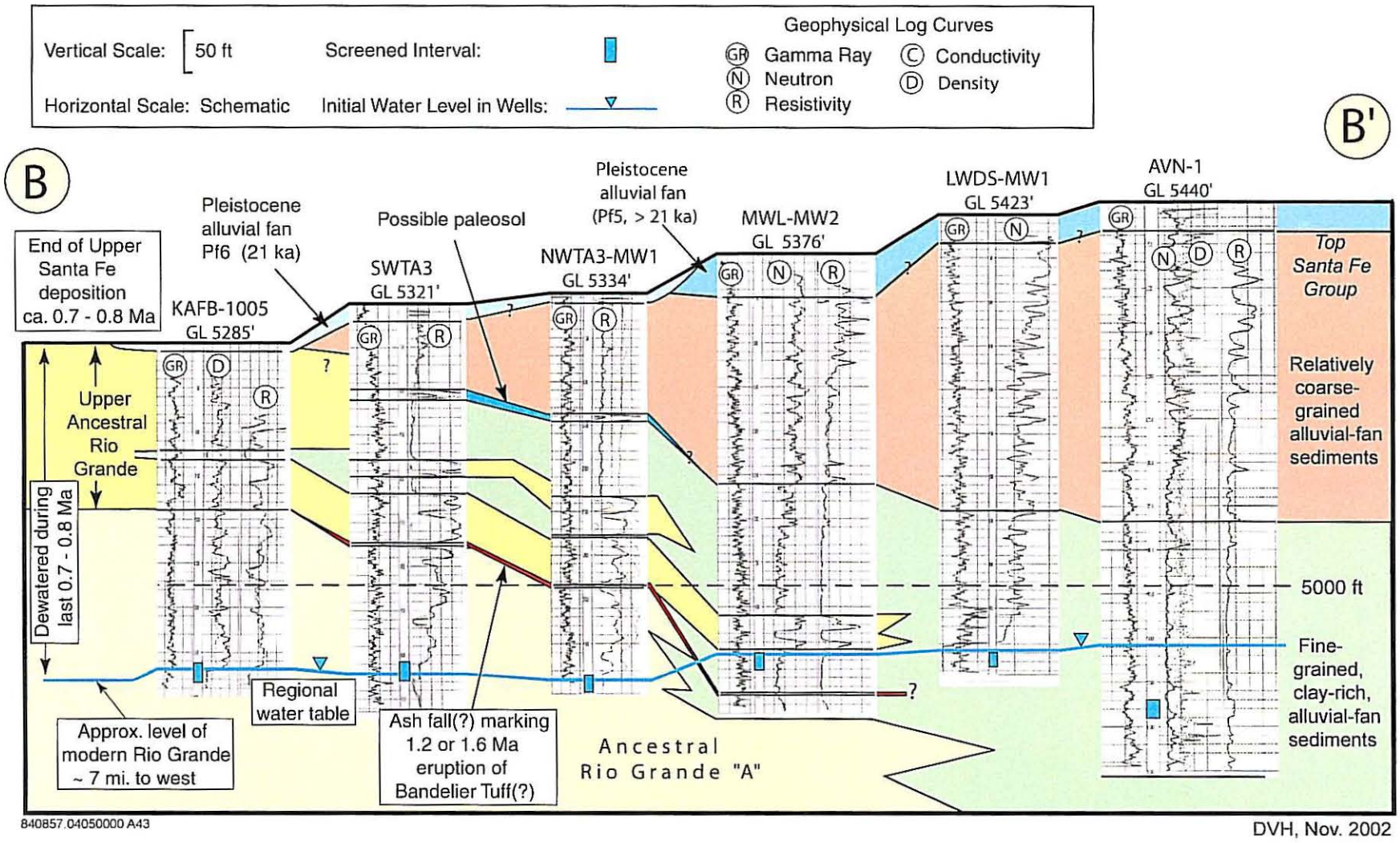

Figure 5-3 Geophysical-Log Correlation Section B-B', Southwest Part of Kirtland Air Force Base (KAFB)
(Location in Figure 5-1)

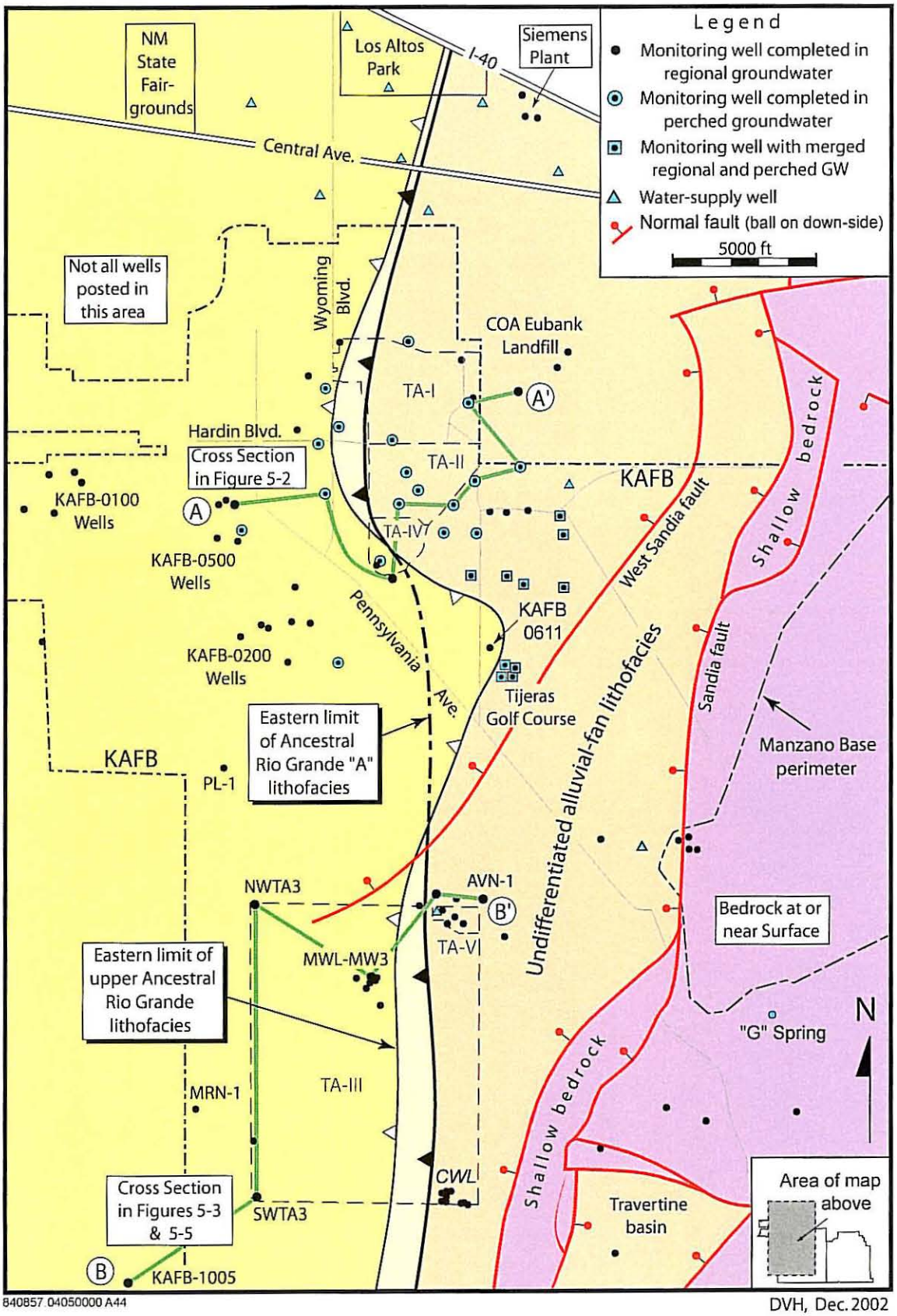

Figure 5-4 Limits of Ancestral Rio Grande and Alluvial-Fan Lithofacies of Upper Santa Fe Group

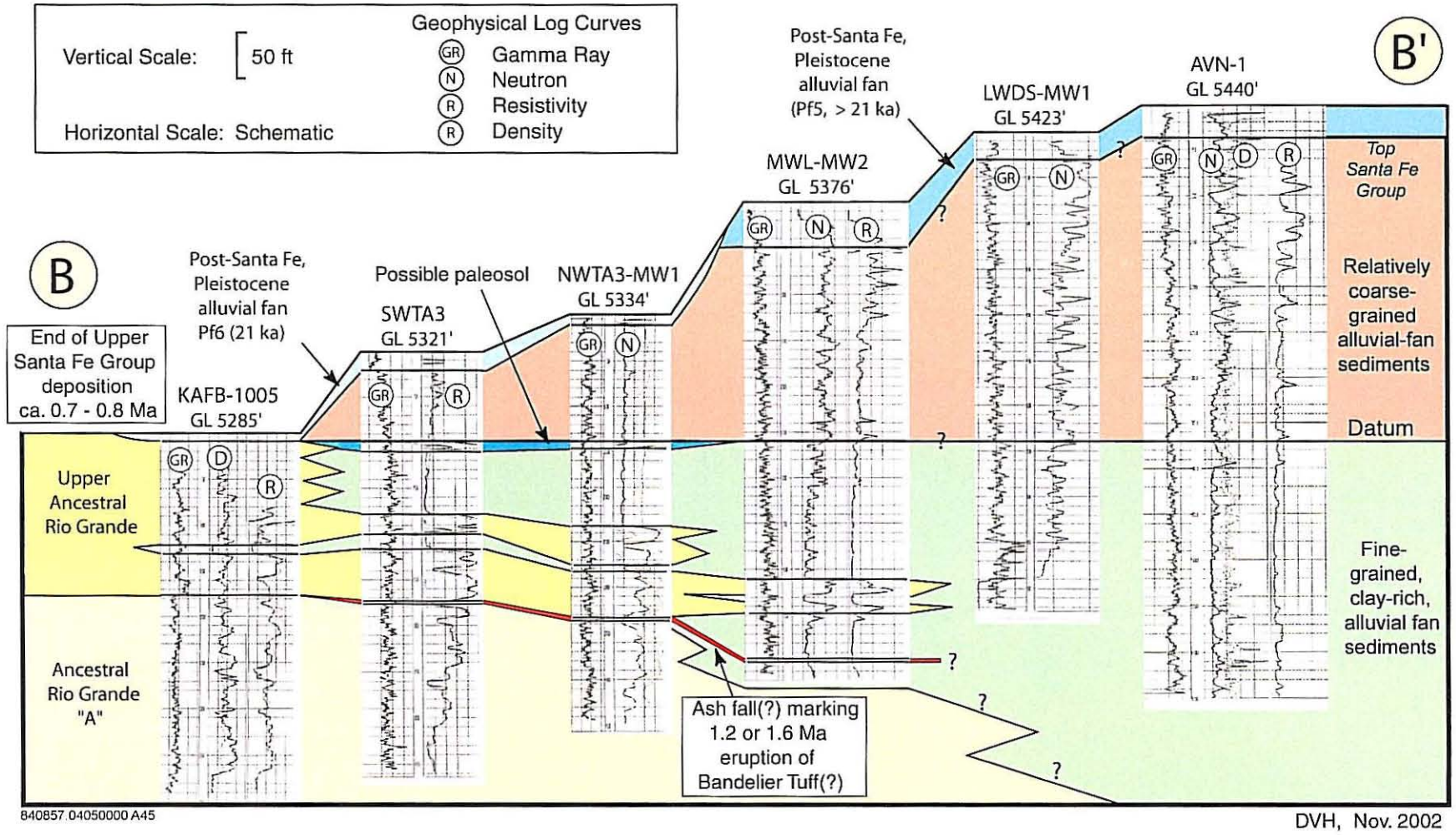

Figure 5-5 Geophysical-Log Stratigraphic Correlation Section B-B', Southwest Part of Kirtland Air Force Base (KAFB)
(Location in Figure 5-1)

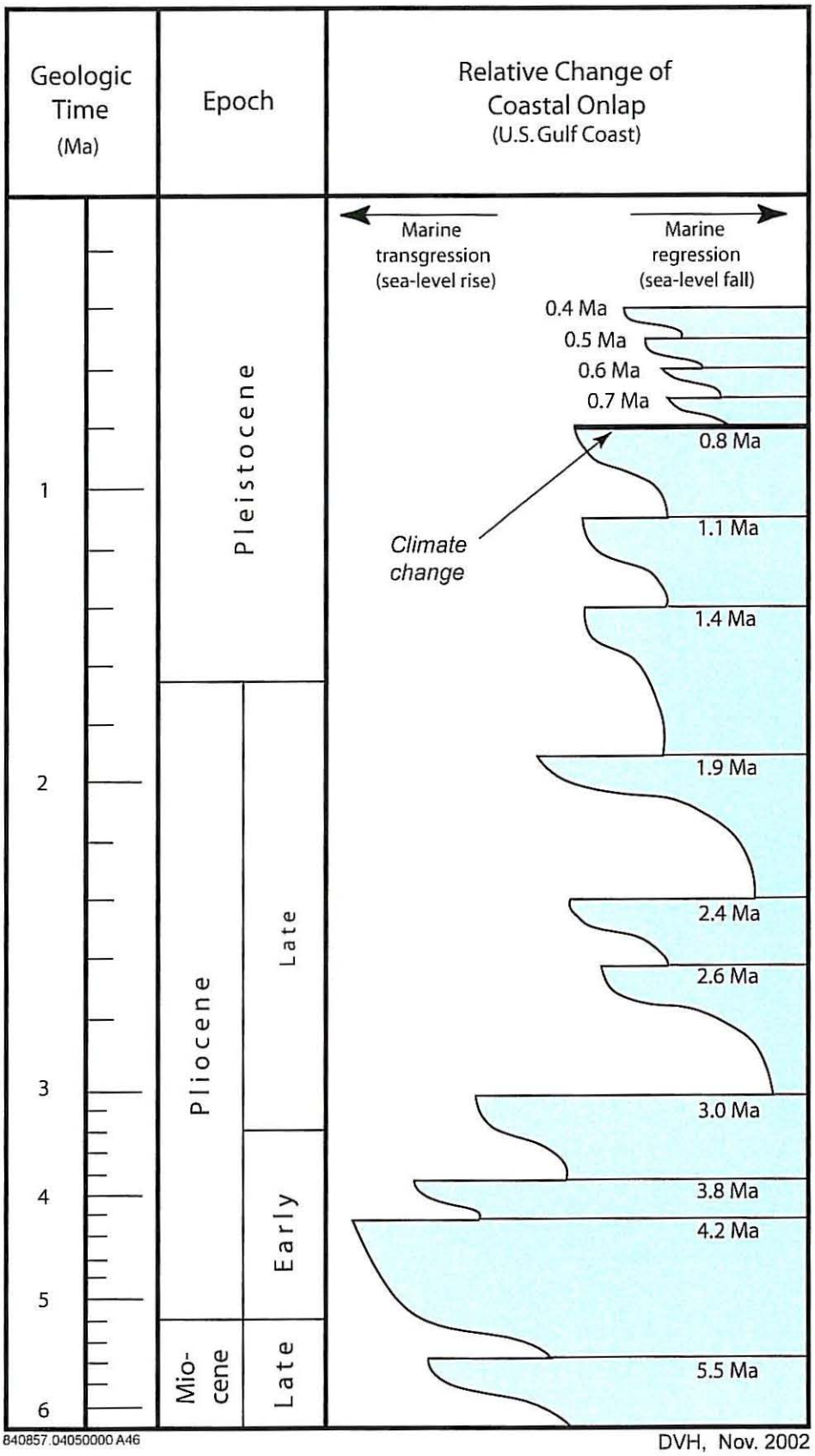

Figure 5-6 Late Cenozoic Changes in Relative Sea Level
(Modified from Paleodata-Schlumberger/Geco-Prakla, 1993)

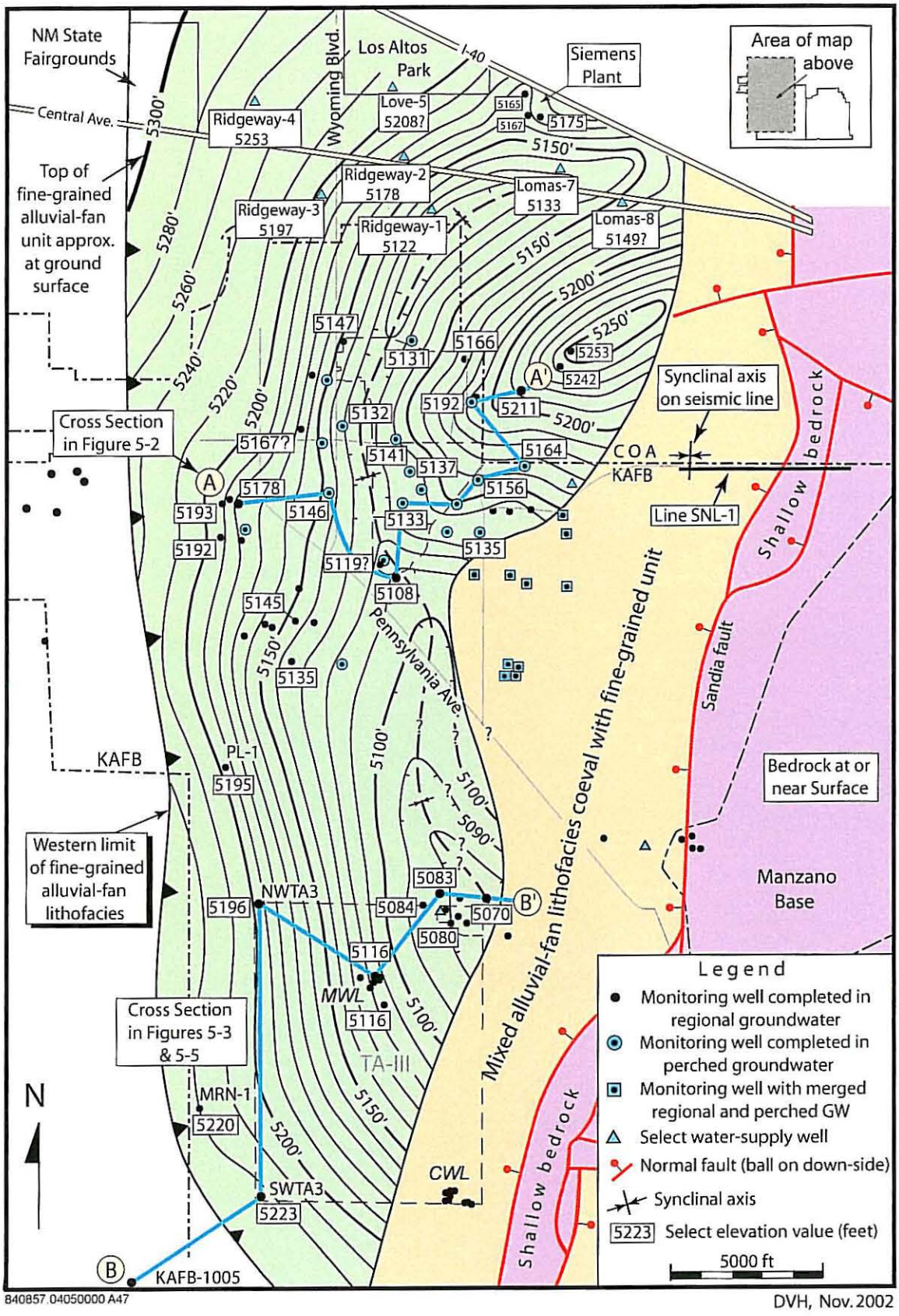

Figure 5-7 Limit of and Structure on Approximate Top of Fine-Grained Alluvial-Fan Lithofacies (green)

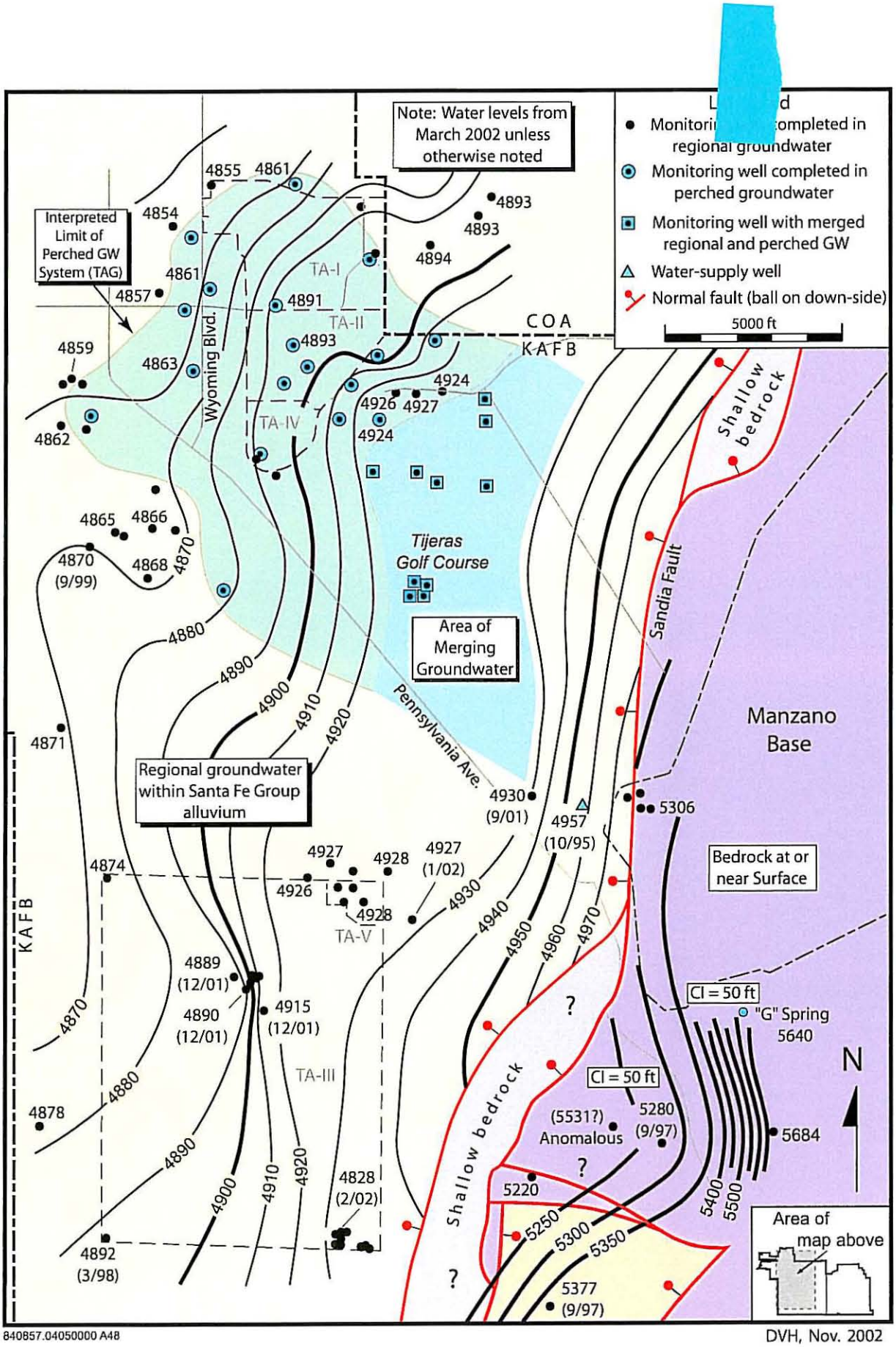

Figure 5-8 Regional Water Table Map
(Cl = 10 ft, except where noted)

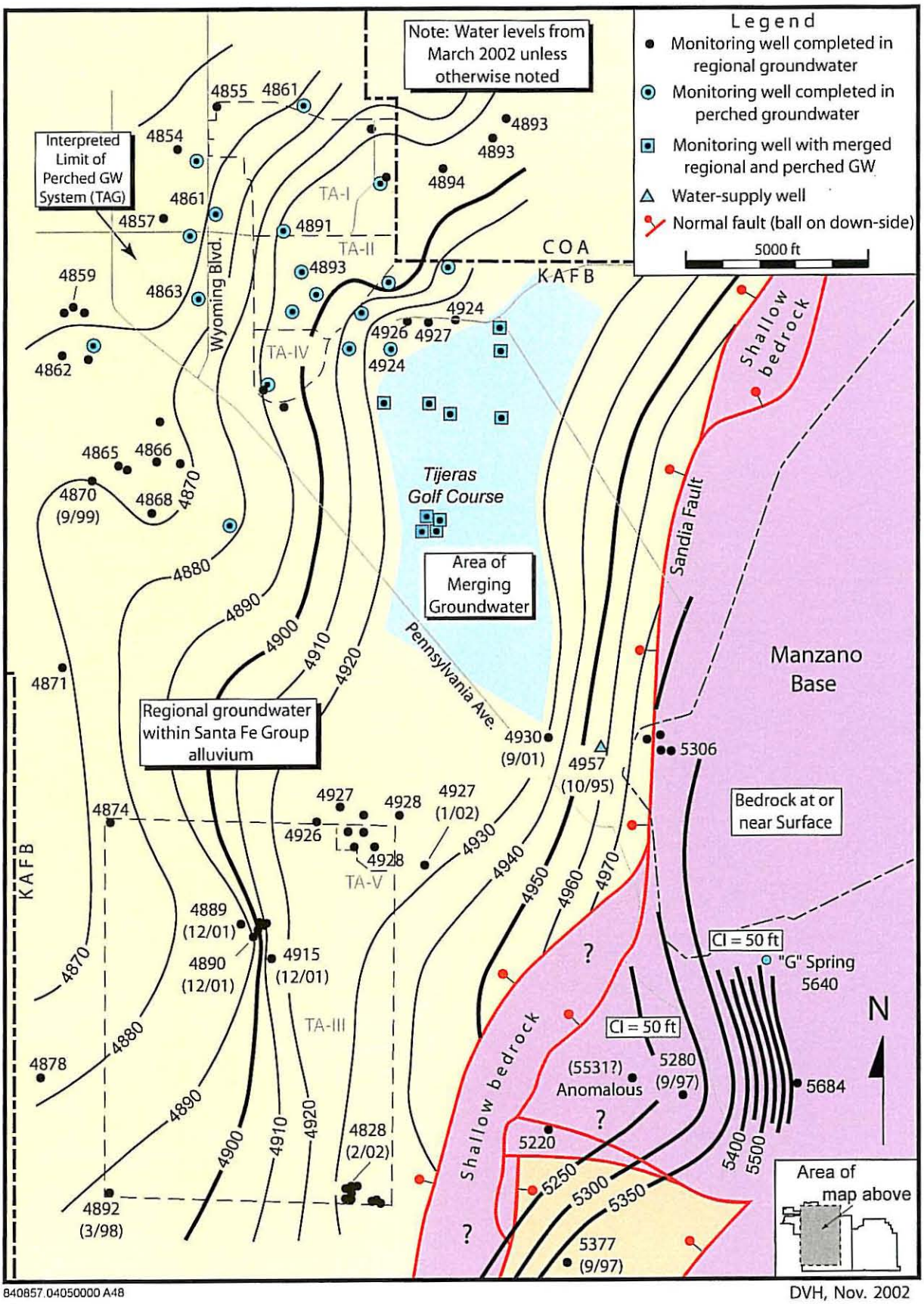

Figure 5-8 Regional Water Table Map
(CI = 10 ft, except where noted)

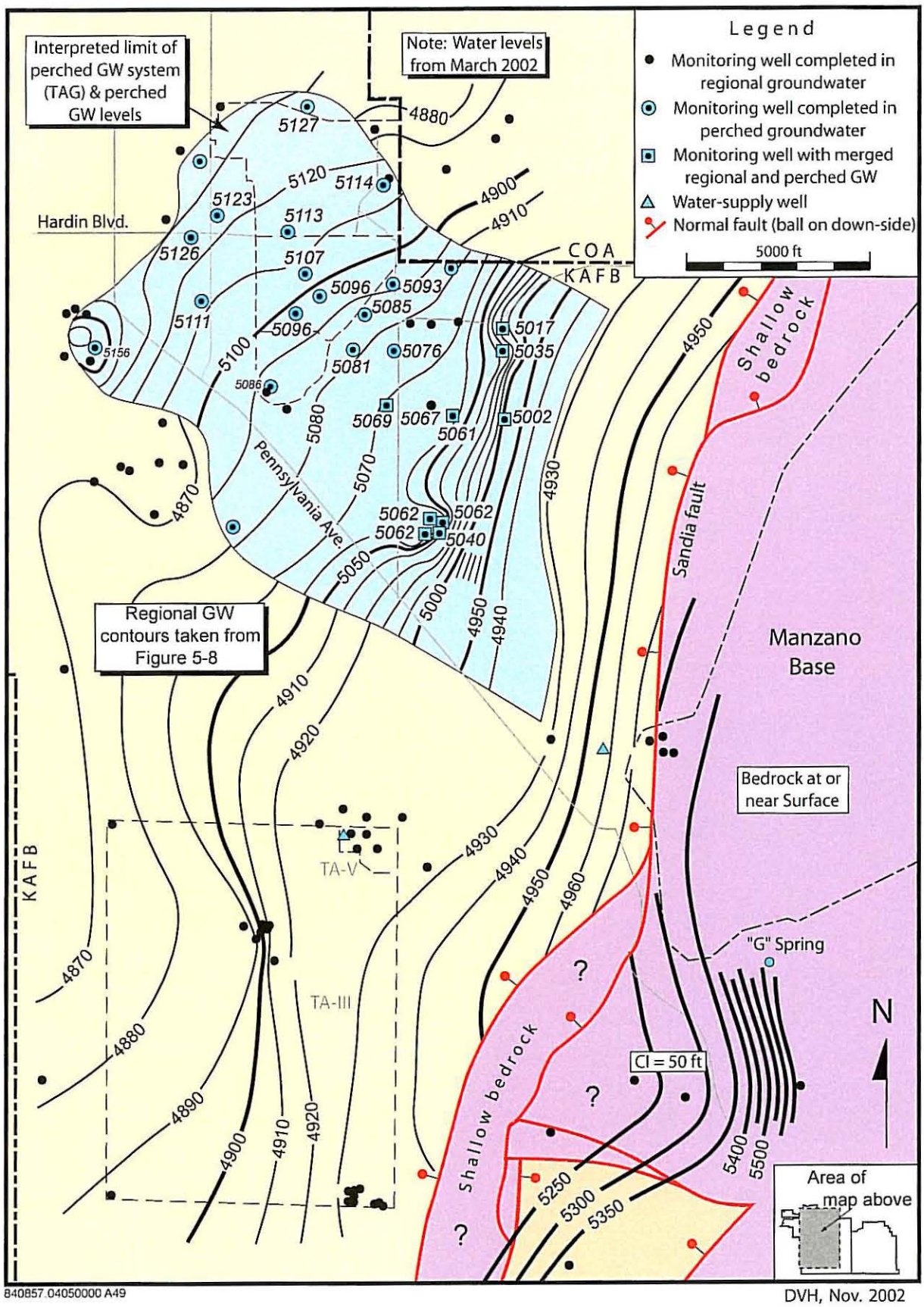

Figure 5-9 Merging of Regional and Perched Groundwater Systems
(CI = 10 ft, except where noted)

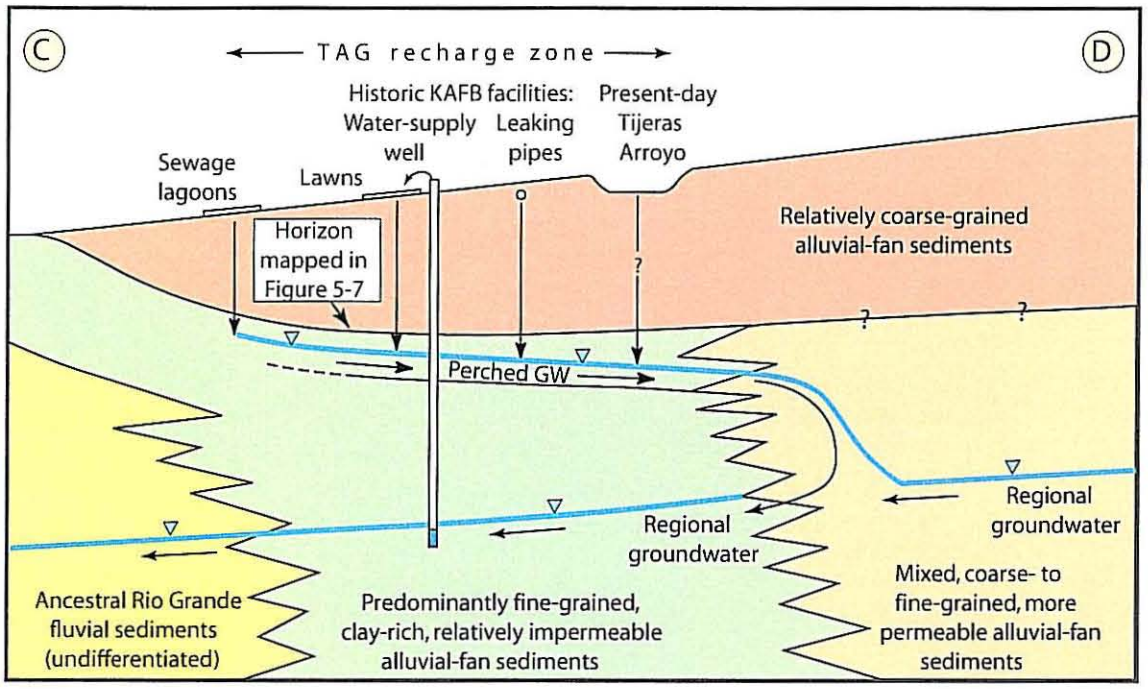

A. Stratigraphic Relationships

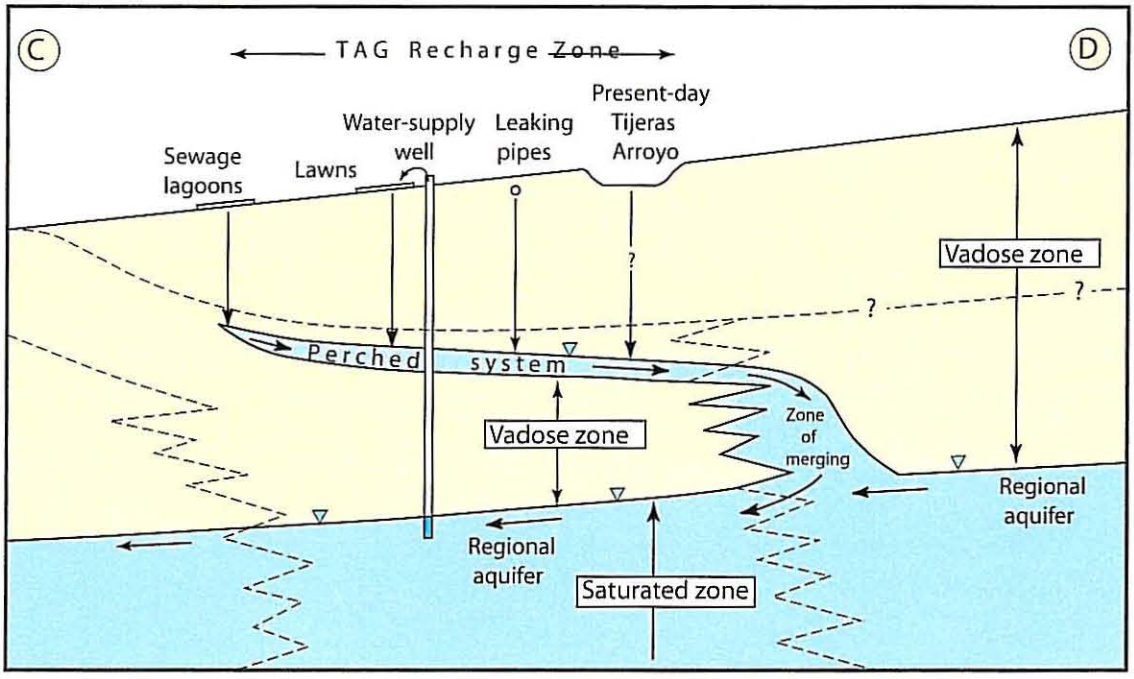

B. Groundwater Flow Model

840857.04050000.A50

DVH, Nov. 2002

Figure 5-10 Schematic Cross Section C-D, Tijeras Arroyo Groundwater (TAG) Area
(Location in Figure 5-1)

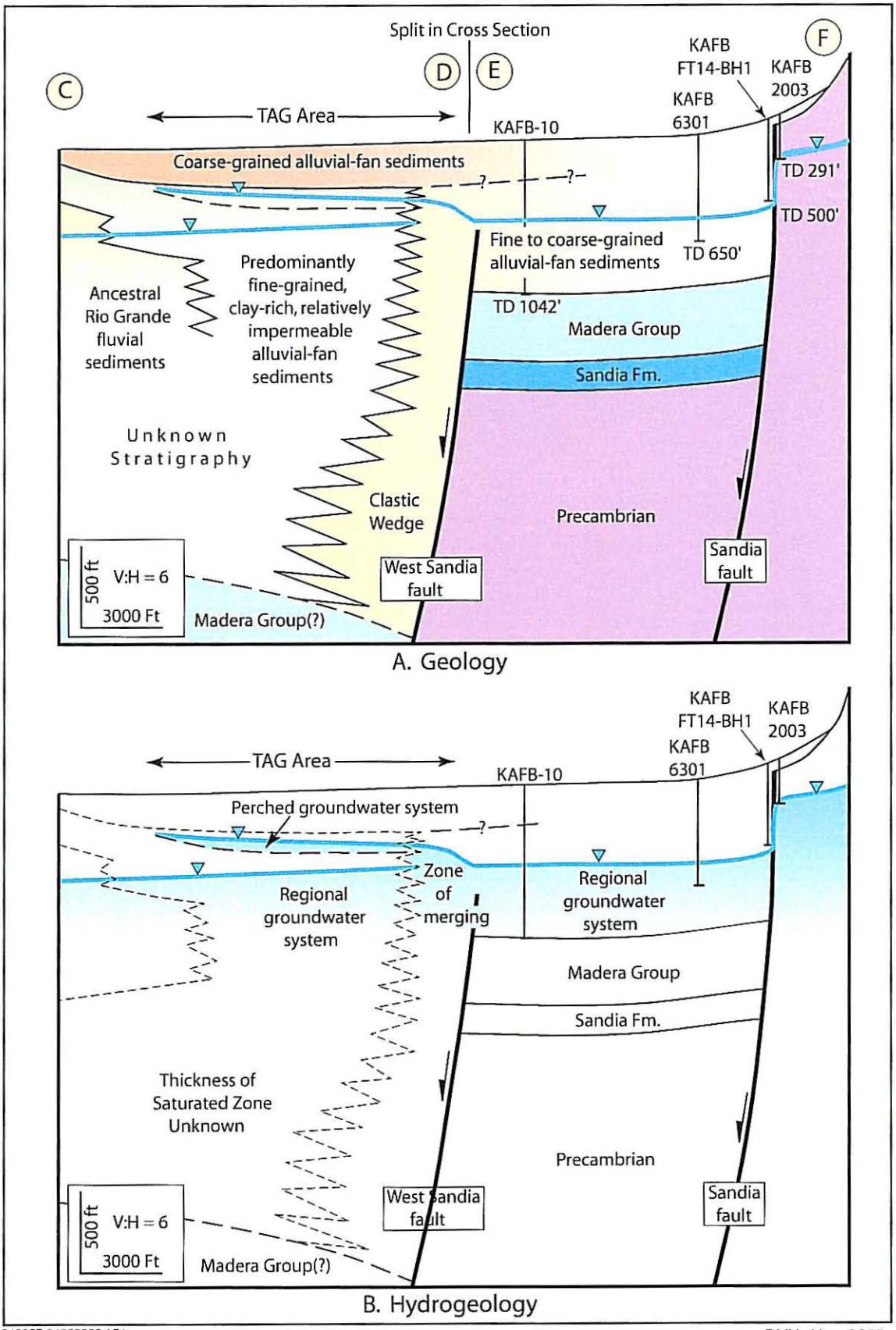

840857.04050000 A51

DVH, Nov. 2002

Figure 5-11 Schematic Cross Section C-D-E-F, Showing Megascopic View of Tijeras Arroyo Groundwater (TAG) System

(Location in Figure 5-1)

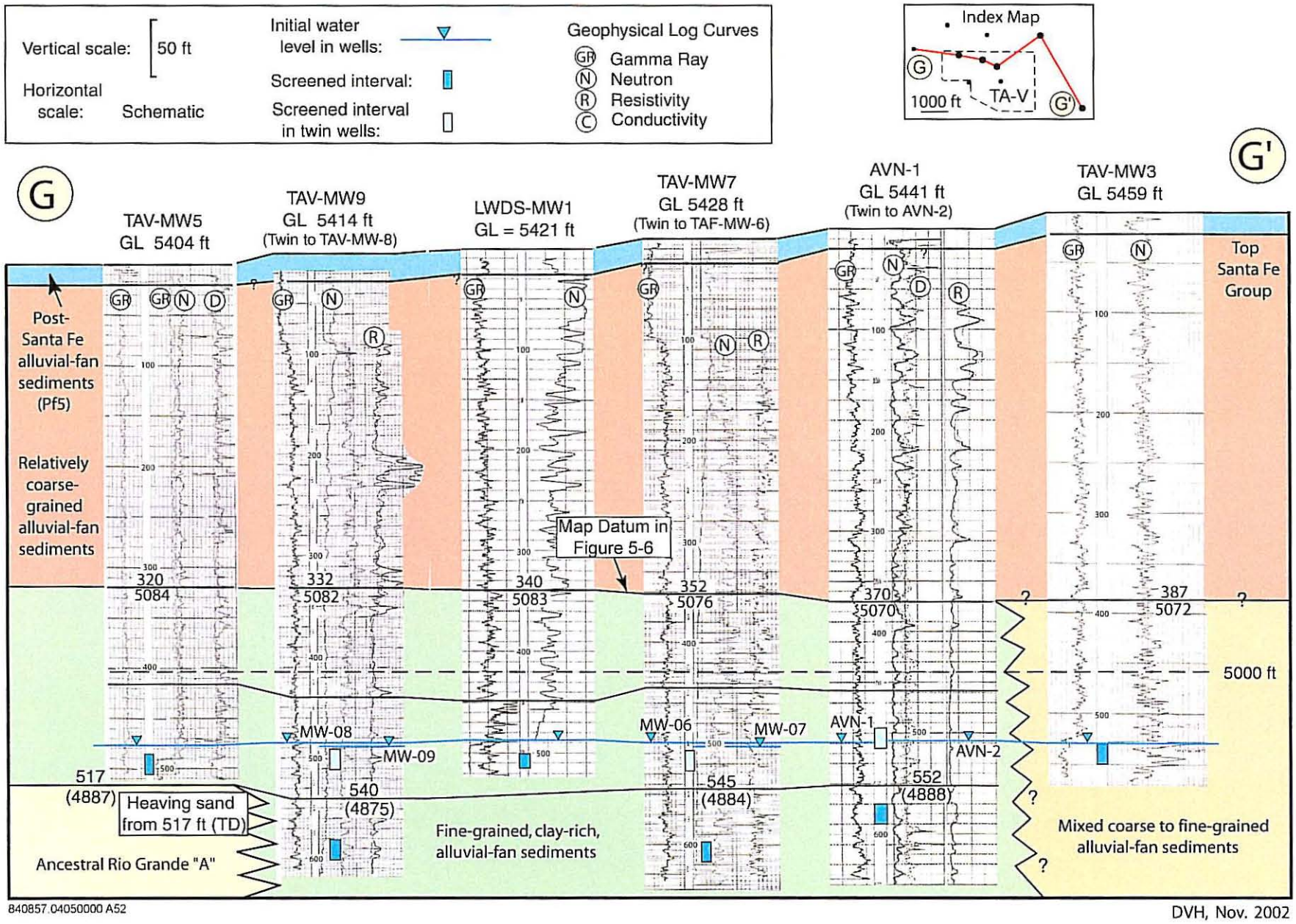

Figure 5-12 Geophysical-Log Correlation Section G-G', Technical Area V

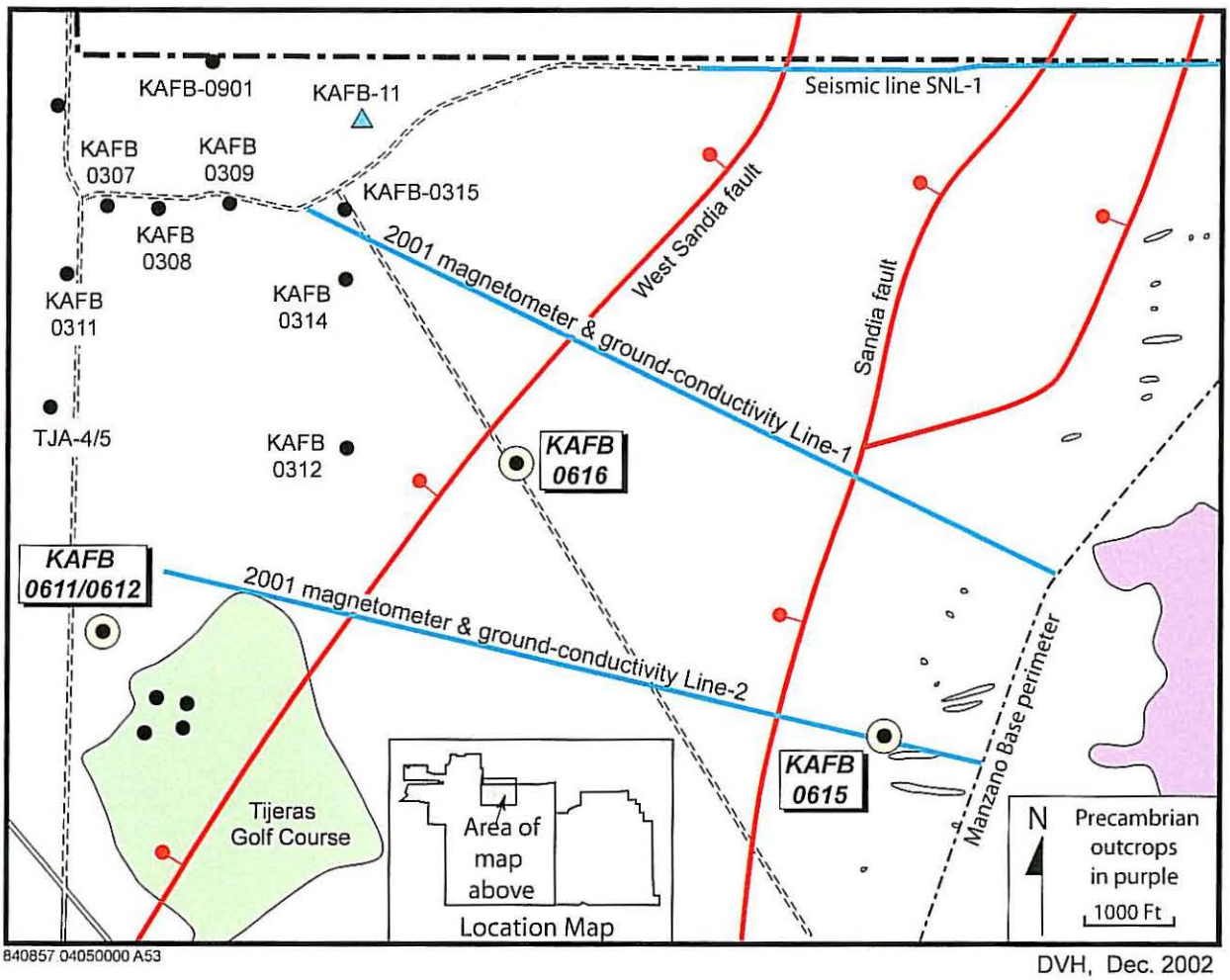

Figure 5-13 Location of New Kirtland Air Force Base (KAFB) Wells

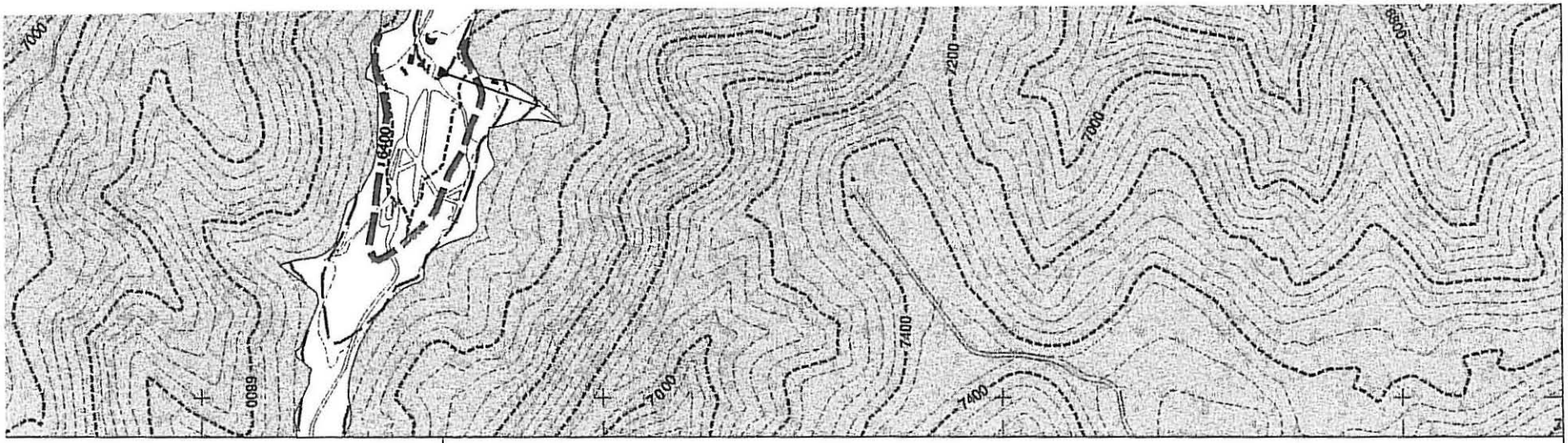

1450000

652500

1000 2000

Scale in Feet

240 480

Scale in Meters

Sandia National Laboratories, New Mexico
Environmental Geographic Information System

PLATE II
LURANCE CANYON
WITH BEDROCK ELEVATIONS
SNL/KAFB

Compiled by photogrammetric methods from aerial photography dated March 1989, March 1990, September 1991 and July 1992

Transverse Mercator Projection, New Mexico State Plane Coordinate System, Central Zone 1927 North American Horizontal Datum, 1929 North American Vertical Datum

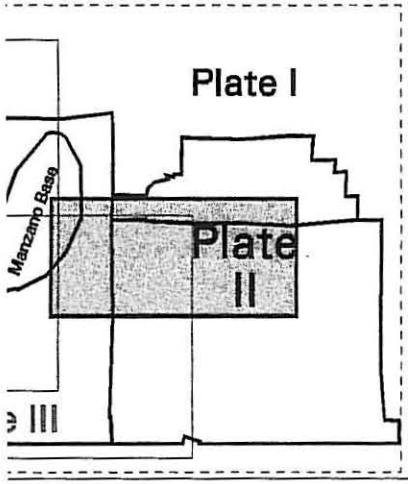

Unclassified	1:12000	05-MAY-2003
SNL EGIS ORG. 6135		
scmorri	sm020415.aml	MAPID=020415

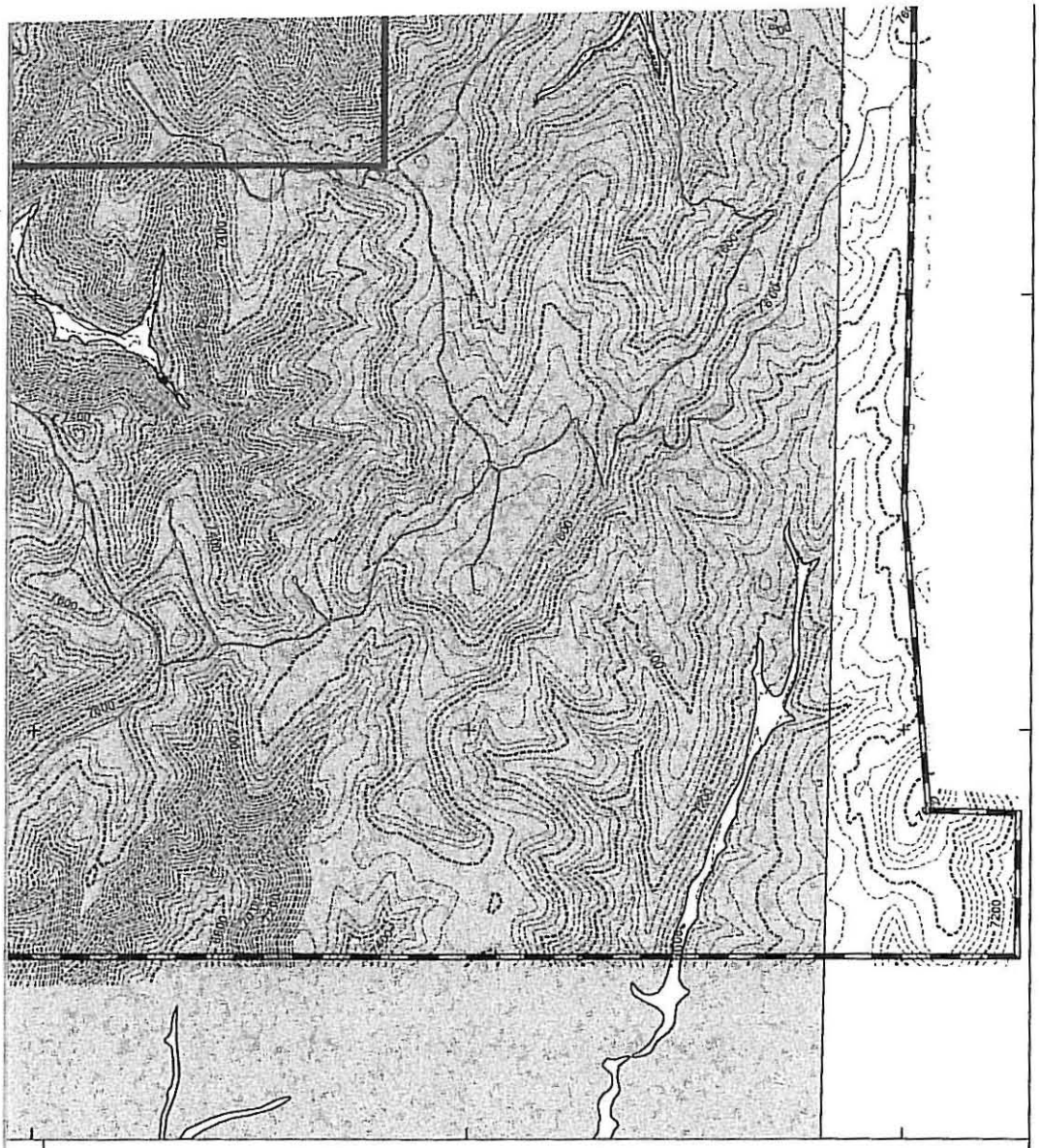

Sandia National Laboratories, New Mexico
Environmental Geographic Information System

PLATE I
LURANCE CANYON, HUBBELL BENCH & MANZANO BASE WEST AREAS WITH BEDROCK ELEVATIONS SNL/KAFB

Compiled by photogrammetric methods from aerial photography dated March 1990, March 1990, September 1991 and July 1992
Transverse Mercator Projection, New Mexico State Plane Coordinate System, Central Zone
1927 North American Horizontal Datum, 1929 North American Vertical Datum

Unclassified	1:36000	22-MAY-2002
SNL EGIS ORG. 6135		
scmorri	sm020414.aml	MAPID=020414

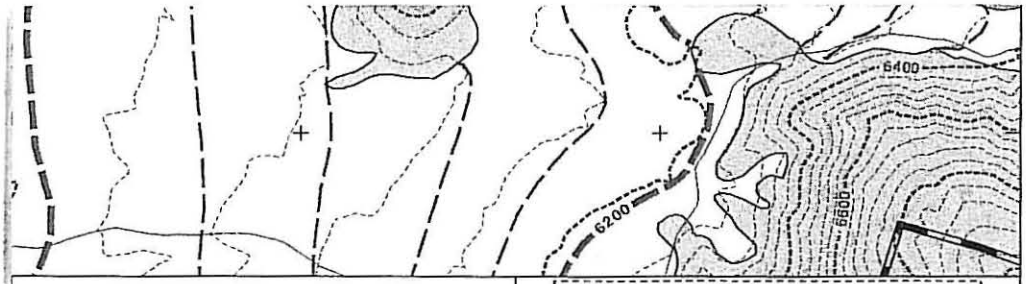

0 1000 2000
Scale in Feet
0 240 480
Scale in Meters

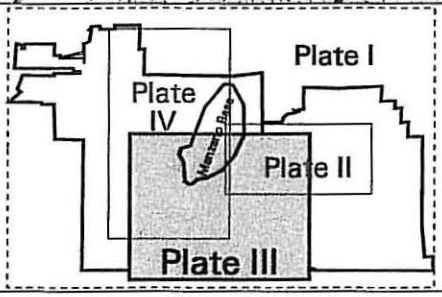

1435000

Sandia National Laboratories, New Mexico
Environmental Geographic Information System

PLATE III
HUBBELL BENCH & LOWER LURANCE CANYON WITH BEDROCK ELEVATIONS SNL/KAFB

Compiled by photogrammetric methods from aerial photography dated March 1989, March 1990, September 1991 and July 1992

Transverse Mercator Projection, New Mexico State Plane Coordinate System, Central Zone 1927 North American Horizontal Datum, 1929 North American Vertical Datum

N

ENVIRONMENTAL GIS OPERATIONS CENTER

Unclassified	1:18000	22-MAY-2002
SNL GIS ORG. 6135		
scmorri	sm020416.aml	MAPID = 020416

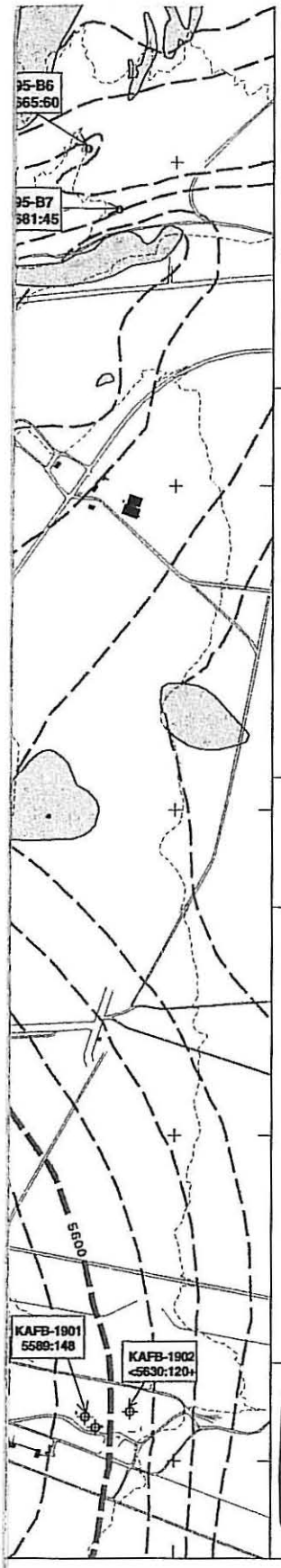

0 1000 2000

Scale in Feet

0 240 480

Scale in Meters

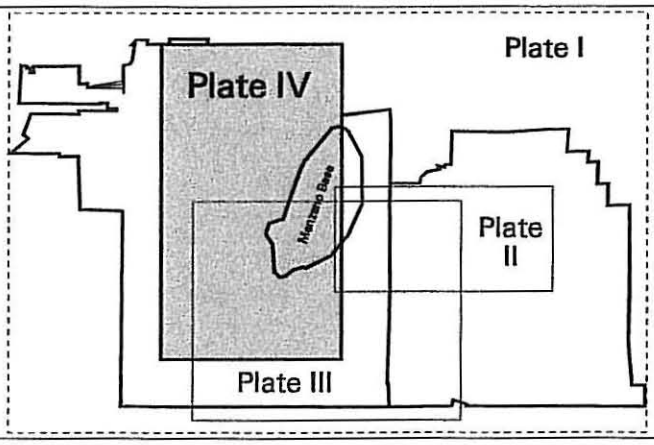

Sandia National Laboratories, New Mexico
Environmental Geographic Information System

PLATE IV
MANZANO BASE WEST AREA WITH BEDROCK ELEVATIONS SNL/KAFB

Compiled by photogrammetric methods from aerial photography dated March 1989, March 1990, September 1991 and July 1992

Transverse Mercator Projection, New Mexico State Plane Coordinate System, Central Zone 1927 North American Horizontal Datum, 1929 North American Vertical Datum

Unclassified	1:18000	04-MAR-2003
SNL EGIS ORG. 6135		
scmorri	sm020417.aml	MAPID=020417

DISTRIBUTION:

1 Geological Associates
Attn: Charles B. Reynolds
4409 San Andres, NE
Albuquerque, NM 87110

1 GRAM, Inc
Attn: Krishan Wahi
8500 Menaul Blvd., NE, Ste. B-335
Albuquerque, NM 87112

1 Hawley Geomatters
Attn: John W. Hawley
P.O. Box 4370
Albuquerque, NM 87196

1 Kirtland Air Force Base, IRP
Attn: Mark Holmes
377 MSG/CEVR
2050 Wyoming Blvd., SE
Albuquerque, NM 87117-5270

1 MWH Americas, Inc.
Attn: Michael Goodrich/Jeff Johnston
6100 Indian School Rd., NE, Ste. 100
Albuquerque, NM 87110-4137

1 NM Bureau of Geology & Mineral Resources
Attn: Sean D. Connell
2808 Central Ave., NE
Albuquerque, NM 87106

1 NM Bureau of Geology & Mineral Resources
Attn: David W. Love,
801 Leroy Pl.
Socorro, NM 87801-4796

1 Pueblo of Isleta, Water Resources Dept.
Attn: John D. Sorrell
P.O. Box 1270
Isleta, NM 87022

1 Sunbelt Geophysics
Attn: David Hyndman
P.O. Box 36404
Albuquerque, NM 87176

1 U.S. Geological Survey
Attn: James R. Bartolino
5338 Montgomery Blvd., NE
Albuquerque, NM 87109

1	MS 0750	Marianne Walck, 6116
1	0750	Jim Krumhansl, 6118
2	1087	Sue Collins, ER 6133
1	1087	John Copland, ER 6133
1	1087	Joe Fritts, ER 6133
1	1087	Stacy Griffith, ER 6133
1	1087	Tim Jackson, ER 6133
1	1087	Bill McDonald, NMED
1	1088	Mike Mitchell, ER 6133
1	1087	Mike Skelly, ER 6133
1	1088	Joe Pavletich, ER 6134
1	1089	Tim Goering, ER 6135
1	1089	Jerry Peace, ER 6135
1	1089	Mike Sanders, ER 6135
1	1089	Dirk Van Hart, ER 6135
1	1087	Will Moats, NMED
1	1042	Franz Lauffer, 03121
1	0612	Review & Approval Desk, 9612 for DOE/OSTI
2	0899	Technical Library, 9616
1	9018	Central Technical Files, 8945-1